ROYAL INSTITUTE OF TECHNOLOGY

POLCA-T code validation against Peach Bottom 2 End of Cycle 2 Turbine Trip Test 2

by:

Henric Lindgren

Master of Science Thesis
Division of Reactor Technology
2004

Department of Energy Technology
Royal Institute of Technology
Stockholm, Sweden

Proposal and approval of a
Master of Science thesis
at the Department of Energy Technology

Title: POLCA-T code validation against Peach Bottom 2 End of Cycle 2 Turbine Trip Test 2		
Author: Henric Lindgren	Report nr:	
Project:	Pages:	Drawings:
Overall responsible at KTH: Dr. Henryk Anglart		
Approved at KTH by:	Signature:	
Overall responsible at industry: Dr. Dobromir Panayotov		
Industrial Partners: Westinghouse Electric Sweden AB		
Approved by industrial partners:	Signature:	

Abstract:

Three Turbine Trip transient experiments were performed prior to shutdown for refueling at the end of cycle 2 at Peach Bottom Unit 2. The aims for the transient tests were to investigate the effects of pressure increase transients on neutron flux in the core. From these experiments, unique transient data was recorded for computer code's validation.

The main objective of the study is to validate the Westinghouse methodology for 3D analysis of pressure increase transients using the coupled 3D neutron kinetics and systems thermal-hydraulics code POLCA-T. Some sensitivity studies on effects of some thermal hydraulic and kinetics parameters, models and options are also performed.

The methodology for performing transient analysis is split up in five major steps: cross section data generation, depletion calculations, system thermal-hydraulics only analysis (initialization of plant model), core 3D neutron kinetics and thermal-hydraulics analysis (initialization of core model), and coupled 3D core and plant systems transient analysis. This report describes the work performed and the results obtained in each of the steps. Cross section data was generated by PHOENIX taking into account fuel exposure, coolant density historical and instantaneous dependencies, control rods, fuel temperature, and xenon dependencies. Westinghouse 3D nodal core simulator POLCA7 was used when performing depletion calculations and xenon transient calculations. Steady state Hot Zero Power and Hot Full Power analyses were performed to initialize the core model, using POLCA7 and POLCA-T.
In the final step of the transient analysis the Westinghouse coupled 3D core neutron kinetics and plant systems thermal hydraulics transient code POLCA-T was validated against the PB2 Boiling Water Reactor Turbine Trip Test 2 (TT2), using multiple table cross section data generated by the Westinghouse PHOENIX code. Obtained results were compared with available measured data and showed good agreement with them. Thus the 3D transient methodology using the POLCA-T code was validated for pressure increase transients.

Distribution List

Name/Company		**Copies**	**Name/Company**		**Copies**

CONTENTS

LIST OF FIGURES

LIST OF TABLES

ABBREVIATIONS

AO	Axial Offset
APRM	Average Power Range Monitor
BA	Burnable Absorber
BWR	Boiling Water Reactor
CD	Cell Data
CR	Control Rod
EFPH	Effective Full Power Hours
EOC	End of Cycle
FA	Fuel Assembly
HFP	Hot Full Power
HZP	Hot Zero Power
KKL	KernKraftwerk Leibstadt
LHGR	Linear Heat Generation Rate
LPRM	Local Power Range Monitor
NEA	OECD Nuclear Energy Agency
NRC	United States Nuclear Regulatory Commission
NW	Northwest
OECD	Organization for Economic Cooperation and Development
PB2	Peach Bottom Atomic Power Station Unit 2
pcm	per cent mille (10^{-5})
PHX	PHOENIX lattice code
PPF	Power Peaking Factor
ppm	parts per million (10^{-6})
PSU	Pennsylvania State University
RMS	Root Mean Square
RPV	Reactor Pressure Vessel
SE	Southeast
SI	Spectrum Interaction
TIP	Traveling In-Core Probe
TSV	Turbine Stop Valve
TT	Turbine Trip

1 INTRODUCTION

Nuclear Power Plants are very complex systems. In order to maintain safe and efficient operation it is important to have models that can predict and simulate the operational conditions before performed by the operational staff. The phenomena that can occur in a Nuclear Power Plant require a theoretical model that can be applied for the entire reactor system. Neutron kinetics models must be applied to the core, along with a thermal hydraulic model for the core and systems.

To simulate transient events, the neutron kinetics and thermal hydraulics models must be coupled in order to consider the interaction of the phenomena. Westinghouse transient code POLCA-T is a 3D core simulator where the core neutron kinetics and the plant thermal hydraulics models are coupled together.

1.1 Background

Three Turbine Trip (TT) transient experiments, and four low-flow stability tests were performed prior to shutdown for refueling at the end of cycle 2 (EOC2) of the Boiling Water Reactor (BWR) Peach Bottom Unit 2 (PB2) in Pennsylvania, in April 1977 [1]. The aims for the TT tests were to investigate the effects of pressure increase transients on neutron flux in the core. The low-flow stability tests were performed to investigate the sensitivity of core stability when small perturbations are made in the operating conditions. From all these experiments, unique transient data was recorded for computer code's validation [1].

In order to verify the capability of different coupled codes during complex transient events, the US Nuclear Regulatory Commission (NRC) and OECD Nuclear Energy Agency (NEA), in cooperation with the Pennsylvania State University (PSU), developed a Boiling Water Reactor transient benchmark. The transient used for the benchmark was the PB2 EOC2 Turbine Trip 2. The benchmark specifications are described in detail in [2].

Previous validations have been made for POLCA-T against PB2 EOC2 Low-Flow Stability tests [3],[4] and the Turbine Trip benchmark [5],[6],[7],[8]. During these validations however, the cross-section data used was generated by PSU using the CASMO and Simulate codes [2]. The fuel exposure, coolant density histories and Xenon distributions were embedded implicitly in the cross section data generated by PSU for the TT2 initial state; and the models in POLCA7 and POLCA-T that utilize fuel exposure and Xenon dependencies were not used in the benchmark analyses. Despite the good agreement between the results in the benchmark and the measured data, the results cannot qualify Westinghouse 3D transient methodology using POLCA-T code due to the requirements of the benchmark specifications. Westinghouse methodology and codes for cross-section data generation differs from the methodology and codes used in the benchmark. In the present POLCA-T code validation against PB2 EOC2 TT2 test, the cross section data is generated using Westinghouse's PHOENIX-code following the standard methodology.

In order to validate the methodology, the results obtained from POLCA7 and POLCA-T have to be compared with available from PB2 measured data.

1.2 Objectives

The main objective of the study is to validate Westinghouse methodology for 3D analysis of pressure increase transients using the coupled 3D neutron kinetics and system thermal-hydraulics code POLCA-T. Some sensitivity studies on effects of some thermal hydraulic and kinetics parameters, models and options are also performed.

1.3 Chapters overview

Chapter 2 describes the 3D transient methodology. The methodology generally used requires five steps in order to perform 3D transient study, and all steps are presented.

Chapter 3 discusses the first step in the procedure which is cross section data generation using Westinghouse PHOENIX code, including definitions and assumptions used. The generated cross section data is used further in the depletion calculations.

The core depletion calculations performed by the Westinghouse POLCA7 code for cycle 1 and 2 are explained in chapter 4. Different options and parameters used in the depletion calculations are explained. The results of the depletion calculations are compared with data from PB2 by performing steady state calculations at the end of cycle 1 and cycle 2.

In chapter 5, the method of initializing the core neutronics model by performing Hot Zero Power calculations is described along with Hot Full Power calculations for the state prior to the TT2 transient with POLCA7 and POLCA-T. A sensitivity study on the influence of the bypass flow rate is performed also. The results are presented and compared to previous calculations using PSU data and also to measured plant data.

In chapter 6 the coupled neutron kinetic and thermal hydraulic transient calculations for the TT2 is performed with POLCA-T. Zero transient calculations and TT transient calculations are performed and sensitivity studies on the cross section models and different POLCA-T options. The results are compared to measured data and to results obtained using PSU data.

In chapter 7, a summary of the work is presented.

Six appendices include the following:

1. The process parameters of cycle 1 and cycle 2
2. The input data used for the depletion calculations
3. Control rod configuration for TT2 initial state and Hot Zero Power state
4. Assembly numbers map for Peach Bottom 2 in POLCA7
5. Radial power distributions for Hot Zero Power and Hot Full Power state prior to TT2
6. Peach Bottom 2 Reactor Pressure Vessel nodalization in POLCA-T

1.4 Westinghouse codes

Westinghouse codes used in the present study for the BWR TT POLCA-T code validation are briefly described below.

PHOENIX

PHOENIX is a 2D lattice neutron transport theory and depletion code which evaluates neutronics behavior in two dimensions of a fuel assembly and individual pin cells, and generates multiple table cross sections. PHOENIX creates spatially smeared (homogenized) microscopic and macroscopic cross-sections for each fuel segment, with discrete energy dependence, using two energy groups (thermal and epithermal) [9].

IFIGEN

IFIGEN is a pre-processor to PHOENIX. In IFIGEN, the depletion steps, boron contents, and moderator density histories are defined for which the cross section tables will be generated with PHOENIX [10].

CoreLink

CoreLink is a post-processing program for PHOENIX. CoreLink prepares the nodal cross section tables for POLCA7 from the files that were generated by PHOENIX. CoreLink processes data for each fuel segment type, and produce cell data tables in ASCII[1] format that will be later used by the program TABBE. The cell data contain all cross section tables for each fuel segment type [11].

TABBE

TABBE is a service program for cell data files. TABBE can convert cross section tables stored in ASCII format to binary format, and also dump tables from the binary file back to ASCII format. TABBE can also list the contents of the cell data files, and list k-infinity tables [12].

POLIN

POLIN is an input processor to POLCA7. All the inputs, where the core is modeled are made in POLIN. The inputs are then checked by POLIN for correctness before POLCA7 is started [13].

POLCA7

The Westinghouse POLCA7 code is a 3D nodal core simulator. POLCA7 solves the coupled neutronics diffusion equation and thermal-hydraulic equations using two energy groups. POLCA7 tracks burnup distributions and important nuclides during all reactor operation conditions; control rod insertions and axial spacer grid positions. In POLCA7, the assemblies are divided in axial nodes that are homogenized, to which fuel segment data is linked [9],[11].

[1] ASCII format in this case means a plain text file

POLDIS

POLDIS is a distribution file service program for POLCA7 which is used for manipulating distributions. One feature of POLDIS is that distribution files can be created. This was the only option used for this program in the present study, where the TIP measurements from PB2 were put into binary format [14],[15].

SKYFFEL

SKYFFEL is a core shuffling program for the free standing POLCA7. In SKYFFEL, the fuel assemblies, control rods and detectors are shuffled between fuel cycles [16].

POLCA-T

POLCA-T is a 3D transient code which brings together the 3D core neutron kinetics and plant system thermal-hydraulics models. The code has a full 3D core model based on the POLCA7 code, and the plant systems thermal hydraulics model is based on the RIGEL code. POLCA-T uses the BISON modules SAFIR for the balance of plant models and PARA for the steam line model. The code is presently under validation with emphases on pressure increase transient analysis and stability [5],[17],[18].

2 3D TRANSIENT ANALYSIS METHODOLOGY

When 3D transient analyses are performed using coupled codes, the methodology generally consists of five steps as follows:

1. Cross section data generation

2. Depletion (core follow) calculations

3. Plant systems thermal hydraulic only transient analysis: initialization of plant model

4. 3D core neutronics and thermal hydraulic hot zero power calculations and hot full power steady state calculations: initialization of core model

5. Coupled 3D core neutron kinetics and plant thermal hydraulic systems transient analysis

These five steps are described in detail in the sections below.

2.1 Cross section data generation

Cross section data generation is the first step in the 3D transient analysis. One of the reasons for generating cross section tables is to obtain the data required by the 3D core simulator and the transient code. The core simulator and transient code are further used in the depletion calculations of the core, and in the steady state and transient analyses, which are the following steps of the methodology.

In a 3D nodal core simulator and in the transient code, each fuel assembly is axially divided into a number of nodes. The 3D nodal core simulator has models with coupled neutronics, thermal-hydraulics and depletion. The core simulator requires data that is homogenized for each material composition in order to solve the neutron diffusion equation. These homogenized data for each material composition are not prepared by the core simulator, but instead by a separate 2D transport theory and depletion code often called lattice code [19].

A fuel assembly can have different axial compositions. Each unique axial composition is called a fuel segment type. A common assumption when generating data for each fuel segment type is that it is surrounded by identical fuel segments, which means that the fuel segment parameters depend primarily on the assembly itself, and not on its position in the core. The position dependency is later modeled in the core simulator [19].

For each fuel segment type, successive independent depletion calculations are performed. This is to model the history effects for fuel exposure and material burnup. Independent non-depletion calculations are also performed to model instantaneous effects by means of branch calculations. In these calculations, the fuel segment state parameters fuel exposure, coolant density and coolant density history are determined [19].

The calculations are performed to create Cell Data (CD) that will be linked to each fuel segment type. The CD consists of macroscopic and microscopic cross section tables, diffusion coefficients, discontinuity factors, pin-power, pin-burnup form factors and delayed neutron data.

When a depletion calculation is performed, all parameters are held constant at their base values, and only the fuel exposure changes. The base values are the parameters for which the core is designed to run during normal operation (rated parameters). Non-depletion off-base branch calculations are based on instantaneous variations from the rated state parameters [19].

The CD is generated for many depletion histories. The data includes all the significant state parameters and is tabulated. From the tables, interpolations can be performed by the core simulator of the history parameters to get the history dependent data for the specified node [19].

The coolant density history and control rod (CR) history are the two history state parameters used by the core simulator, where the coolant density history is the only independent parameter in the cross section tables. The CR history is regarded only for pin-power form factor maps and neutron flux discontinuity factors. This is done explicitly in supplementary cross section tables [19].

The non-depletion off-base calculations are made for the instantaneous steps, for all state parameters independently. However, in some cases some parameters are combined and varied simultaneously. The active coolant density is the most important parameter for the off-base calculations and is always varied simultaneously with the other parameters. This means that the CD is a tabulation of three independent variables, namely the fuel exposure, the instantaneous coolant density and the coolant density history [19].

The base values for a BWR are defined in [19] as:

- Hot Full Power (HFP) moderator[2] density corresponding to a saturated or sub-cooled condition with no void at rated core pressure
- HFP coolant density corresponds to the reference coolant density (coolant density at a selected void condition)
- HFP nominal power density
- HFP nominal fuel temperature
- No control rods or spacer grids present
- Reference boron concentration of zero ppm
- Equilibrium xenon at nominal power density

For the off-base parameter values, instantaneous variations of the coolant density are made for each depletion case, and variations with the following state parameters are calculated, as explained in pp. 8-9 of [19]:

- Average fuel Doppler temperature

[2] The moderator and active coolant are treated differently in a BWR. The active coolant is the internal assembly flow. The moderator includes also the internal and external assembly bypasses.

- Control rod presence for each control rod type
- Spacer grid presence for each spacer grid type
- Xenon concentration (non-equilibrium)

The presence of CR during the depletion is treated specially with the control rod history tables for pin-power form functions and discontinuity factors. This is done to capture the impact they have on reactivity and pin powers. When a CR is inserted the fissile isotope Pu-239 is built up and the depletion of U-235 retardates in the near vicinity of the CR. When the CR is removed very large pin power peaking may occur. The CR history tables are generated assuming the control rods have been inserted for certain depletion periods, and withdrawn after some period [19].

The base CD tables are generated with base dependencies in three state parameters; the fuel exposure, the reference coolant density and the coolant density history. All other parameters also affect these base CD-tables, and are additional contributors to the base CD tables [19].

The inputs to the lattice code when generating the CD is design data for the fuel and the other materials present in the core, and a microscopic cross section library.

The reason for generating nodal data by means of a separate lattice code is that the microscopic cross section library is very large, and the 3D core simulator cannot acquire data directly from the library. Separate CD tables including only the homogenized compositions present in each fuel segment and in the CR and detectors are generated. In these tables, the core simulator interpolates in order to achieve data for the desired state of the reactor.

When the CD is generated, the next step in the 3D transient analysis can be performed: the depletion calculations with the core simulator up to the desired operational point when the transient analysis is to be performed.

The cross section generation process for PB2 cycle 1 and cycle 2 along with used assumptions and results are presented in chapter 3.

2.2 Depletion calculations

The second step in the 3D transient analysis is depletion (core follow) calculations. During operation of a nuclear power plant, the initial isotopes are depleted, and some isotopes are built up and then depleted. In order to obtain the actual distributions of the isotopes at the state prior to the transient analysis, the core must be depleted to model all the history effects in the core during the operation up until the time of the transient analysis.

The parameters that determine the depletion of the core are several. Among them are core thermal power, coolant flow, control rod presence, pressure and core coolant inlet subcooling. The variation of these parameters during the operation must be considered in order to model the local depletion effects in the core. The cross section tables are used by the core simulator where all different operating states and exposures are modeled by interpolating in the tables.

3D neutronics core simulators are used for the calculations where the fuel, control rods and detectors are depleted. In the core simulators, the fuel assemblies are divided in axial nodes. These nodes may consist of several material compositions, to which cell data is linked.

Burnup steps no larger than 1 MWd/kg are recommended in order to model all local depletion effects in the core sufficiently. At the end of each depletion calculation, the calculated distributions for the isotopes and the histories are saved. Having all these distributions saved, a new set of depletion calculations for the next burnup step is performed.

In order to check the accuracy of the depletion calculations and the generated cell data, instantaneous steady state power calculations can be performed, and compared with measured plant data. The calculated TIP (Traveling In-core Probe) detector response can be compared with measured TIP detector response. If the deviations between the calculated and measured TIP response are within certain acceptable limits, the core depletion calculations are considered to be satisfactory.

Between the fuel cycles, a specialized code or a core simulator is used to shuffle and reload the core, and to initiate distributions for the fresh fuel assemblies.

When the core is depleted during the cycles, the xenon is assumed to be equilibrium. If the reactor has not been operating with steady conditions prior to the transient test, xenon transient calculations must be performed in order to model the non-equilibrium xenon distributions in the core. This is important because xenon has an extremely large absorption cross section [20].

The distribution of xenon in the core is assumed to be in equilibrium in the core if the reactor has been operating with steady conditions for a long time period (more than 72 hours). However, if significant changes in the operating conditions are made in a shorter time period prior to the transient test, the xenon will not be in equilibrium. Xenon is formed in two ways in the core, directly from the fission process and from the decay of Iodine. It is the xenon that is formed from the decay of Iodine that requires approximately 72 hours to reach a new equilibrium.

The depletion calculations and xenon transient calculations for PB2 during cycle 1 and cycle 2 up to the state prior to the TT2 test are described in detail along with the achieved results in chapter 4.

2.3 Plant systems thermal hydraulic transient analysis: initialization of plant model

The third step in the 3D transient analysis is the development of the thermal hydraulic plant model. The purpose of this step is to develop, initialize and test the response of the plant model from the thermal hydraulic system, and compare the results with available measured data.

The boundary conditions necessary to perform the initialization of the model for the TT simulation are assumed to be the following:

- power versus timetable

- turbine pressure controller set-point versus time
- steam bypass valve position versus time
- feed water mass flow and temperature versus time

The development of the plant model is independent of the cross section model used.

When the plant model is developed, the response of the model is tested by performing transient calculations using the above mentioned boundary conditions. The calculated parameters, steam dome and core exit pressures, main steam line and turbine inlet pressures, reactor pressure vessel (RPV) water level etc. are compared to measured data [5].

This step was performed in previous validations, [5], [21], and is independent of the cross section model used and will not be performed again in this study. The plant model is described in more detail in chapter 6.

The next step in the 3D transient analysis is to initialize the core model. When the core model is initialized, it is coupled with the thermal hydraulics model in the final step, which is coupled 3D core and plant systems transient analysis.

2.4 3D core steady state calculations (Hot Zero Power and Hot Full Power calculations): initialization of core model

In the fourth step of the 3D transient analysis the 3D core model is initialized. By means of performed steady state calculations, the response of the 3D core neutronics and thermal hydraulics models with lower and upper plenum boundary conditions is tested. The analyses are performed by the core simulator.

The first part of initializing the core model is performing Hot Zero Power (HZP) calculations. The HZP is an artificial state where the core neutronics model is initialized and verified. The HZP calculations are performed at 1% of the rated power. The thermal hydraulic parameters (fuel temperature and coolant density) are fixed in each node which turns off the thermal hydraulic feedback in the core, hence only the core neutronics model and the generated cross section data are tested [2].

When the core model is initialized, steady state Hot Full Power (HFP) calculations are performed for the state prior to the transient test. The process parameters for the state prior to the transient experiment are used when calculating the steady state.

The calculated power and its distributions are compared to measured plant data for the state.

The calculation procedure is described in detail in chapter 5 along with the process parameters at PB2 for the state prior to the TT2 tests, and the results of the calculations.

Now all first four steps have been completed in order to prepare the coupled 3D core and plant systems transient analysis. The cross section tables have been generated; the core has been depleted up to the desired state; the thermal hydraulic and core models have been initialized. The fifth and final step is to perform calculations for the transient with coupled core and thermal hydraulic models.

2.5 Coupled 3D core and plant systems transient analysis

In the final step of the 3D transient analysis the thermal hydraulic plant model is coupled with the 3D neutron kinetics model and transient analysis is performed.

The first step is to perform zero transient calculations. Zero transient calculations are performed in order to avoid that any numerical noise or input errors are superimposed on the results in the transient calculations.

Immediately following the zero transient calculations, the system is perturbed in the way that was used in the test and the transient calculations are performed.

A sensitivity study is performed in order to check the effect of some input parameters, code's options and models on results. The choice of parameters, options and models is made considering their uncertainty and importance for phenomena assumed to be important for simulated transient.

The calculated parameters fission power, steam dome pressure, main steam line pressure, turbine inlet pressure, etc. are compared to measured plant data.

The transient calculations, and the steps involved are explained in detail in chapter 6 along with the analysis, results and comparison with measured data.

3 CROSS SECTION DATA GENERATION

Cross section data generation was the first step in the 3D transient analysis. The methodology described in section 2.1 was applied using Westinghouse codes.

In the Westinghouse 3D nodal core simulator POLCA7, each fuel assembly is axially divided into nodes. Each node may contain a number of fuel segment types, to which cell data[3] (CD) is linked. POLCA7 requires data that is homogenized for each fuel segment (often called material composition) in order to solve the neutron diffusion equation. The homogenization means that all materials and their temperatures, densities and exposure are assigned to the whole composition [19]. These homogenized data for each material composition are not prepared by the core simulator, but instead by Westinghouse 2D transport theory and depletion code PHOENIX [22], [23].

In order to model the neutron transport for each fuel segment type in PHOENIX, the design data of PB2 [24] was used to describe all materials that the core consisted of during cycle 1 and cycle 2.

A description of the PB2 reactor and the design data for cycle 1 and cycle 2 used when generating the cell data is described in the next section. A thorough description of PB2 during cycle 1 and cycle 2 is found in [24].

3.1 Peach Bottom 2 Core Data

Peach Bottom 2 is a General Electric BWR/4 Nuclear Power Plant. The core consisted of 764 fuel assemblies with an active length of 144 inches (365.76 cm). 185 control rods provided reactivity control. Local Power Range Monitors (LPRM) and a Traveling In-core Probe (TIP) system were used to detect neutron flux in the core.

During cycle 1, the core was loaded with 764 7x7 fuel assemblies. When the core was shuffled and reloaded for cycle 2, 576 7x7 fuel assemblies remained in the core, and 188 8x8 assemblies were loaded.

The fuel assembly geometry and data is shown in Table 3.1 for the assembly types that were present in cycle 1 and cycle 2 (Table 1, 2 and 3 in [24]).

In the 7x7 assemblies, the spacer was connected to the fuel rod by a Zirconium connector located on the fuel rod. In the 8x8 assemblies, the water rods were spacer positioning rods.

In [24], there is no distinction between fuel assemblies of type 4-1 and 4-2 in the fuel assembly identification map. Therefore all type 4 fuel assemblies are assumed to be of type 4-1, since only eight assemblies of sixty-eight are of type 4-2. The only difference between fuel type 4-1 and 4-2 is the fuel box thickness, see Table 3.1.

The core loading patterns are shown below in Figure 3.1 and Figure 3.2 for cycle 1 and cycle 2 respectively.

[3] The macroscopic and microscopic cross section tables, diffusion coefficients, discontinuity factors, pin-power and pin-burnup form factors for each fuel segment type are assembled and called Cell Data

Table 3.1. PB2 fuel assembly data for cycle 1 and cycle 2

Assembly type	**1**	**2**	**3**	**4-1**	**4-2**	**5**	**6**
No of assemblies, initial core	168	263	333	0	0	0	0
No of assemblies, cycle 2	0	261	315	60	8	116	4
Geometry	7x7	7x7	7x7	8x8	8x8	8x8	8x8
Assembly pitch, in	6.0	6.0	6.0	6.0	6.0	6.0	6.0
Fuel rod pitch	0.738	0.738	0.738	0.640	0.640	0.640	0.640
Fuel rods per assembly	49	49	49	63	63	63	62
Water rods per assembly	0	0	0	1	1	1	2
Fuel rods containing Gd_2O_3	0	4	5	5	5	5	5
No of spacer grids	7	7	7	7	7	7	7
Inconel per grid, lb	0.102	0.102	0.102	0.102	0.102	0.102	0.102
Zr-4 per grid, lb	0.537	0.537	0.537	0.614	0.614	0.614	0.614
Spacer width, in	1.625	1.625	1.625	1.625	1.625	1.625	1.625
Assembly average fuel composition:							
Gd_2O_3, g	0	441	547	490	490	328	313
UO_2, kg	222.44	212.21	212.06	207.78	207.78	208.00	207.14
Total fuel, kg	222.44	212.65	212.61	208.27	208.27	208.33	207.45
1/2 Width of wide water gap, in	0.375	0.375	0.375	0.355	0.335	0.355	0.355
1/2 Width of narrow water gap, in	0.188	0.188	0.188	0.167	0.147	0.167	0.167
Bundle average enrichment	1.10	2.50	2.50	2.74	2.74	2.74	2.60
Weight of U per fuel assembly, kg	196.1	187.1	186.9	183.2	183.2	183.3	182.6
Channel geometry							
Outside width, in	5.438	5.438	5.438	5.478	5.518	5.478	5.478
Thickness, in	0.08	0.08	0.08	0.10	0.12	0.10	0.10
Inside corner radius, in	0.38	0.38	0.38	0.38	0.38	0.38	0.38
Material	Zr-4	Zr-4	Zr-4	Zr-4	Zr-4	Zr-4	Zr-4

Core loading pattern Peach Bottom 2 Cycle 1

	01	03	05	07	09	11	13	15	17	19	21	23	25	27	29	31	33	35	37	39	41	43	45	47	49	51	53	55	57	59
60									2	2	2	2	2	2	2	2	2	2	2	2	2	2								
58								2	2	1	1	2	2	1	1	2	2	2	1	2	2	2	2							
56						2	2	2	2	2	2	2	2	2	2	2	2	2	2	2	2	2	2	2	2					
54						2	1	2	2	1	1	2	2	1	1	2	2	1	1	2	2	1	1	2	2					
52					2	1	1	2	3	1	1	3	3	1	1	3	3	1	1	3	3	1	1	2	1	2				
50			2	2	2	2	2	3	3	3	3	3	3	3	3	3	3	3	3	3	3	3	3	2	2	1	2	2		
48			2	2	2	2	3	3	3	3	3	3	3	3	3	3	3	3	3	3	3	3	3	3	2	2	2	2		
46		2	1	2	2	1	1	3	3	1	1	3	3	1	1	3	3	1	1	3	3	1	1	3	3	1	1	2	2	
44	2	2	1	2	3	1	1	3	3	1	1	3	3	1	1	3	3	1	1	3	3	1	1	3	3	1	1	2	2	2
42	2	2	2	2	3	3	3	3	3	3	3	3	3	3	3	3	3	3	3	3	3	3	3	3	3	3	2	2	2	2
40	2	2	2	2	3	3	3	3	3	3	3	3	3	3	3	3	3	3	3	3	3	3	3	3	3	3	2	2	2	2
38	2	2	1	2	3	1	1	3	3	1	1	3	3	1	1	3	3	1	1	3	3	1	1	3	3	1	1	2	1	2
36	2	2	1	2	3	1	1	3	3	1	1	3	3	1	1	3	3	1	1	3	3	1	1	3	3	1	1	2	2	2
34	2	2	2	2	3	3	3	3	3	3	3	3	3	3	3	3	3	3	3	3	3	3	3	3	3	3	2	2	2	2
32	2	2	2	2	3	3	3	3	3	3	3	3	3	3	3	3	3	3	3	3	3	3	3	3	3	3	2	2	2	2
30	2	2	1	2	3	1	1	3	3	1	1	3	3	1	1	3	3	1	1	3	3	1	1	3	3	1	1	2	1	2
28	2	2	1	2	3	1	1	3	3	1	1	3	3	1	1	3	3	1	1	3	3	1	1	3	3	1	1	2	1	2
26	2	2	2	2	3	3	3	3	3	3	3	3	3	3	3	3	3	3	3	3	3	3	3	3	3	3	2	2	2	2
24	2	2	2	2	3	3	3	3	3	3	3	3	3	3	3	3	3	3	3	3	3	3	3	3	3	3	2	2	2	2
22	2	2	1	2	3	1	1	3	3	1	1	3	3	1	1	3	3	1	1	3	3	1	1	3	3	1	1	2	1	2
20	2	2	1	2	3	1	1	3	3	1	1	3	3	1	1	3	3	1	1	3	3	1	1	3	3	1	1	2	1	2
18	2	2	2	2	3	3	3	3	3	3	3	3	3	3	3	3	3	3	3	3	3	3	3	3	3	3	2	2	2	2
16		2	2	2	2	3	3	3	3	3	3	3	3	3	3	3	3	3	3	3	3	3	3	3	3	2	2	2	2	
14			2	1	2	1	1	3	3	1	1	3	3	1	1	3	3	1	1	3	3	1	1	3	2	1	1	2		
12			2	2	2	1	1	3	3	1	1	3	3	1	1	3	3	1	1	3	3	1	1	2	2	1	2	2		
10					2	2	2	2	3	3	3	3	3	3	3	3	3	3	3	3	3	3	2	2	2	2				
08						2	1	2	2	2	2	2	2	2	2	2	2	2	2	2	2	2	2	2	2					
06						2	2	2	2	1	1	2	2	1	1	2	2	1	1	2	2	1	1	2	2					
04								2	2	2	2	2	2	2	2	2	2	2	2	2	2	2	2							
02									2	2	2	2	2	2	2	2	2	2	2	2	2	2								

Figure 3.1. Core loading pattern cycle 1

Core loading pattern Peach Bottom 2 Cycle 2

	01	03	05	07	09	11	13	15	17	19	21	23	25	27	29	31	33	35	37	39	41	43	45	47	49	51	53	55	57	59
60									3	2	2	2	2	2	2	2	2	2	2	2	2	3								
58								2	2	5	2	5	2	5	5	5	5	2	5	2	5	2	2							
56						2	3	3	5	2	5	2	5	2	2	2	2	5	2	5	2	5	3	3	2					
54						2	2	5	2	2	2	3	2	3	3	2	3	3	2	3	2	3	5	2	2					
52					3	2	5	2	5	3	5	3	5	3	4	4	3	5	3	5	3	5	3	5	2	3				
50			2	2	2	5	3	2	3	2	3	2	3	2	3	3	2	3	2	3	2	3	2	3	5	2	2	2		
48			2	2	5	3	6	3	5	3	5	3	4	3	3	2	3	4	3	5	3	5	2	6	3	5	2	3		
46		2	3	5	2	2	3	3	3	3	3	3	3	2	3	3	3	3	2	3	3	3	2	2	2	3	5	3	2	
44	3	2	5	2	5	3	5	3	4	3	4	3	4	3	4	4	3	4	3	4	3	4	3	5	3	5	3	5	2	3
42	2	5	2	2	3	2	3	2	3	2	3	3	3	2	3	3	3	3	3	3	3	3	2	3	2	3	2	2	5	2
40	2	2	5	2	5	3	5	3	4	3	4	3	4	3	3	3	3	4	3	4	3	4	3	5	3	5	3	5	2	2
38	2	5	2	2	3	2	2	3	3	2	2	3	3	3	3	3	3	3	2	3	3	3	2	3	2	2	2	2	5	2
36	2	2	5	2	5	3	4	3	4	3	4	3	4	3	4	4	3	4	3	4	3	4	3	4	3	5	3	5	2	2
34	2	5	2	3	2	3	3	3	3	3	3	3	3	3	3	3	3	3	3	3	3	3	3	3	2	3	2	2	5	2
32	2	5	2	2	4	2	3	2	4	3	3	3	4	3	3	3	3	4	3	3	3	4	3	3	3	4	3	2	5	2
30	2	5	2	3	4	3	3	3	4	3	3	3	4	2	3	3	3	4	3	3	3	4	3	3	2	4	3	2	5	2
28	2	5	2	2	3	3	3	3	3	2	3	3	3	3	2	3	3	3	3	3	3	3	3	2	3	3	3	2	5	2
26	2	2	5	3	5	3	4	3	4	3	4	3	4	3	4	4	3	4	3	4	3	4	3	4	3	5	3	5	2	2
24	2	5	2	2	3	2	2	3	3	3	3	3	3	2	3	3	3	3	2	3	2	3	3	3	2	2	3	2	5	2
22	2	2	5	2	5	3	5	3	4	3	4	3	4	3	2	3	3	4	3	4	3	4	3	5	3	5	3	5	2	2
20	2	5	2	2	3	2	3	2	3	3	3	3	3	2	3	3	3	3	2	3	2	3	2	3	2	3	2	2	5	2
18	3	2	5	2	5	3	5	3	4	3	4	3	4	3	4	4	3	4	3	4	3	4	3	5	3	5	2	5	2	2
16		2	3	5	2	2	3	2	3	3	3	3	3	2	3	2	2	3	3	3	3	3	2	3	2	2	5	2	2	
14			3	2	5	3	6	3	5	3	5	3	4	3	2	2	3	4	3	5	3	5	3	6	3	5	2	3		
12			2	2	2	5	3	2	3	2	3	2	3	3	3	3	3	2	2	3	2	3	2	3	5	2	2	2		
10					3	2	5	2	5	3	5	3	5	3	4	4	3	5	3	5	2	5	2	5	2	3				
08						2	2	5	2	2	2	2	2	2	3	2	3	2	2	2	2	2	5	2	2					
06						2	3	3	5	2	5	2	5	2	2	2	2	5	2	5	2	5	3	3	2					
04								2	2	5	2	5	2	5	5	5	5	2	5	2	5	2	2							
02									3	2	2	2	2	2	2	2	2	2	2	2	2	3								

Figure 3.2. Core loading pattern cycle 2

The individual fuel bundle design for each fuel assembly is shown in Figure 3.3 through Figure 3.10, where the individual pin enrichment is shown, along with the rods containing the burnable absorber (BA) Gd_2O_3.

For the fuel assemblies of type 2 and type 3, the BA is not distributed over the entire fuel rod length. This is shown in Figure 3.5 and Figure 3.7. For the assemblies of type 4, 5 and 6, the BA is distributed over the entire fuel rod length. The figures are taken from [24].

wide-wide corner

2	1	1	1	1	1	1
1	1	1	2	1	1	1
1	1	2	2	2	2	1
1	2	2	2S	2	2	1
1	1	2	2	2	2	1
1	1	2	2	2	1	1
1	1	1	1	1	1	1

Rod type	U-235 (wt%)	Gd_2O_3 (wt%)	No. of rods
1	1.33	0	31
2	0.71	0	18

S=spacer positioning rod

Figure 3.3. Bundle design for Fuel Assembly type 1

The “wide-wide corner” presented in Figure 3.3 represents the corner where the control rod will be located. The wide-wide corner is also referred to as the northwest (NW) corner. The same analogy is used for the opposite corner, which is called the southeast (SE) corner. The control rods are always located in the NW corner, and the detectors are always located in the SE corner in the PHOENIX simulation.

wide-wide corner

4	3	3	2	2	2	2
3	2	1	1	1	1	2
3	1	5A	1	1	5A	1
2	1	1	1S	1	1	1
2	1	1	1	6B	1	1
2	1	5A	1	1	1	2
3	2	1	1	1	2	2

Rod type	U-235 (wt%)	Gd_2O_3 (wt%)	No. of rods
1	2.93	0	26
2	1.94	0	12
3	1.69	0	6
4	1.33	0	1
5A	2.93	3.0	3
6B	2.93	3.0	1

S=spacer positioning rod

Figure 3.4. Bundle design for Fuel Assembly type 2

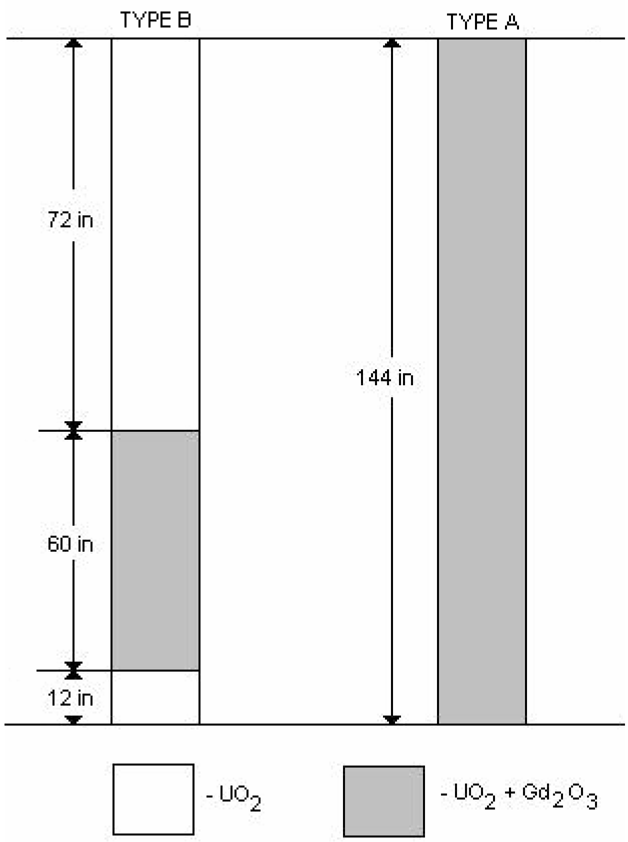

Figure 3.5. Axial variation of Burnable Absorber in Fuel Assembly type 2

wide-wide corner

4	3	3	2	2	2	3
3	8D	1	1	1	1	2
3	1	1	1	1	5A	1
2	1	1	6C	1	1	1
2	1	1	1	1	1	1
2	1	5A	1	1	7E	2
3	2	1	1	1	2	2

Rod type	U-235 (wt%)	Gd_2O_3 (wt%)	No. of rods
1	2.93	0	26
2	1.94	0	11
3	1.69	0	6
4	1.33	0	1
5A	2.93	3.0	2
6C	2.93	3.0	1
7E	2.93	4.0	1
8D	2.93	4.0	1

6C=spacer positioning rod

Figure 3.6. Bundle design for Fuel Assembly type 3

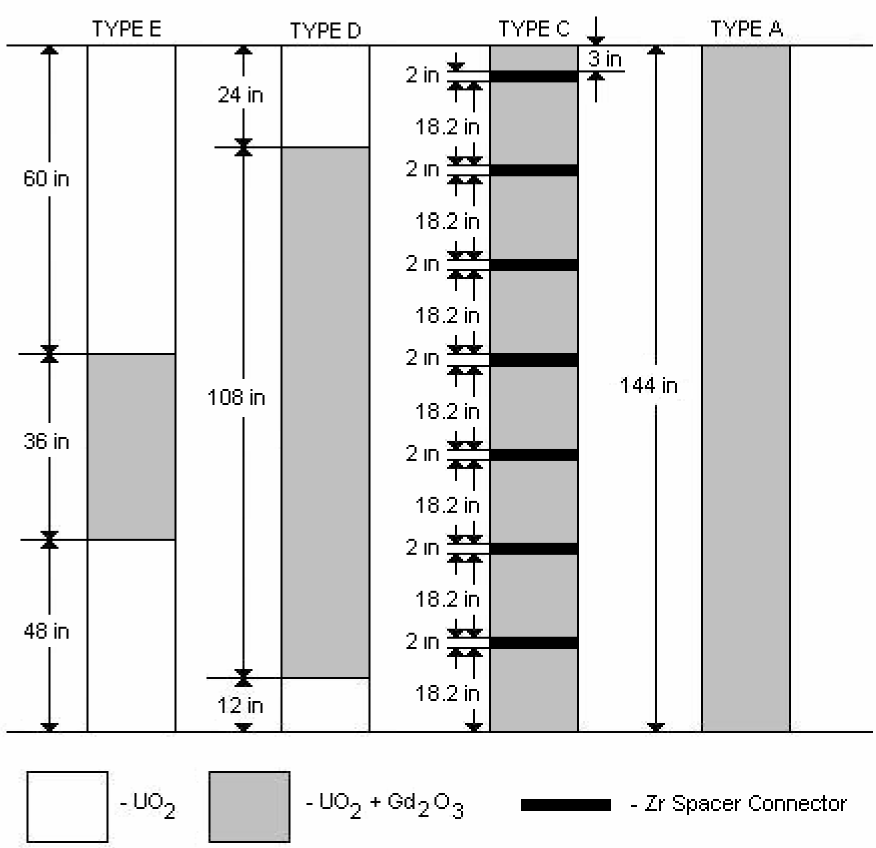

Figure 3.7. Axial variation of Burnable Absorber in Fuel Assembly type 3

wide-wide corner

4	3	2	2	2	2	2	3
3	2	1	5	1	1	1	2
2	1	1	1	1	1	5	1
2	5	1	1	1	1	1	1
2	1	1	1	WS	1	1	1
2	1	1	1	1	1	1	1
2	1	5	1	1	1	5	1
3	2	1	1	1	1	1	2

Rod type	U-235 (wt%)	Gd_2O_3 (wt%)	No. of rods
1	3.01	0	39
2	2.22	0	14
3	1.87	0	4
4	1.45	0	1
5	3.01	3.0	5
WS	-	-	1

WS=spacer positioning water rod

Figure 3.8. Bundle design for Fuel Assembly type 4

wide-wide corner

4	3	2	2	2	2	2	3
3	2	1	5	1	1	1	2
2	1	1	1	1	1	5	1
2	5	1	1	1	1	1	1
2	1	1	1	WS	1	1	1
2	1	1	1	1	1	1	1
2	1	5	1	1	1	5	1
3	2	1	1	1	1	1	2

Rod type	U-235 (wt%)	Gd_2O_3 (wt%)	No. of rods
1	3.01	0	39
2	2.22	0	14
3	1.87	0	4
4	1.45	0	1
5	3.01	2.0	5
WS	-	-	1

WS=spacer positioning water rod

Figure 3.9. Bundle design for Fuel Assembly type 5

wide-wide corner

4	3	2	2	2	2	2	3
3	2	1	5	1	1	1	2
2	1	1	1	1	1	5	1
2	5	1	1	WR	1	1	1
2	1	1	WS	1	1	1	1
2	1	1	1	1	1	1	1
2	1	5	1	1	1	5	1
3	2	1	1	1	1	1	2

Rod type	U-235 (wt%)	Gd_2O_3 (wt%)	No. of rods
1	3.01	0	38
2	2.22	0	14
3	1.87	0	4
4	1.45	0	1
5	3.01	2.0	5
WS	-	-	1
WR	-	-	1

WS=spacer positioning water rod
WR=water rod

Figure 3.10. Bundle design for Fuel Assembly type 6

The fuel rods in assembly type 6 have a length of 140 inches. The difference between type 6 and the other fuel types is that type 6 has an end plug containing natural uranium at the top and bottom. The bottom end plug is 4 inches long, and the top end plug is 6 inches long. Since the active fuel length is 144 inches, the assumption was made that fuel assembly 6 contained of the bottom 4 inch end plug, and the fuel rods of 140 inches. The top end plug containing natural uranium was not modeled, see Figure 3.11.

The different fuel assembly types are modeled separately in PHOENIX as individual fuel segment types. Assembly types 2, 3 and 6 are split up into several fuel segment types due to the variation in axial material composition. The fuel segment types are defined in the next section.

3.2 Definition of fuel segment types

In order to generate the cross section data, the different fuel segment types had to be defined. A fuel segment type is a detailed 2D radial cross section description of an assembly, including fuel pins, assembly boxes and water gaps, to which nodal data is associated.

Six different fuel assembly types were used in PB2 cycle 1 and 2. They are described by eleven different fuel segment types due to the variation in axial geometry and material compositions. The different fuel segment types are illustrated in Figure 3.11. The eleven unique axial layers are modeled according to Figure 3.3 through Figure 3.10.

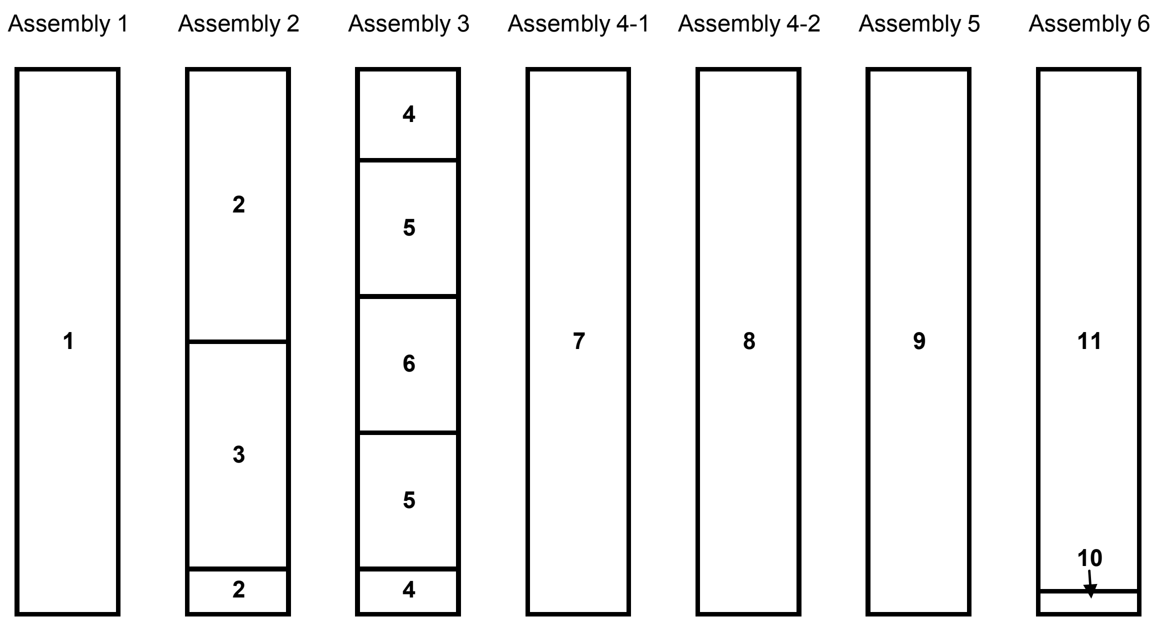

Figure 3.11. Definition of the different fuel segment types generated in PHOENIX

Separate cross section tables were generated for each fuel segment type and assembled in one cell data file using the Westinghouse program chain IFIGEN/PHOENIX/CoreLink/TABBE. The assumptions used and the calculations that were performed are explained in the next sections.

3.3 PHOENIX input data

In order to model the neutron transport in the fuel segment, each fuel segment type must be modeled with the corresponding geometries and masses.

For each fuel segment type, all the materials are modeled by their masses and densities. Examples of those are; the enrichment of the fuel, the contents of BA, materials in fuel cladding and fuel boxes, compositions of coolant, detectors, control rods and spacer grids, etc.

The geometry of the fuel assembly is described in the PHOENIX input. All the geometries of the pins, gaps and boxes etc. were given, as well as the geometries of the control rods and detectors. The position of each pin in the assembly was also input to PHOENIX.

In addition to the design data [24], PHOENIX requires a cross section library for the isotopes that are present in the considered design materials. The cross section library is a data base containing data for 308 materials [25], and is based on the ENDF/B-VI.

Some calculations are required of the design data before it can be input to PHOENIX. An example is the geometries of the fuel assemblies, which is described in the next section.

3.3.1 PHOENIX geometry representation

PHOENIX requires a certain geometry model for the fuel rods, assembly box, control rods and detectors. Some modifications are required to the original design data in order to get it into PHOENIX geometry. An example of a 7x7 assembly with PHOENIX geometry is shown in Figure 3.12. The calculations that were necessary for the inputs to PHOENIX were generated following the recommendations given in [10], [11], [22] and [23].

The average fuel temperature is a required input to PHOENIX. This is explained in the next section.

3.3.2 Fuel temperature

The average fuel temperature is used as a reference when generating the CD. A variation from the average fuel temperature is later modeled in IFIGEN. This is done in order to model the Doppler Effect in the CD tables.

The average fuel temperature for each fuel assembly was calculated as an input to PHOENIX. The Linear Heat Generation Rate (LHGR) was used in order to determine the average fuel temperature. The procedure is explained in [11] as

$$LHGR = \frac{0.96 \cdot Q}{M \cdot n \cdot l} \qquad (3.1)$$

where

Q - rated thermal reactor power, kW
M - number of bundles in core
n - number of fuel rods in each bundle
l - active length of fuel bundle, m

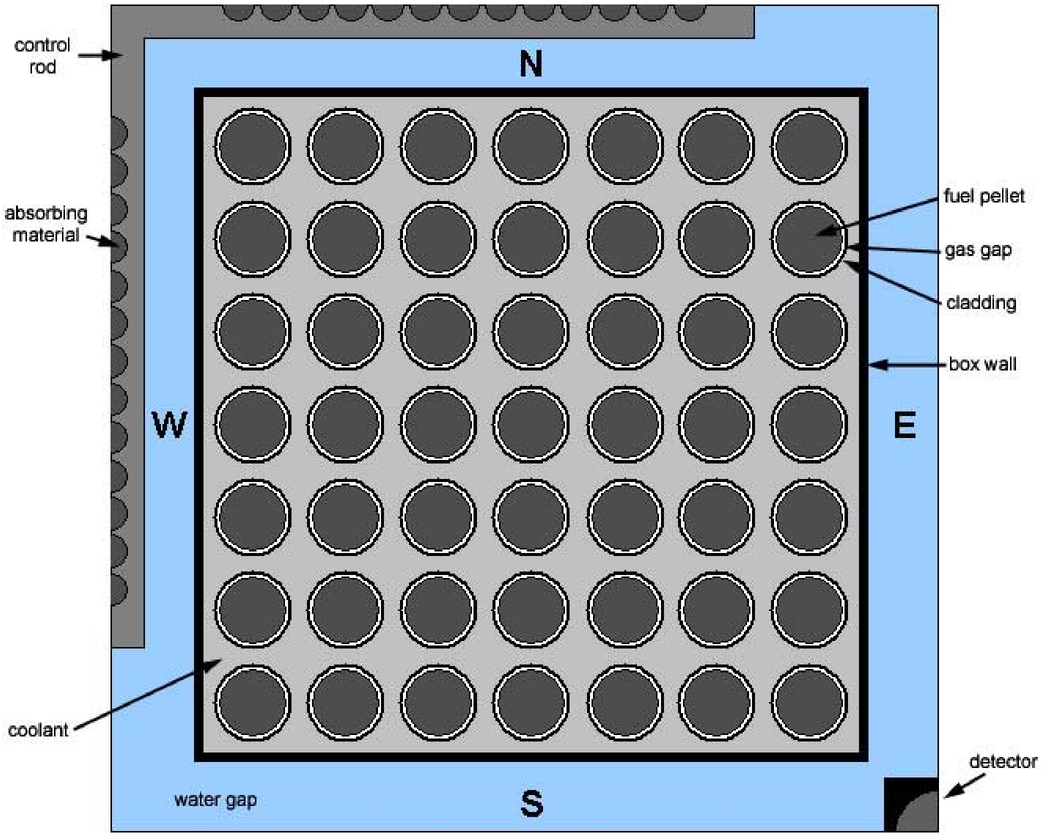

Figure 3.12. PHOENIX geometry model of a 7x7 assembly

The fuel temperature is found using equation (3.1) and a graph for the relation between the LHGR and average fuel temperature [11]. The calculated average fuel temperatures for cycle 1 and cycle 2 are presented in Table 3.2. During cycle 2, both 7x7 and 8x8 fuel assemblies were present, and hence the average number of active fuel rods in each bundle is used in the calculations.

The in-core flux detectors at PB2 during cycle 1 and cycle 2 were neutron detectors [24]. The neutron detectors are modeled in the SE corner in PHOENIX, and the calculations to model them in PHOENIX (Figure 3.12) are described in the next section.

Table 3.2. Average fuel temperature for cycle 1 and cycle 2

input data	**cycle 1**	**cycle 2**
Q, kw	3293000	3293000
M	764	764
n	49	52.44*
l, m	3.6576	3.6576
calculated:		
LHGR, kW/m	23.088	21.573
Tfuel, K	933	909

* average value in core

3.3.3 Detectors data

The neutron flux in the core during cycle 1 and cycle 2 of PB2 was detected by fixed Local Power Range Monitors (LPRM) and a Traveling In-core Probe (TIP) system. The LPRM and TIP system give a representation of the spatial distribution of the neutron flux in the water gaps in the core. The LPRM are fixed in the core, and are distributed evenly in 43 radial positions throughout the core and with 4 detectors axially. The TIP is a 1 inch long fission chamber containing U-235 which is connected to a cable and can be positioned in any axial position in one of the 43 detector strings [24].

The TIP system is used to give an accurate representation of the axial neutron flux distribution in the core. The TIP system is generally used approximately once per month in order to calibrate the LPRM. During transient situations, the TIP system is not used. The LPRM however are always located in the core, and are used to measure the neutron flux during transients. The LPRM positions and the TIP system arrangement are illustrated in Figure 3.13, where the 43 detector strings are shown. The core orificing is shown also in the figure.

When modeling the detectors in PHOENIX, some assumptions had to be made in order to get it into PHOENIX geometry. The location of the detector in the PHOENIX geometry model is shown in Figure 3.12. First of all, the fuel type with the smallest narrow gap (south and east gaps) had to be calculated (it turned out to be fuel 4-2, since it has the thickest box). This was because in PHOENIX the detectors, modeled with square geometry in the SE corner, cannot overlap the pin-cells; this would have generated an error. Another assumption needed was that the space between the pin cell and the detector needed to be at least 0.002 cm for numerical reasons [26].

The half thickness of the narrow gap was calculated to be 0.398 cm. The height and width of the detector with PHOENIX geometry was 0.398 - 0.002 = 0.396 cm. This size was modeled for all fuel types since the detector pin is assumed to have the same geometry for the entire core when modeled later in POLCA7.

The mass of the steel in the detector pin must be kept constant when changing the geometry to maintain the correct absorption cross section. The mass was kept constant by modifying the steel density when the area was changed.

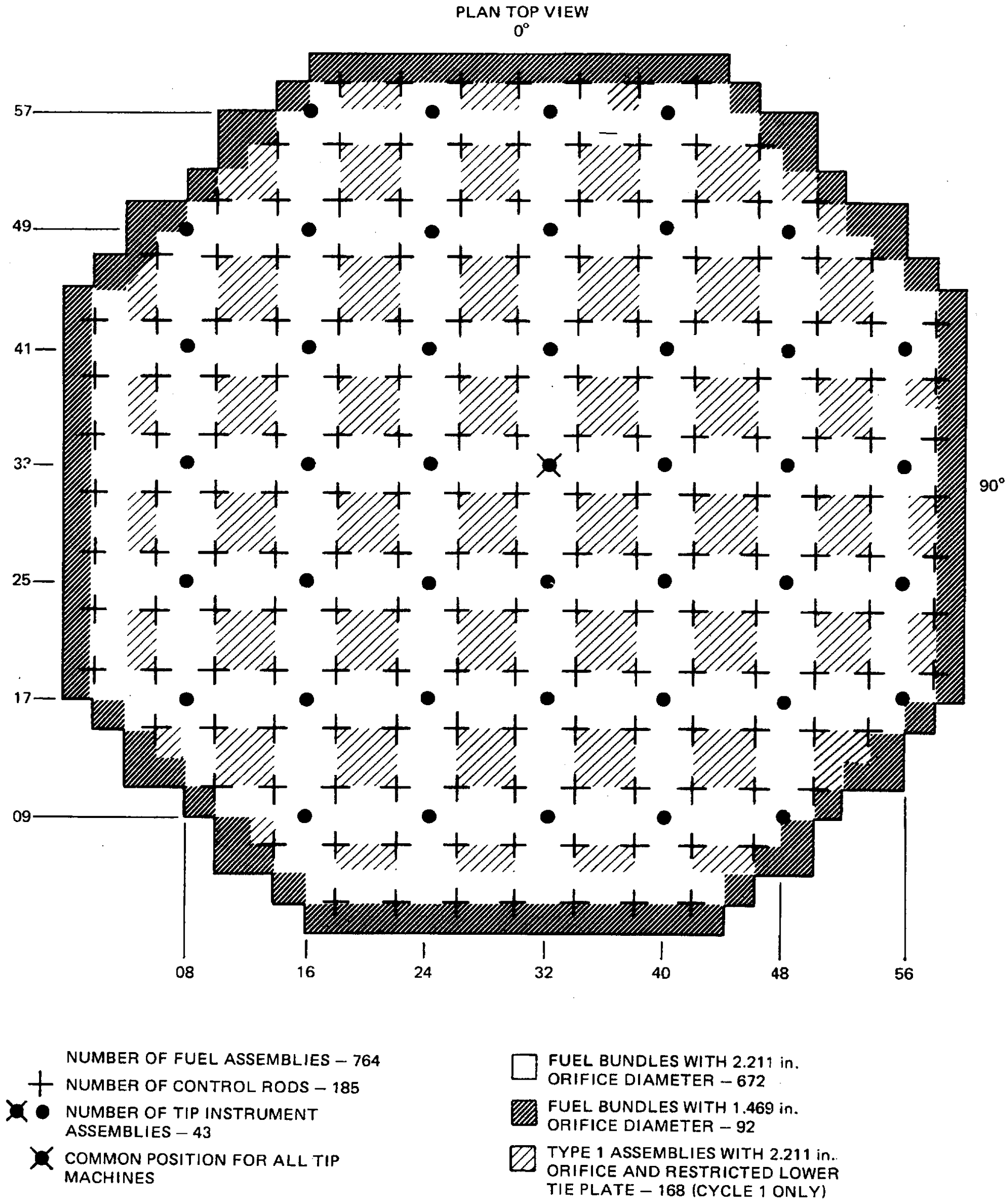

Figure 3.13. Core orificing and TIP system arrangement, [24] Figure 23.

3.3.4 Additional assumptions in the PHOENIX input data

The steel composition was assumed to be SS-type 304 as given in [24].

The formula for calculating the relative spacer grid area for the spacers in [11] was modified, because of the presence of Zircalloy in the spacers, to

$$A_{sg} = \frac{m_{inc} + m_{Zr-4}}{\rho_{avg} \cdot h_{sg}} \quad \text{where} \quad \rho_{avg} = \frac{(m_{inc} + m_{Zr-4}) \cdot \rho_{Zr-4} \cdot \rho_{inc}}{m_{inc} \cdot \rho_{Zr-4} + m_{Zr-4} \cdot \rho_{inc}} \tag{3.2}$$

and

A_{sg} - relative area of spacer grid, cm^2

m_{inc} - mass of Inconel in spacer grid, g

m_{Zr-4} - mass of Zircalloy-4 in spacer grid, g

ρ_{avg} - average density of spacer grid, g/cm^3

h_{sg} - height of spacer grid, cm

ρ_{inc} - density of Inconel, g/cm^3

ρ_{Zr-4} - density of Zircalloy-4, g/cm^3

The input values to equation (3.2) are given in Table 3.1.

The detector and the neutron absorbing material B_4C in the control rods were modeled using the compositions given in [11]. The steel in the control rods, and the water in the water paths of the control rods were homogenized into a mixture of steel and water. The steel-water mixture in the control rods was assumed to be the same as for the composition “BWR2/3/4 D-lattice” in [11]. The composition and geometry for the control rod-handle was extracted from KKL data, since there was no geometry data on the CR-handle in [2] or [24] for PB2.

In PHOENIX, all data necessary to generate the base case cross section tables are input. Base case means unrodded fuel, no spacers or detectors present, equilibrium xenon, nominal power density and reference coolant density etc. The data necessary to perform the branch calculations are input in IFIGEN, which is a pre-processor to PHOENIX. In IFIGEN code’s input data the depletion steps, boron contents, and coolant and moderator density histories are defined, along with the geometries for the control rods, spacers and the detectors. This is explained in the next section.

3.4 IFIGEN input data

IFIGEN is a pre-processor to PHOENIX where the data required to perform the branch calculations are defined. In IFIGEN the burnup steps, control rod and spacer presence, number of active coolant densities, fuel temperatures and xenon contents are defined in an operational matrix [10]. The operational matrix and the IFIGEN inputs are described along with some assumptions in the sections hereafter.

3.4.1 The operational matrix

In order to have a comprehensive overview of all necessary calculations in the CD generation process, IFIGEN uses an operational matrix that defines the following [10]:

- Burnup values where base tables are generated, and for which burnup values branch calculations should be performed.

- Number of active coolant density conditions (including branches) for which tables should be generated.

- For which burnup values branch calculations will be performed with control rod and/or spacer presence.
- The number of non-base boron conditions and fuel temperatures (for Doppler calculations).
- For which burnup values Xenon branch calculations should be performed.

Each of these parameters defined in the operational matrix are described further in the next sections.

3.4.2 Burnup steps

Base cross section tables are generated for several burnup values. This is done in order for the core simulator POLCA7 to be able to use the tables for any burnup value and interpolate the corresponding cross sections. Branch calculations are made for all, or some selected burnup steps. All the burnup values are defined in the matrix, and according to Westinghouse methodology the cross section tables are generated in a span from 0 MWd/t to 70 000 MWd/t, with burnup steps no larger than 2 000 MWd/t between the generated tables [11]. In the low burnup region, the burnup steps are 500 MWd/t in order to model the fast burnup of the BA accurately.

3.4.3 Coolant density histories

The base cross section tables are generated for a reference coolant density, which is the active coolant density at a specified void. Branch calculations are also performed to generate tables for conditions other than the reference case.

The reference coolant density used to generate the base tables is specified in [11] as:

- 40 % void at saturated conditions for a pressure of 70 bars (286 °C).

The branch tables are generated for the following conditions:

- 0 % void at 20 °C subcooled conditions (266 °C) for a pressure of 70 bars.
- 20 % void at saturated conditions for a pressure of 70 bars.
- 60 % void at saturated conditions for a pressure of 70 bars.
- Subcooled conditions, 20 °C at 1 bar pressure.
- Subcooled conditions, 80 °C at 1 bar pressure.
- Subcooled conditions, 160 °C at 70 bars pressure.

The last three cases are zero-power conditions. These tables are used in zero power calculations, and in Doppler calculations [10].

3.4.4 Control rods and spacers

The base tables are generated for unrodded fuel assemblies, which means that the control rod is withdrawn. Branch calculations are performed for cases with an inserted control rod for the specified burnup values.

The same is applied for spacer grids. The base tables are generated without spacer grid presence. Branch calculations are again performed for cases with spacer grid presence.

3.4.5 Boron contents and Doppler temperature

The base tables are generated with a boron content of 0 ppm. One non-base boron condition is calculated and the boron variation is assumed to be 1000 ppm according to [11]. Branch calculations are performed at the specified burnup values in order to model the boron content.

In order for the core simulator to model the Doppler effect, one variation from the base fuel temperature is tabularized. The base value for the fuel temperature was calculated for the PHOENIX input and was 933 K and 909 K for cycle 1 and cycle 2 respectively. The recommendation in [11] is that the Doppler variation should be $T_f^{base} + 400K$, where T_f^{base} is the base value for the fuel temperature for each cycle. However, in this case the Doppler variation was set to 1199 K, when the recommendations were that it should be less than 1200 K due to numerical reasons [11].

3.4.6 Xenon branches

The base cross section tables are generated assuming equilibrium xenon. Branch calculations are performed to generate tables with zero xenon. This is done in order to model the indirect and most important effect that xenon has on the neutron spectrum (called xenon spectrum effect).

Xenon has an extremely large absorption cross section. The neutron absorption changes considerably when the xenon number density deviates from its equilibrium. The secondary effect of this is the neutron spectrum that changes and this in turn affect all fissionable isotopes' cross sections. The dependence of the xenon on the neutron spectrum is close to linear.

Tables are generated for equilibrium xenon at rated conditions and for zero xenon. By doing this, all deviations from the xenon equilibrium state can be modeled for the cross sections of the fissionable isotopes [28].

3.5 Calculation procedure

The calculations when generating the CD tables are divided in two major steps, illustrated in Figure 3.14 for a single coolant density history. First of all a depletion case for each single coolant density is performed for the base conditions. At certain burnup values the calculated data is saved. The saved data represents the base conditions for the coolant density at the specified burnup.

In the second step, the saved data is used in a restart where branch calculations are performed for each off-base case that is specified in the matrix. For the branch calculations, no further depletion is performed.

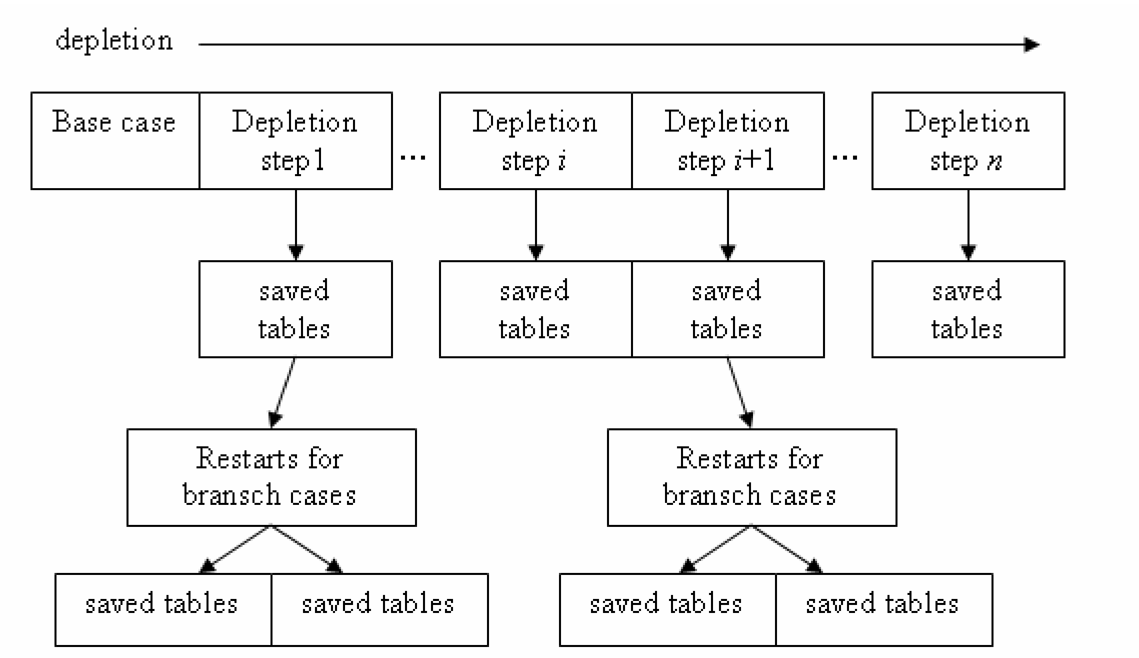

Figure 3.14. Calculation procedure for a single coolant density history

3.6 Results of cross section calculations

The results from the calculations are multiple cross section tables with dependencies in the three state parameters: fuel exposure, coolant density history, and reference coolant density. The results also include pin maps that contain the enrichment and BA content in the fuel pins, the pin power and exposure. The cross section tables are generated for all eleven different fuel segment types, and put into one binary CD file using the Westinghouse code TABBE [12]. The reflection of neutrons escaping the core is not modeled in PHOENIX. The neutron reflection is treated specially and is described in the next section.

3.7 Reflector data

Neutrons that escape the core are slowed down and/or reflected in both the radial and axial direction. Two different methods can be applied to model the neutron reflection, either by explicit reflectors which are represented as material regions, or by albedo boundary conditions. A common practice is to use explicit reflectors for the radial reflection, and albedo boundary conditions for the axial reflection. In this specific case generic BWR reflectors CD were used for the radial reflector region and albedo boundary conditions for the top and bottom of the core according to [29].

3.8 Conclusions

The CD was generated using Westinghouse methodology. The data will be used in the depletion calculations for PB2 cycle 1 and 2, and tested by means of steady state calculations. Finally the data will be used in the transient calculations. The CD takes into account xenon number density, fuel exposure and historical and instantaneous coolant density dependencies explicitly, as is required by the 3D core simulator POLCA7.

4 DEPLETION CALCULATIONS

During the operation of a nuclear power plant the initial isotopes are depleted, and some isotopes are built up and then depleted. The TT2 test was performed at the EOC 2. In order to model the state prior the TT2 test correctly, depletion calculations were performed to obtain the actual distributions of isotopes in the core.

The depletion calculations were performed by modeling the operational states during cycle 1 and cycle 2 using POLCA7 and is described in the next section. The process parameters used for the calculations were taken from figures 63-100 in [24].

The accuracy of the depletion calculations was checked by performing steady state power calculations at the end of cycle 1 and cycle 2, using instantaneous process parameters given in [24]. The calculated TIP response by POLCA7 was then compared to the measured TIP signals. The results of the depletion calculations are presented in section 4.2.2 for cycle 1 and section 4.4.1 for cycle 2.

4.1 Process parameters and input data

The process and input parameters of PB2 cycle 1 and 2 used for the POLCA7 depletion calculations are presented in this section. The rated conditions of PB2 are presented in Table 4.1 (Table 3.1.1.3 in [2]).

Table 4.1. Peach Bottom 2 rated conditions

Parameter	Value
Core thermal power, MW	3 293
Core total flow rate, kg/s	12 915
Bypass flow rate, fraction of total core flow	Figure 4.7
Fraction of core thermal power passing through fuel cladding	0.96
Approximate bypass coolant total power fraction	0.02
Approximate active coolant total power fraction	0.02
Rated reactor dome pressure, MPa	7.033
Rated core pressure, MPa	7.1361
Core pressure drop at rated conditions, MPa	0.1517
Core inlet enthalpy, kJ/kg	1212.5
Average enthalpy rise across core, kJ/kg	254.91
Reactor average exit quality	0.129
Design hot channel active coolant exit quality	0.25
Design bypass exit quality	0
Total feedwater flow rate, kg/s	1 679.70
Feedwater temperature, °C	191.17

4.1.1 Process parameters for cycle 1 and 2

The process parameters core thermal power, total number of inserted CR notches, total flow and core inlet subcooling for the two cycles were used as input data to POLCA7 in order to repeat the operational conditions at PB2. The process parameters are given in figure 63-100 of [24] as daily average values. These parameters were used when calculating the POLCA7 input process parameters for each burnup step and are plotted in Figure 4.1 and Figure 4.2 for the entire cycle 1 and cycle 2 respectively. The process parameters were converted in SI units and tabulated in Appendix 1 as daily average values.

The depletion calculations were performed in 43 steps for cycle 1 and 22 steps for cycle 2. The local burnup is affected by the CR positions, the flow rate, core inlet coolant subcooling and power level. The process parameters shown in the figures below were processed in order to get input data for the depletion calculations, and are described in the next section.

4.1.2 Input data

The steps for which the depletion calculations were performed had to be smaller than 1 MWd/kg in order to model the local burnup properly [28]. During each burnup step, the process parameters power, total flow, core inlet subcooling and the number of inserted CR notches were integrated and averaged. The average core thermal power for a burnup step is calculated as follows:

$$Q_{avg} = \frac{1}{\Delta t}\int_{t} Q\,dt \tag{4.1}$$

where

Q_{avg} - Averaged core thermal power for the burnup step, MW

Q - Daily average core thermal power, MW

Δt - Time for the burnup step, h

The inputs to the equation above are the daily average values from figure 63-100 of [24] (tabulated in Appendix 1). The same procedure is used when calculating average flow, inlet subcooling and average number of inserted CR notches for the burnup step. All the calculated parameters for input to POLCA7 are found in Appendix 2.

The CR positions are described by the number of notches *withdrawn* in the CR configuration maps (data set 01 – 37 in [24]), where one notch is equal to 3 inches. The physical notches at PB2 were 6 inches apart; hence the number of withdrawn notches was always even [24].

The CR positions changes many times between the measured data sets due to power regulations, sudden shutdowns and changes of CR sequences. In the data summaries in [24] figures 63-100, only the total number of *inserted* CR notches is given for each day. The exact CR configuration is only given for the data sets. For the burnup steps where the CR configuration is not given, the CR positions must be derived using CR sequences. The CR sequence groups A and A2 are shown in Figure 4.3, where the 185 control rods are divided in 21 groups. The CR positions can be assumed according to the CR sequence groups that are defined in [24], figures 56-61. The sequence groups are ordered, so CR groups with high sequence numbers are inserted first and CR groups with low sequence numbers withdrawn first. Using this knowledge, the actual CR positions were derived.

The exact position of each control rod in the core for each burnup step is given in Appendix 2.

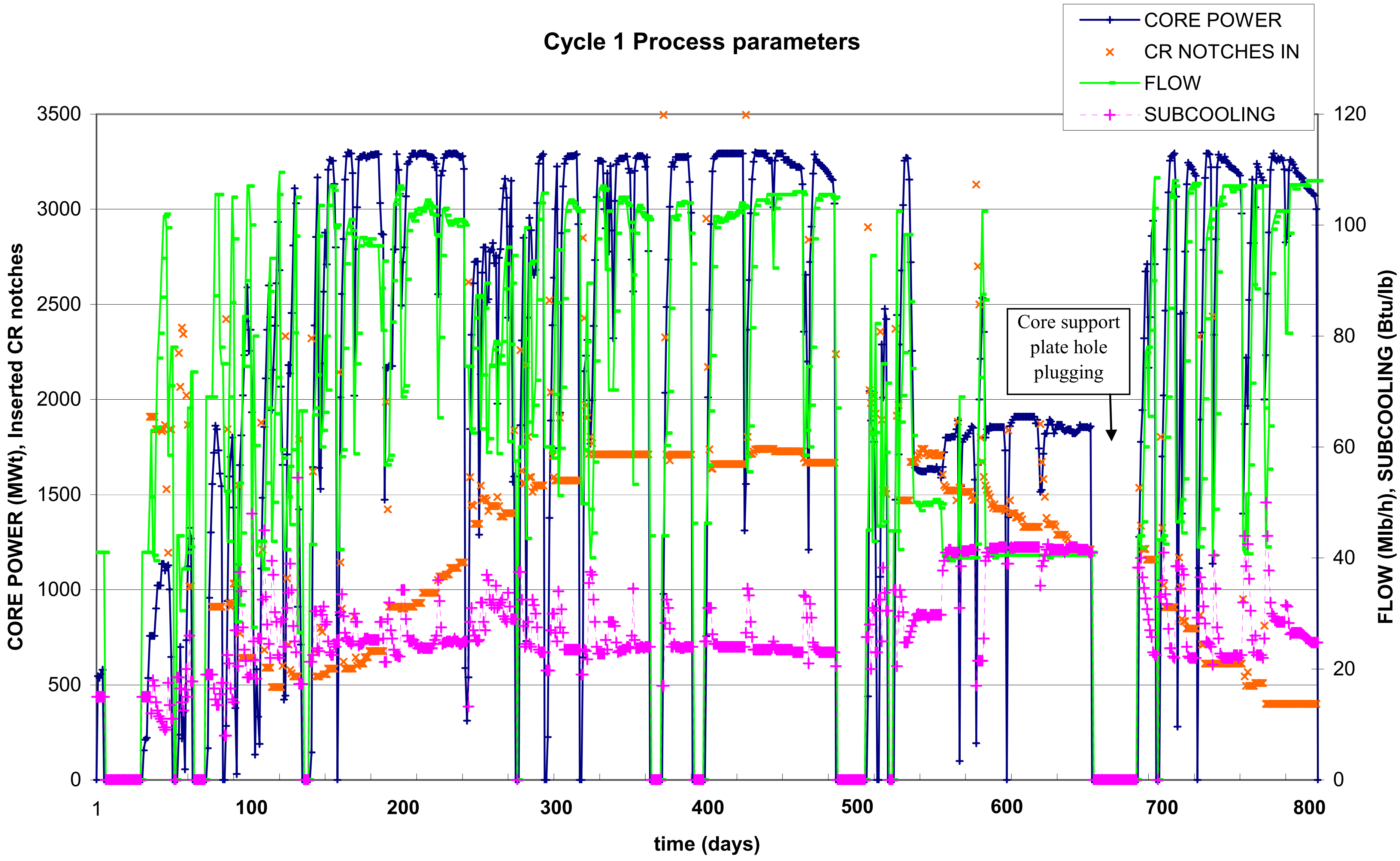

Figure 4.1. Data summaries for process parameters at PB2 during cycle 1

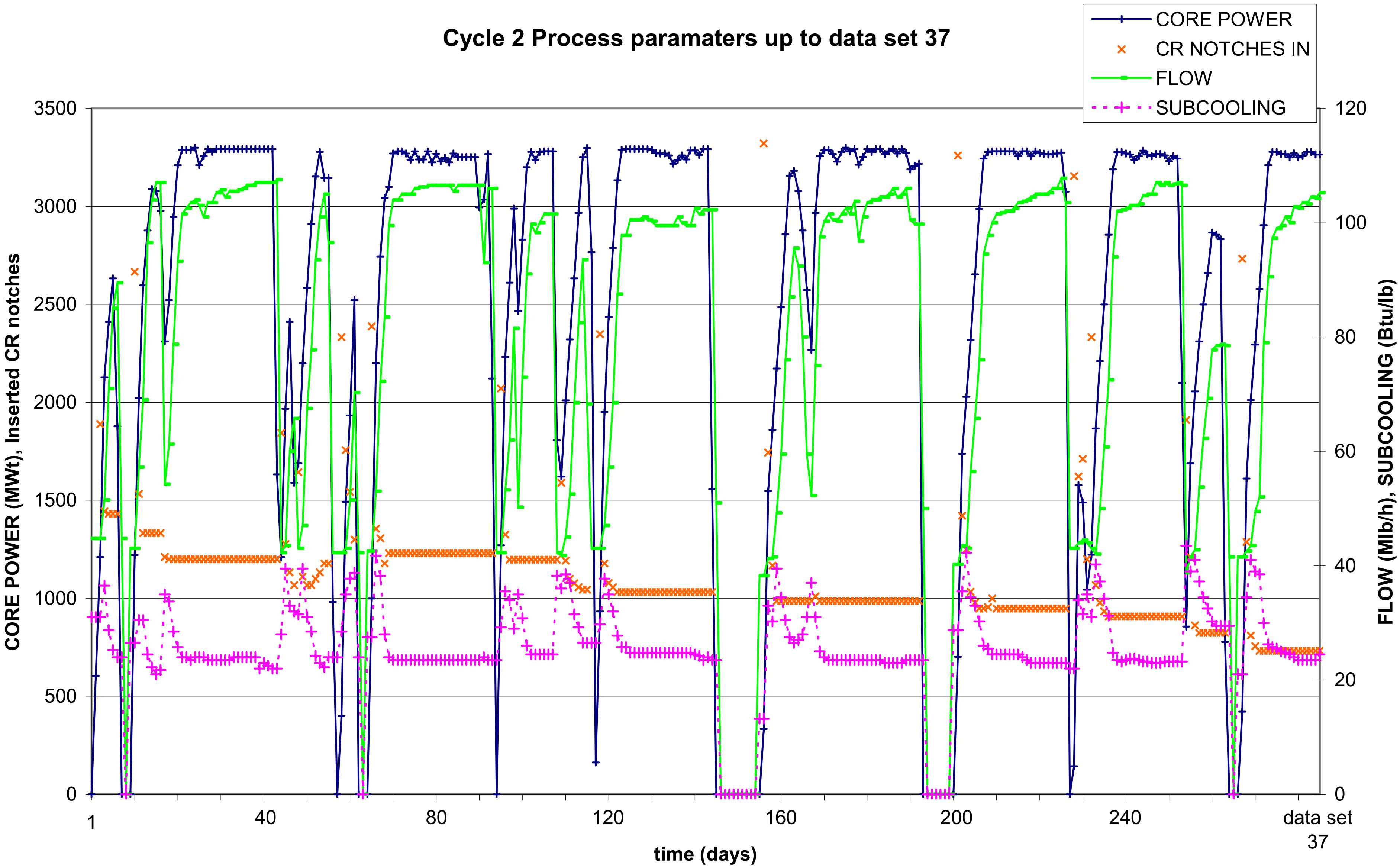

Figure 4.2. Data summaries for process parameters at PB2 during cycle 2 to data set 37

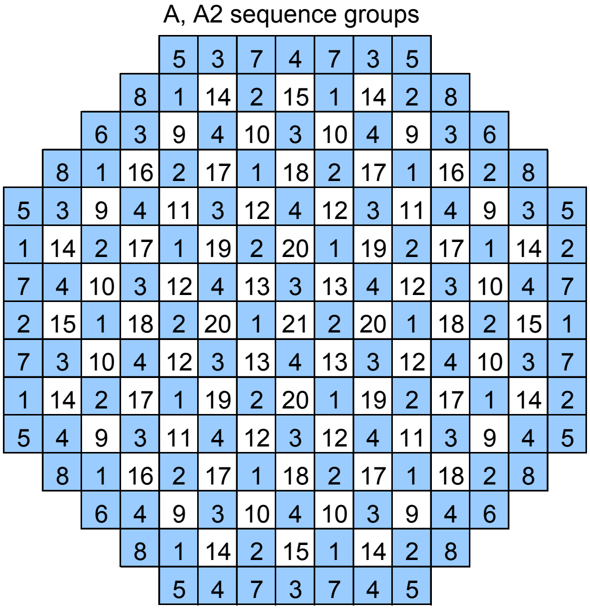

Figure 4.3. Control rod sequence groups A and A2 at Peach Bottom 2

The burnup steps must also be calculated, and can be expressed in terms of burnup or time units, either as MWd/kg or Effective Full Power Hours (EFPH) as shown in the following equations respectively [30]:

$$\Delta E_{core} = \frac{Q_{avg} \cdot \Delta t}{m_{tot} \cdot 24} \qquad (4.2)$$

$$\Delta t_{EFPH} = \frac{Q_{avg} \cdot \Delta t}{Q_{nom}} \qquad (4.3)$$

These two equations are related as

$$\Delta E_{core} = \frac{Q_{nom} \cdot \Delta t_{EFPH}}{m_{tot} \cdot 24} \qquad (4.4)$$

where

ΔE_{core} - Burnup step, MWd/kg (“d” stands for days)

Δt_{EFPH} - Burnup step, EFPH

m_{tot} - Mass of initial heavy nuclides for all fuel bundles, kg

Q_{nom} - Nominal core thermal power, MW

Q_{avg} - Averaged core thermal power for the burnup step, MW

Δt - Time for the burnup step, h

The burnup steps decide the burnup range for which the core was depleted using the specified process parameters. When significant changes were made in the operation, new operational parameters were used for the next step in the depletion calculations. An example of this is illustrated in Figure 4.4 below.

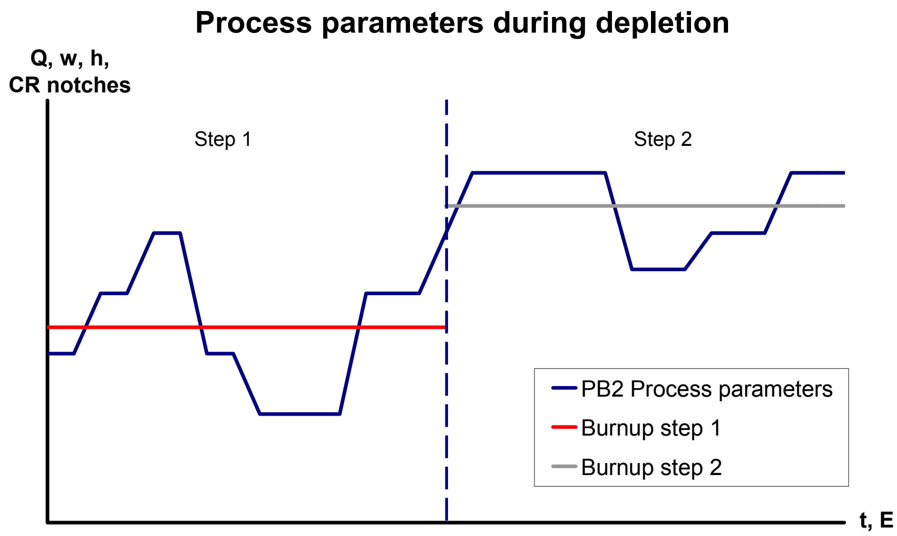

Figure 4.4. Calculation of process parameters for depletion calculations

The burnup step size was calculated as EFPH when performing the depletion calculations by using equation (4.3). The averaged process parameters for core power, flow, subcooling, CR notches used as POLCA7 input data in the depletion calculations are shown in Appendix 2 along with the calculated EFPH for each step.

4.1.3 POLCA7 models and options used and investigated

Some of the parameters used as input data to the depletion calculations involve certain uncertainties. In order to check the sensitivity to some parameters and calculation options in POLCA7, several different cases were performed for the depletion calculations. The parameters and options that were studied and varied were the Dittus-Boelter heat transfer coefficient, the fuel Doppler temperature, the option for describing the bypass flow, and parameters describing leakage flow through leakage path 1. These parameters and options are described in more detail in sections 4.1.3.1- 4.1.3.4.

Eight different cases were performed in the depletion calculations. However, only four of them were found to be valuable. They are described in section 4.2.1. The cases represent different combinations of the above mentioned parameters and options.

4.1.3.1 <u>Dittus-Boelter heat transfer coefficient</u>

The Dittus-Boelter correlation is used to calculate the single-phase heat transfer coefficient between the fuel wall and the liquid coolant

$$\mathrm{Nu} = C_{DB}\,\mathrm{Re}^{0.8}\,\mathrm{Pr}^{0.4} \tag{4.5}$$

Where Nu, Re and Pr are Nusselt, Reynold and Prandtl numbers respectively and C_{DB} is a constant that for the best-estimate correlation for turbulent flow is $C_{DB} = 0.023$, [31], [32]. This is also the default value for the constant in POLCA7 [13].

From equation (4.5) the heat transfer coefficient H_{DB} is obtained as:

$$H_{DB} = C_{DB}\frac{G^{0.8}}{D_h^{0.2}}\left(\frac{c_p}{\mu_l}\right)^{0.4}\lambda_l^{0.6} \tag{4.6}$$

The other parameters in the equation are:

G - mass flux, kg/(m^2·s)
D_h - hydraulic diameter, m
c_p - heat capacity of liquid coolant, J/(kg·K)
μ_l - dynamic viscosity of liquid coolant, kg/(m·s)
λ_l - liquid conductivity, W/(m·K)

Two different values were used for C_{DB} in the calculations. Both the default $C_{DB} = 0.023$, and also $C_{DB} = 0.030$ which was used in previous validations and is recommended in [32] when using subcooled boiling correlation EPRI [32],[33]. In the present validation the Levy subcooled boiling correlation was used [32],[33]. The reason for using $C_{DB} = 0.030$ was that using $C_{DB} = 0.023$ generated bypass void in the calculations when combined with certain options. The bypass void did not occur when using $C_{DB} = 0.030$ in these cases. These results are not physical and the bypass void is explained in detail in section 4.1.4. For the final case, the default value $C_{DB} = 0.023$ was used.

The influence of the Doppler temperature was also studied in the depletion calculations, and is described in the next section.

4.1.3.2 Fuel Doppler Temperature

During a pressure increase transient in a BWR, the boiling of the coolant after the void collapse has the main influence on the negative reactivity feedback. A secondary and smaller effect during a pressure increase transient on the reactivity feedback is the Doppler Effect. When the fuel temperature increases, more neutrons are absorbed and give a decrease in reactivity.

In the CD generation process, the fuel temperature was 933 K for 7x7 fuel and 909 K for 8x8 fuel. A new set of CD was generated that had a fuel temperature of 750 K for all fuel segment types. The CD with fuel temperatures 933 K for 7x7 fuel and 909 K for 8x8 fuel, and the CD with fuel temperatures 750 K for all fuel types, were used in different runs to see the influence of the Doppler temperature on the calculated axial power. However both sets showed no differences in results and for the final calculations the CD set with fuel temperatures 933 K and 909 K was used.

The flow in the bypass channel can be specified in POLCA7 in two different ways by using two different options. Both options were used in the calculations and are described in next section.

4.1.3.3 Bypass flow

In the BWR core the coolant flow is separated into active coolant flow and bypass flow. Active coolant flow is the water that directly cools the fuel rods inside the fuel assemblies. The inter assembly water flow and the flow inside the water pins is called bypass flow. The amount of the total flow that goes into the bypass is determined by the leakage from the main channel to the bypass.

In GE BWR/4 reactors with 7x7 and 8x8 fuel, two different leakages appear as shown in Figure 4.5; one between the main channel before the orifice inlet and the core support plate (leakage path 1), and the second (leakage path 2) from the main channel into the bypass before the lower tie plate [13]. In the 8x8 fuel with water pins, a part of the coolant flow goes into the water pins also.

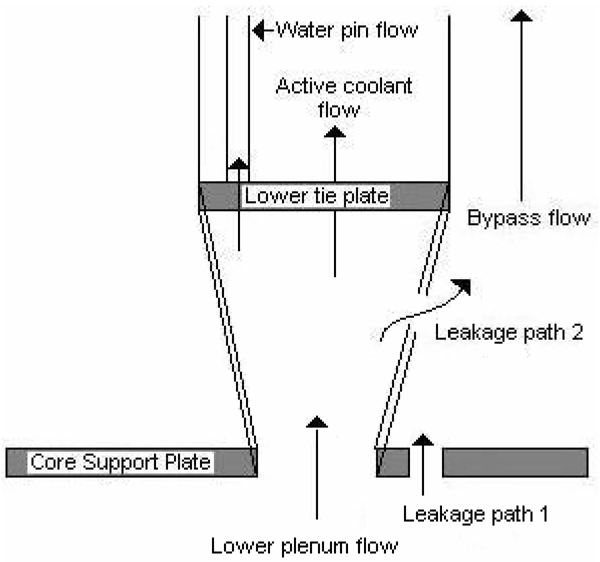

Figure 4.5. Coolant and bypass flow in a fuel assembly

The fraction (expressed as a percentage) of the total core flow that goes into the bypass can be specified in POLCA7 in two different ways. One option is to specify one value for the bypass flow fraction that will stay constant in the thermal hydraulic iterative process. The other option is to specify a minimum and a maximum bypass flow fraction (SPLMIN and SPLMAX). With this information, the initial guess of the bypass flow fraction used in the iteration process is found according to Figure 4.6 in POLCA7. The two different options will not necessarily calculate the same final result for the bypass flow.

Both options were used in the depletion calculations. The option where POLCA7 guess the initial bypass flow fraction, and improves it by iteration was used in the final calculations. The reasons for this are elaborated in section 4.1.4.

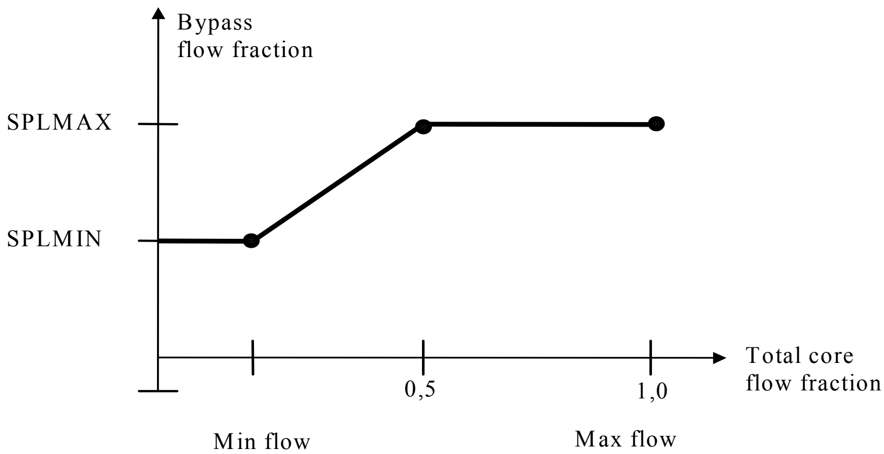

Figure 4.6. POLCA7 method for determining initial guess of bypass flow. [13] p. 150

During the first part of cycle 1, holes were drilled in the core support plate increasing the bypass flow fraction. The holes in the core support plate would increase the flow area of leakage path 1. The plant was shutdown and the holes in the core support plate were plugged in November of 1975 (see Figure 4.1). After the core support plate holes plugging, the leakage of the total flow into the bypass channel was decreased. During cycle 2, 8x8 fuel assemblies were added, which changed the leakage areas due to the different dimensions of the fuel and the waterpins, which did not exist in the 7x7 fuel, and hence affected the bypass flow fraction.

Three different relations between total flow and bypass flow appear for cycle 1 and 2:

1. Cycle 1 with 7x7 fuel assemblies before core support plate holes plugging.

2. Cycle 1 with 7x7 fuel assemblies after core support plate holes plugging.

3. Cycle 2 with 7x7 and 8x8 fuel assemblies.

When the option of specifying the bypass flow fraction explicitly in POLCA7 was used, the three different situations were modeled separately for the different parts of the depletion calculations. This was done in order to model the correct bypass flow fraction. The core bypass flow rate is expressed as a function of total core flow in fig. 54-55 of [24], reproduced below in Figure 4.7. The three lines represent cases 1, 2 and 3 respectively.

From these figures, the bypass flow fraction was calculated as a function of total core flow rate. This function was then used in the bypass flow fraction calculations for each burnup step.

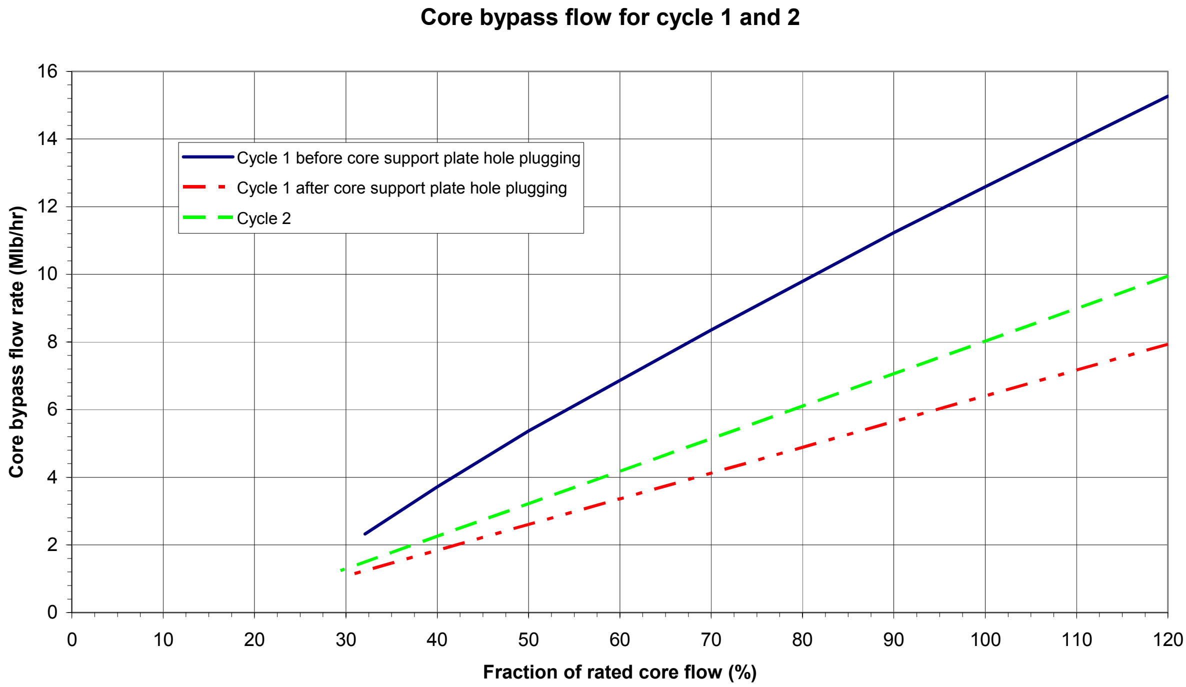

Figure 4.7. Core bypass flow rate for cycle 1 and 2. [24] figures 54-55

After the core support plate holes plugging during cycle 1, and during cycle 2, there was a linear dependence between the core bypass flow rate and the fraction of rated core flow. From this, the bypass flow fraction was expressed as a function of the total core flow rate:

$$w_{bp,\%} = \frac{(c_1 \cdot w_{tot} + c_2) \cdot 126}{w_{tot}} \cdot 100 \qquad (4.7)$$

where $c_1 \cdot w_{tot} + c_2$ describes the linear function with the constants c_1 and c_2 and

$w_{bp,\%}$ - bypass flow fraction of total flow, %

w_{tot} - total core flow, kg/s

$w_{bp,i,Mlb/hr}$ - core bypass flow rate from Figure 4.7, Mlb/hr

$w_{tot,i,kg/s}$ - core total flow from Figure 4.7, kg/s

126 - conversion factor from Mlb/hr to kg/s

However, for case 1, before the core support plate holes plugging during cycle 1, there was not a linear dependence between the core bypass flow rate and the fraction of rated core flow as seen in Figure 4.7. The approach in this case was to select certain points in Figure 4.7 and interpolate linearly between these points. Due to this, several linear functions were obtained. For each of those linear functions, equation (4.7) was applied to calculate the bypass flow fraction. The results of the calculations are shown in Figure 4.8 and Table 4.2.

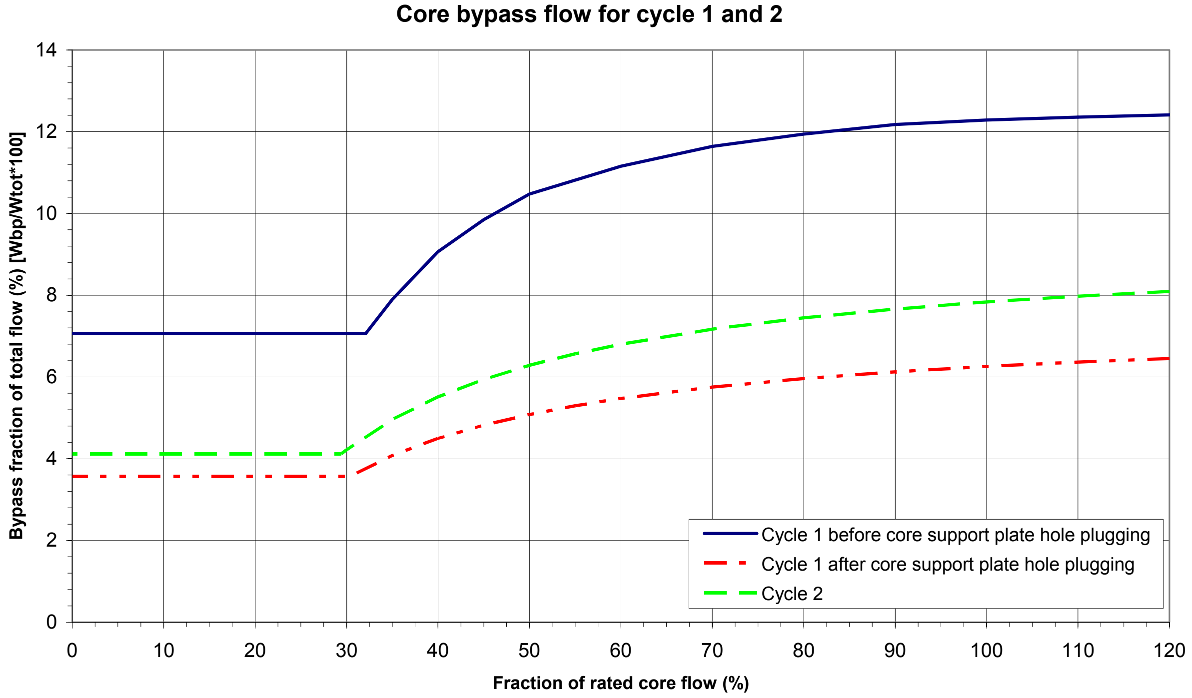

Figure 4.8. Core bypass flow fraction for cycles 1 and 2

Table 4.2. Constants for equation (4.7)

case	valid for flow range: (% of rated flow)	c1	c2
1	32.1 - 40.0	0.001364	-3.331923
	40.0 - 50.0	0.001281	-2.904110
	50.0 - 70.0	0.001154	-2.082192
	70.0 - 90.0	0.001116	-1.736986
	90.0 - 100.0	0.001052	-0.997260
	100.0 - 120.0	0.001035	-0.778082
2	30.3 - 120.0	0.000589	-1.200414
3	29.4 - 120.0	0.000744	-1.584851

The last parameters that were investigated were the leakage path 1 area and loss coefficients and are described in the next section.

4.1.3.4 <u>Leakage path 1 area and loss coefficient</u>

A sensitivity study was performed on the area and flow loss coefficient of leakage path 1. The reason for performing this sensitivity study was that the value of this area is not well known. When the core is loaded, there are some leakages between the fuel assemblies and the core support plate through which coolant flows. The value of the leakage path 1 area and its loss coefficient depends on the core support plate and fuel assemblies manufacture tolerances and roughness of their surfaces. For these reasons both parameters have very high uncertainty.

4.1.4 Sensitivity study of bypass flow options and leakage path 1 area and loss coefficient

In the very first depletion cases bypass void occurred that were for some depletion steps as high as 16%. This is not realistic and some investigation had to be made in order to realize why the high bypass void occurred. A sensitivity study was performed where the two different options of describing the bypass flow fraction were tested, along with the influence of the leakage path 1 area and loss coefficient.

The bypass flow fraction can be specified explicitly in POLCA7. This is done by setting the input parameter `SPLFIX` > 0. If the input parameter `SPLFIX` = 0, the bypass flow fraction is calculated by POLCA7.

The leakage flow into the bypass through leakage path 1 (w_{leak1}^{CSP}) is calculated as:

$$w_{leak1}^{CSP} = s_{bp}^{0} \cdot w_{tot} \tag{4.8}$$

where s_{bp}^{0} is the bypass flow fraction, and w_{tot} is the total flow in kg/s

When `SPLFIX` = 0, s_{bp}^{0} is initially guessed according to Figure 4.6, and is later improved in an iterative process [33]. In the iterative process the distribution of the coolant between the active channels and the bypass is adjusted to fulfill the criteria that the pressure drop over all channels is equal. When the flow distribution is determined, the leakage flow through the core support plate is calculated according to equation (4.8). This flow is used when calculating the pressure drop over the core support plate.

When `SPLFIX` > 0, s_{bp}^{0} is set to that specific value, and stays constant in the iterative process. In this case, w_{leak1}^{CSP} is not calculated to satisfy the flow distribution criteria. Consequently, POLCA7 does not calculate the pressure drop over the core support plate properly (see Figure 4.9). If the calculated pressure drop is too large, the pressure in the bypass will be too low. This in turn leads to a low saturation enthalpy in the bypass, and a bypass steam quality that is too large. This is the reason for the high bypass void when using `SPLFIX` > 0.

The loss coefficient ξ_{leak1} affects the bypass flow in the case when `SPLFIX` = 0, when it is used in the iterative process of finding the flow distribution [33]. In both cases for the `SPLFIX` input, the pressure drop is affected by ξ_{leak1}.

A sensitivity study was performed to see the influences of the loss coefficient and `SPLFIX` on the results. The loss coefficient ξ_{leak1} is called `L1RC` in the POLCA7 input. The values used for `L1RC` in the study were 1900, 240 and 80. The values for `SPLFIX` were 7.8574 and 0.0. In the study the PSU CD was used and the TT2 initial steady state process parameters (Table 5.1). The results are shown in Table 4.3. The value of `L1RC` in the first sets of depletion calculations was 1900, which was considered to be too large to be realistic [27], [34].

Steady state calculations were also performed using POLCA-T with PSU CD for the TT2 initial conditions to compare the results and get a better understanding of the source of the high bypass void. POLCA-T uses a more advanced thermal hydraulic model, and the calculated pressure drop over the core support plate was reasonable. This in turn predicted a much lower bypass void than POLCA7. The results below and the results from the POLCA-T calculations showed that the high predicted void in the bypass came from using the calculation option where the bypass flow was given explicitly.

Table 4.3. Sensitivity study on bypass flow fraction and leakage path 1 loss coefficient

L1RC **SPLFIX**	**1900** **7.8574**	**1900** **0.0**	**240** **7.8574**	**240** **0.0**	**80** **7.8574**	**80** **0.0**
Bypass flow (% of total)	7.86	8.12	7.86	12.04	7.86	16.08
Bypass outlet void (%)	15.37	2.95	5.03	0.00	0.00	0.00
Keff	0.99860	1.00286	1.00271	1.00126	1.0032	0.99923
Power Peaking Factor total	2.286	2.261	2.277	2.226	2.273	2.190
Power Peaking Factor radial	1.470	1.459	1.465	1.461	1.465	1.462
Power Peaking Factor axial	1.482	1.480	1.483	1.456	1.481	1.430
Axial Offset (%)	3.00	10.99	10.19	10.35	11.10	9.31
Core average void	33.50	31.74	31.81	32.92	31.59	34.33
dP (active channels - bypass) in node 1 (MPa)	0.2509	0.0277	0.0490	0.0251	-0.0164	0.0226
dP (active channels - bypass) in node 24 (MPa)	0.2250	0.0032	0.0243	0.0027	-0.0409	0.0022
dP active channels, core average (MPa)	0.0509	0.0503	0.0505	0.0485	0.0504	0.0467
dP bypass (MPa)	0.0250	0.0258	0.0258	0.0261	0.0259	0.0263

In Table 4.3 it is clearly shown how `SPLFIX` influence the pressure in the bypass. For all cases when `SPLFIX` = 0, the pressure difference between the bypass and the active channels are in the same range. The pressure difference between the active channel and the bypass at the outlet (node 24) is small, which is realistic when the two channels exit into the same upper plenum.

When `SPLFIX` > 0, the pressure drop into the bypass channel is not calculated correctly, and the pressure differences between the active channel and the bypass do not show consistency in the calculations. In the case of `L1RC` = 80, the pressure is higher in the bypass channel than in the active channel, which is not realistic. The pressure in the active channels and the bypass is plotted for `L1RC` = 1900 in Figure 4.9. The figure demonstrates that core support plate pressure drop has been calculated incorrectly for the case when `SPLFIX` > 0. There is a pressure difference between the active channels and the bypass channel which is larger than 2 bars. The pressure difference between the active channels and the bypass channel at the top of the core (node 24) should be small, as is the case when using `SPLFIX` = 0.

The results in Table 4.3 and Figure 4.9 show that the option `SPLFIX` > 0 should never be used in POLCA7 calculations.

It is also shown in Table 4.3 that `L1RC` affects the bypass flow fraction when the option `SPLFIX` = 0 is used.

In the first sets of depletion calculations, the option `SPLFIX` > 0 together with `L1RC` = 1900 were used. From the results in Table 4.3, it is shown that this combination produce results that cannot be trusted, hence new sets of depletion calculations were performed using different options and data and are explained in the next section.

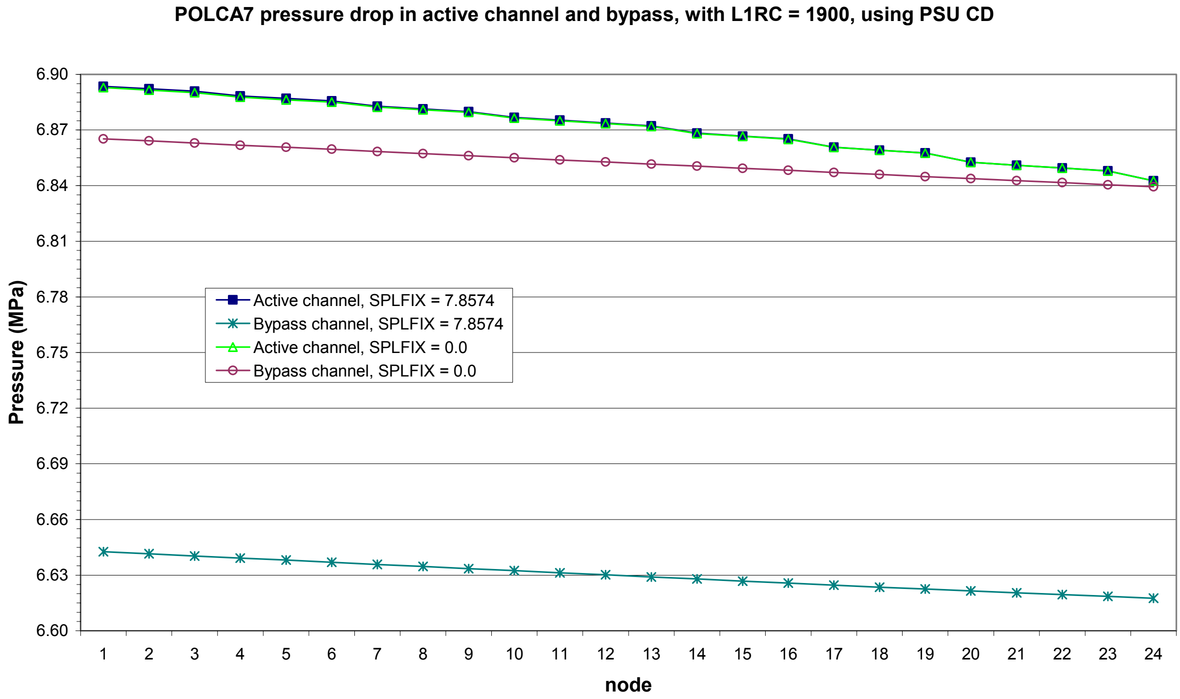

Figure 4.9. Influence of SPLFIX on pressure drop in active channels and bypass

4.2 Depletion calculations of cycle 1

Eight different cases were run for the depletion calculations, however only four of them were found to be valuable. The parameters and options that were studied and varied were the Dittus-Boelter heat transfer coefficient, the fuel Doppler temperature, the option for describing the bypass flow, and parameters describing leakage path 1 flow. The depletion cases represent different combinations of the above mentioned parameters and options.

4.2.1 Description of depletion cases

Below is an explanation of the four different depletion calculations which results will later be discussed.

Case 3: In this case the bypass option SPLFIX > 0, the Dittus-Boelter heat transfer coefficient constant $C_{DB} = 0.030$, and the original set of CD with fuel temperatures 933 K and 909 K were used.

Case 6, 7 and 8: These cases used the bypass option SPLFIX = 0, Dittus-Boelter heat transfer coefficient constant C_{DB} (called htrdit in the POLCA7 input) was set to its default value of 0.023. Different bypass flow area A_{leak1} and loss coefficients ξ_{leak1} were used. These two parameters are called L1AREA and L1RC in the POLCA7 input.

Table 4.4 presents a summary of the depletion cases.

Table 4.4. Summary of the depletion cases

case	SPLFIX	htrdit	L1AREA*	L1RC
3	> 0	0.030	10431.86 / 10431.86	1900
6	= 0	0.023	10431.86 / 7000.00	240
7	= 0	0.023	12620.00 / 5215.00	240
8	= 0	0.023	10431.86 / 7000.00	100

* - before and after core support plate holes plugging

The accuracy of the depletion calculations was checked by performing power calculations at the end of each cycle and comparing the calculated TIP distribution with the measured TIP distribution from PB2 [24].

4.2.2 Results of depletion calculations cycle 1

In order to check the accuracy of the depletion calculations, steady state calculations were performed at the end of cycle 1 with POLCA7. The calculations used the process parameters for data set 24 as input data [24]. In the steady state calculations, the neutron TIP detector response was calculated by POLCA7. The calculated TIP response was then compared with the measured TIP detector response from PB2 [24].

The results of depletion cases 3, 6, 7 and 8 are shown in Table 4.5, where the influence of the parameters specified in the previous section is shown. Case 3 is presented in this section as a reference only to demonstrate the use of the option `SPLFIX` > 0.

The power shape is also described by the axial offset, which is given in Table 4.5. A negative axial offset means that the core power has a bottom peak; a positive axial offset means top peaked power. The axial offset (AO) is similar for cases 6-8, while it differs for case 3. The same behavior is shown for the power peaking factor (PPF). The PPF shows the relation between the nodal maximum volumetric power density compared to the core average volumetric power density. The PPF are in the same range for cases 6-8, and different for case 3. From the results of the AO and the PPF the conclusion is that the values of the `L1AREA` and the `L1RC` used for cases 6-8 give small differences in the results.

It is shown in Table 4.5 that the results of cases 6, 7 and 8 are very similar. This is confirmed in Figure 4.10, where the calculated core average axial TIP responses for the four cases are compared with the measured TIP response. The power shapes for cases 6, 7 and 8 are almost impossible to tell apart. The differences between the different cases are the leakage path 1 area and loss coefficient and all three combinations of the parameters give results that are very similar, hence the results of the depletion calculations are insensitive to changes in these parameters if they are varied within this range (`L1AREA` between 5000-7000, and `L1RC` between 100-240).

Table 4.5. Results of depletion cases 3, 6, 7 and 8 at end of cycle 1

TIP 24	End of Cycle 1	**case 3**	**case 6**	**case 7**	**case 8**
input data	htrdit	0.03	0.023	0.023	0.023
	SPLFIX	> 0	= 0	= 0	= 0
	L1RC	1900	240	240	100
	L1AREA at EOC1	10431.86	7000	5215	7000
results	k-effective	0.99324	0.99154	0.99203	0.99147
	Avg diff. (TIPMEA, TIPNEU)	5.9	9.3	8.7	8.9
	RMS diff. (TIPMEA, TIPNEU)	7.2	11.5	10.8	11.0
	Max diff. (TIPMEA, TIPNEU)	20.7	33.4	31.2	31.8
	Axial Offset (%)	-3.60	-10.03	-9.50	-9.80
	Power Peaking Factor total	2.067	1.934	1.948	1.947
	Power Peaking Factor radial	1.318	1.317	1.317	1.316
	Power Peaking Factor axial	1.397	1.321	1.326	1.329
	bypass void (%)	0.00	0.00	0.90	0.00
	core average void (%)	31.39	35.28	34.82	35.79
	bypass flow (% of total)	6.32	7.77	6.72	9.95

At the EOC 1, the calculated core average TIP response for case 3 shows better agreement with the measured TIP response. Cases 6-8 all show the same axial shape for the TIP response, although with slightly worse agreement than for case 3. The reason for the observed deviation is the difficulty of modeling the correct burnup during cycle 1 when many startup tests were performed, as seen in Figure 4.1. In the recorded data summaries of cycle 1 (figures 63-89 in [24]) some process parameters are not recorded each day, especially not during the first six calendar months where many parameters are missing. The process parameters were estimated for these days, which imposed additional uncertainties in the results.

Taking into account the above reasons, the axial power for cases 6-8 have a reasonable deviation from the P1 edit power, and the results can be used for further calculations of cycle 2 [27].

Between cycle 1 and cycle 2, the core was shuffled, as it is described in the next section.

4.3 Core shuffling between cycles 1 and 2

Between cycle 1 and cycle 2, some fuel assemblies were discharged from the core, some assemblies were shuffled, and some fresh fuel assemblies loaded. This was modeled by using the Westinghouse code Skyffel [16]. In Skyffel, the fuel assemblies, the control rods and the detectors are shuffled. There was no information in [24] about CR or detector shuffling, so they were assumed to remain unshuffled.

After cycle 1 all fuel assemblies of type 1 were discharged from the core, along with some of type 2 and type 3 assemblies according to Table 3.1. New 8x8 fuel was loaded into the core. The core loading patterns for cycle 1 and 2 are shown in Figure 3.1 and Figure 3.2.

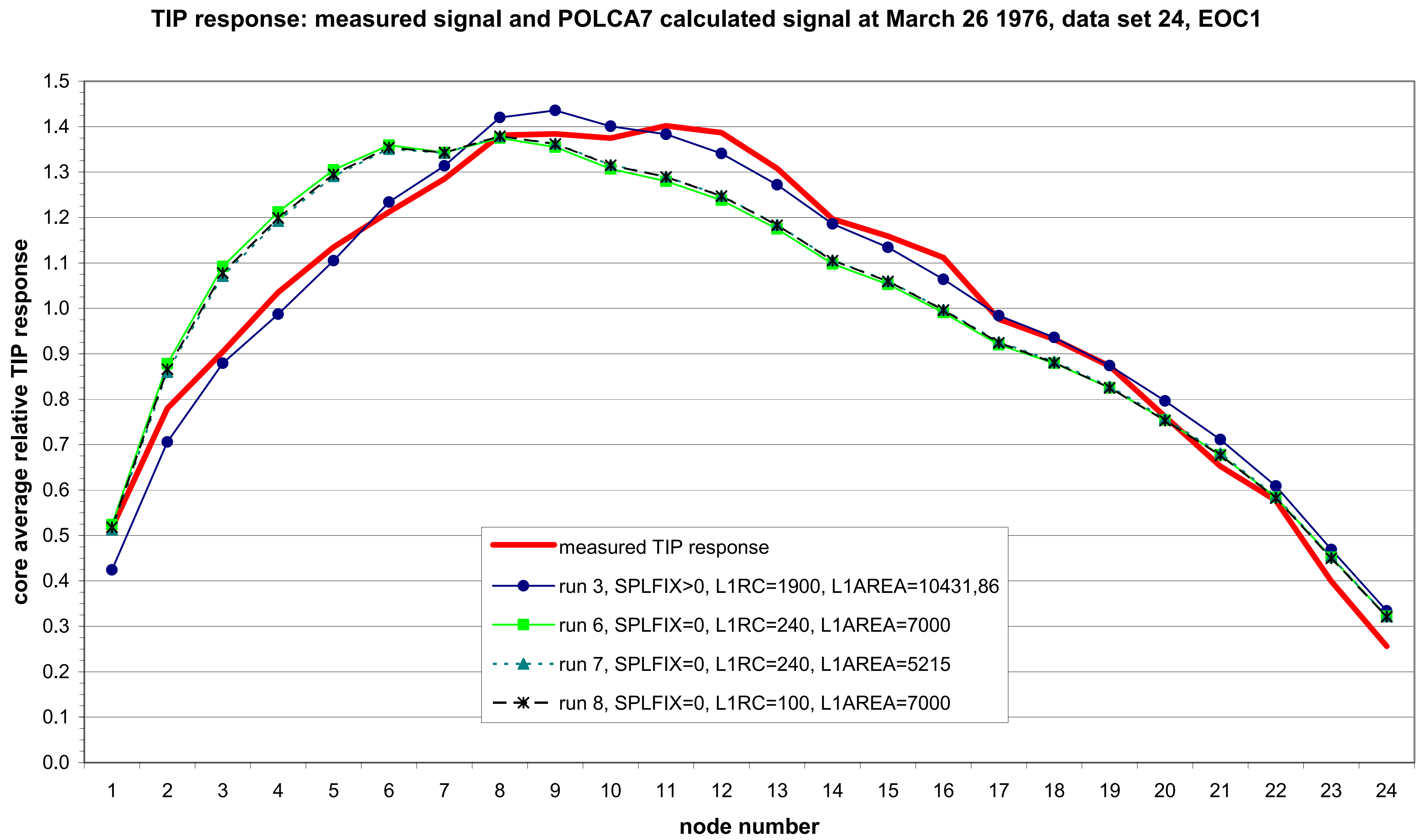

Figure 4.10. Comparison between measured and calculated TIP response at the end of cycle 1

In order to keep track of each individual fuel assembly and their calculated histories, the fuel bundle identification maps for cycle 1 and 2 (Table 13-14 in [24]) were input to Skyffel. Skyffel uses the identification map along with a map containing which assembly type is associated with the identification number to transfer all calculated distributions from cycle 1 to cycle 2. Skyffel also initiates distributions for fresh fuel assemblies.

In [24], there was no distinction between fuel assemblies of type 4-1 and 4-2 in the fuel bundle identification map. Therefore all type 4 fuel assemblies were assumed to be of type 4-1 when reloading the core for cycle 2, since only eight assemblies of sixty-eight were of type 4-2. The only difference between fuel type 4-1 and 4-2 was the fuel box thickness, see Table 3.1.

Once the core had been shuffled using Skyffel, the depletion calculations for cycle 2 were continued in the same manner as for cycle 1.

4.4 Depletion calculations of cycle 2

For cycle 2, depletion calculations were performed using the same procedures as for cycle 1. Following the conclusions of section 4.2.2, only cases 3, 6, 7 and 8 were run in the depletion calculations for cycle 2. Case 3 was performed only as a reference to see the influence of the different `SPLFIX` options.

The core was depleted up to data set 37, when the last TIP measurements were collected prior to the turbine trip and stability tests. The input data used in the depletion calculations are found in Appendix 2. For all depletion calculations during cycle 1 and cycle 2 up to data set 37, equilibrium Xenon was assumed. Prior to the TT2 transient test, non-equilibrium Xenon was assumed. The depletion and Xenon calculations after data set 37 are treated separately in section 4.4.2. The results of the depletion calculations up to data set 37 are presented in the next section.

4.4.1 Results of depletion calculations cycle 2

Steady state calculations were performed at the end of cycle 2 with POLCA7, using the process parameters for data set 37 (p. 188 in [24]), which was the last TIP measurement taken prior to the tests. As for data set 24, the neutron TIP detector response was calculated by POLCA7 and compared with the measured TIP detector response from PB2 [24].

The results of depletion cases 3, 6, 7 and 8 are shown in Table 4.6, where the influence of the parameters specified in Table 4.4 is shown.

It is shown in Table 4.6 that the results of cases 6, 7 and 8 are very similar for cycle 2. This is shown well in Figure 4.11, where the calculated core average axial TIP responses for the four cases are compared with the measured TIP response. At the end of cycle 2 all calculated cases show very good agreement with the measured TIP response.

The axial offset and the power peaking factors are very similar for all cases 6-8 for TIP measurement 37. These results prove also for cycle 2 that the results of the depletion calculations are insensitive to changes in the leakage path 1 area and loss coefficient if they are varied within the range (L1AREA between 5000-7000, and L1RC between 100-240).

Table 4.6. Results of depletion cases 3, 6, 7 and 8 at end of cycle 2

TIP 37	End of Cycle 2	**case 3**	**case 6**	**case 7**	**case 8**
input data	htrdit	0.030	0.023	0.023	0.023
	SPLFIX	> 0	= 0	= 0	= 0
	L1RC	1900	240	240	100
	L1AREA at EOC2	10431.86	7000	5215	7000
results	k-effective	0.99375	0.99433	0.99465	0.99395
	Avg diff. (TIPMEA, TIPNEU)	5.9	5.8	5.8	5.8
	RMS diff. (TIPMEA, TIPNEU)	7.3	7.2	7.2	7.2
	Max diff. (TIPMEA, TIPNEU)	24.1	23.2	23.5	23.0
	Axial Offset (%)	-1.51	-3.53	-3.24	-3.60
	Power Peaking Factor total	1.805	1.852	1.844	1.844
	Power Peaking Factor radial	1.264	1.280	1.280	1.280
	Power Peaking Factor axial	1.274	1.293	1.292	1.294
	bypass void (%)	0.00	0.00	0.00	0.00
	core average void (%)	35.95	38.31	37.94	38.94
	bypass flow (% of total)	7.88	9.27	8.24	11.42

Case 7 bypass flow is closer to the value obtained from Figure 4.7 and Figure 4.8. At the same time this case shows better agreement with TIP measurements in cycle 1 than cases 6 and 8, and almost exactly the same as these cases in cycle 2. The differences in the other parameters (k-effective, AO, PPF, radial and axial power factors) between case 7 and the other two cases are negligible.

The final depletion case used for further depletion and transient calculations was case 7.

In order to verify the depletion calculations for the entire 3D model of the core, a complete comparison of each TIP position was performed and is explained in the next section.

4.4.1.1 <u>3D core TIP response</u>

In order to check the results of the depletion calculations for the entire core, the results must be compared for each TIP position. The positions of the 43 detector strings in the core are shown in Figure 3.13 and are numbered 1-43, from left to right and top to bottom. 145 measurements were taken for each detector string. The measurements were processed and presented as 24 values axially in the data sets in [24].

For depletion case 7, a summary of the TIP comparison is presented below in Table 4.7 for data set 37.

As seen in Table 4.7, the core average radial difference show largest deviations on the core perimeter with the largest difference in string 43, where the calculated detector response is 11.6% lower than the measured. In the detectors located in the central parts of the core, the core average radial difference is less than 5%. The radial string RMS difference is 4.5%.

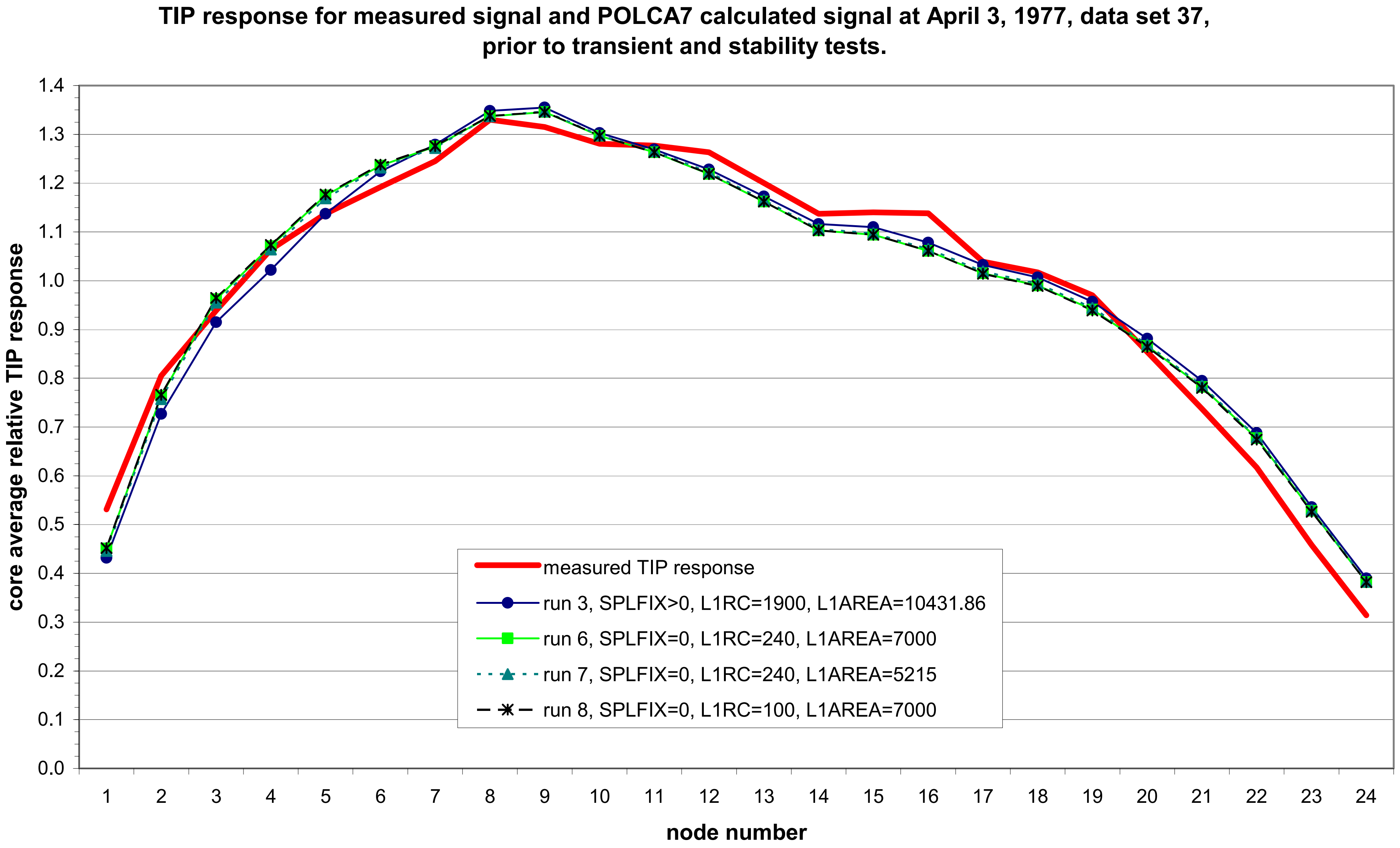

Figure 4.11. Comparison between measured and calculated TIP response at the end of cycle 2

Table 4.7. Summary of TIP comparison for each detector string

TIP string number	Average difference (%)	RMS difference (%)	Max difference (%)	location in core xx-yy*	location of max difference node no.**	TIP string number	Average difference (%)	RMS difference (%)	Max difference (%)	location in core xx-yy*	location of max difference node no.**
1	4.6	5.6	-13.3	16-57	1	25	5.4	6.2	-11.9	08-25	16
2	5.6	6.8	-17.7	24-57	1	26	4.7	6.2	13.2	16-25	22
3	7.3	8.3	-19.6	32-57	1	27	6.0	7.0	14.6	24-25	22
4	10.5	11.4	-17.6	40-57	16	28	6.0	7.0	-15.3	32-25	1
5	10.0	11.4	-23.5	08-49	1	29	4.7	5.8	13.5	40-25	22
6	8.2	9.9	17.5	16-49	9	30	5.7	6.7	-12.3	48-25	16
7	5.2	6.6	-14.3	24-49	1	31	4.1	4.8	-9.6	56-25	16
8	4.5	5.5	-11.4	32-49	16	32	6.0	7.3	-15.3	08-17	16
9	7.0	8.3	-15.6	40-49	1	33	5.6	6.5	11.4	16-17	22
10	4.5	5.4	10.2	48-49	11	34	4.5	5.8	-12.8	24-17	1
11	6.8	8.2	-16.6	08-41	16	35	4.3	6.2	-17.0	32-17	1
12	4.3	5.8	13.2	16-41	22	36	4.2	5.1	10.2	40-17	22
13	3.8	4.7	-9.5	24-41	16	37	4.6	5.6	-11.1	48-17	1
14	5.1	5.8	-12.6	32-41	16	38	4.3	5.4	-15.4	56-17	1
15	4.2	5.2	10.3	40-41	22	39	6.5	7.0	11.8	16-09	7
16	4.6	5.5	-12.7	48-41	16	40	7.9	9.0	17.0	24-09	7
17	8.1	9.4	-15.8	56-41	12	41	4.7	5.5	-11.6	32-09	16
18	4.1	5.0	9.7	08-33	24	42	7.4	8.9	17.9	40-09	7
19	9.1	9.8	17.0	16-33	22	43	12.1	13.5	-21.9	48-09	12
20	4.7	5.7	11.6	24-33	22						
21	3.7	4.6	-10.1	32-33	13	core average					
22	6.5	7.7	-17.1	40-33	16	overall	5.8	7.2	-23.5	-	-
23	5.7	6.6	13.1	48-33	22	axially	3.6	4.3	-8.5	-	-
24	3.9	4.8	10.3	56-33	4	radially	3.5	4.5	-11.6	-	-

* - coordinates as in Figure 3.13
** - node 1 at core inlet and node 24 at core outlet

For the core average axial difference (plotted in Figure 4.11), the largest difference is in node 1, where the calculated TIP response is underestimated with 8.5%. The largest underestimations in the calculated TIP response occur in node 1 and 16 most frequently. The largest overestimations in the calculated TIP response occur most frequently in node 22. This can also be seen in the plot of the core average axial TIP response in Figure 4.11, where the largest differences are in node 1, 16 and 22.

The overall maximum TIP difference is in the first node of string number 5, where the calculated TIP detector response is underestimated by 23.5% as compared to the measured. The overall core average RMS difference is 7.2%.

The RMS deviations are acceptable and the results of the depletion calculations for case 7 show good agreements with the measured data from PB2, and can be used further in the calculations. During all depletion calculations up to data set 37 equilibrium Xenon distributions were assumed. Prior to the TT2 test however, the reactor did not operate at steady state for a long time period, and non-equilibrium Xenon was assumed. How this was treated is explained in the next section.

4.4.2 Depletion and Xenon calculations prior to tests

The calculated distributions of isotopes at data set 37 were used in a restart when performing depletion calculations after data set 37 up to the state prior to the TT3 test. The TT3 test was the last test performed before shutdown for refueling.

4.4.2.1 Operating conditions prior to the Turbine Trip test 2

The operating conditions for the time period between data set 37 and the TT3 test are shown in Figure 4.12. The daily average values for the core thermal power, number of inserted CR notches, flow and core inlet subcooling are given. The times for the turbine trip transient tests TT1-TT3 and the low flow stability tests PT1-PT4 are also shown.

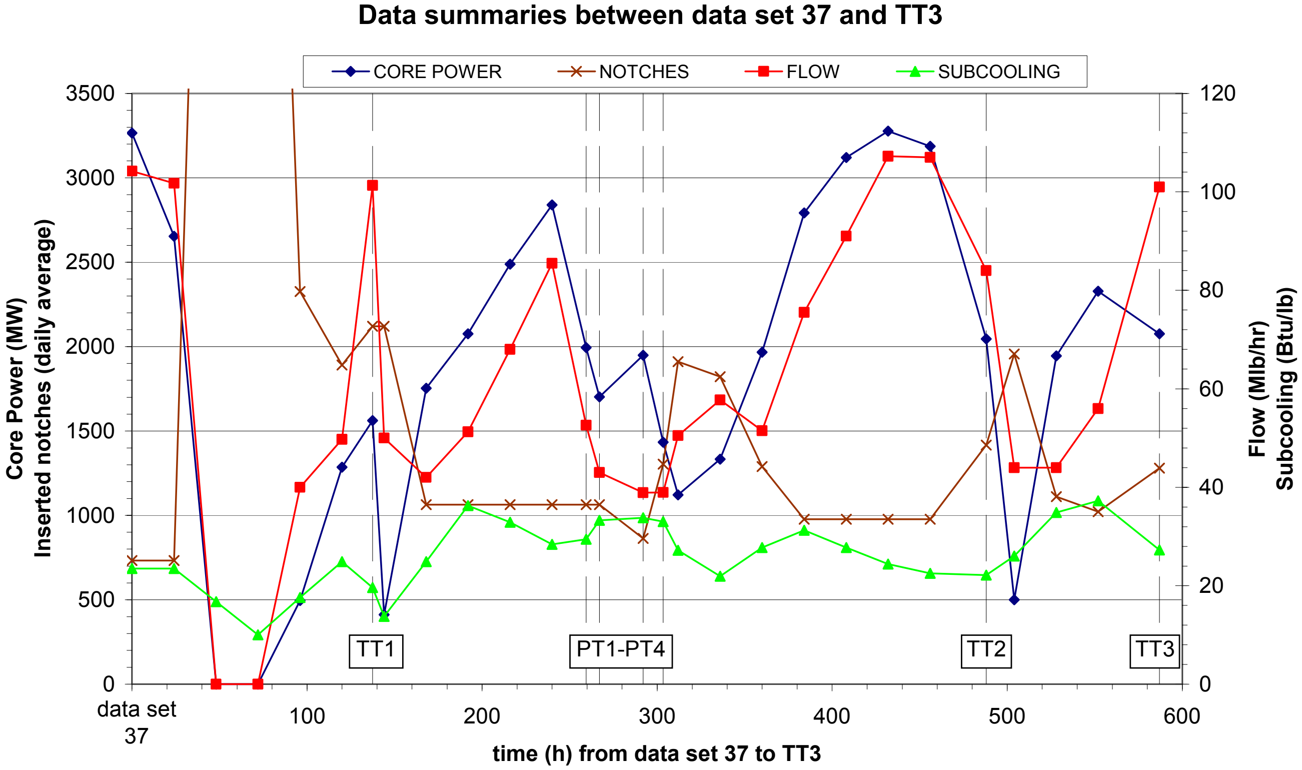

Figure 4.12. Data summaries between data set 37 and TT3.

Prior to the seven tests, the reactor had not been operating at steady conditions for a long time. This requires that the non-equilibrium Xenon distributions had to be calculated. The Xenon concentration in the core is not at equilibrium when the plant has not been in steady state for more than 72 hours. For all depletion calculations performed for cycle 1 and cycle 2, equilibrium Xenon was assumed.

4.4.2.2 Xenon poisoning

Xenon has an extremely large absorption cross section. At stationary operation, the amount of Xenon is constant in the core, and gives a decrease in reactivity (Xenon poisoning). After a power change, there is a transient change in Xenon poisoning. After a decrease in power, there is an increase in Xenon poisoning and vice versa. An increase or decrease in Xenon strongly affects the neutron flux in the core [20]. This phenomenon is illustrated in Figure 4.13, where the transient Xenon poisoning effect is shown for different changes in core power.

Figure 4.12 and Figure 4.13 demonstrate the importance of updating the Xenon distributions, when the reactor was not operating with steady conditions prior to TT2.

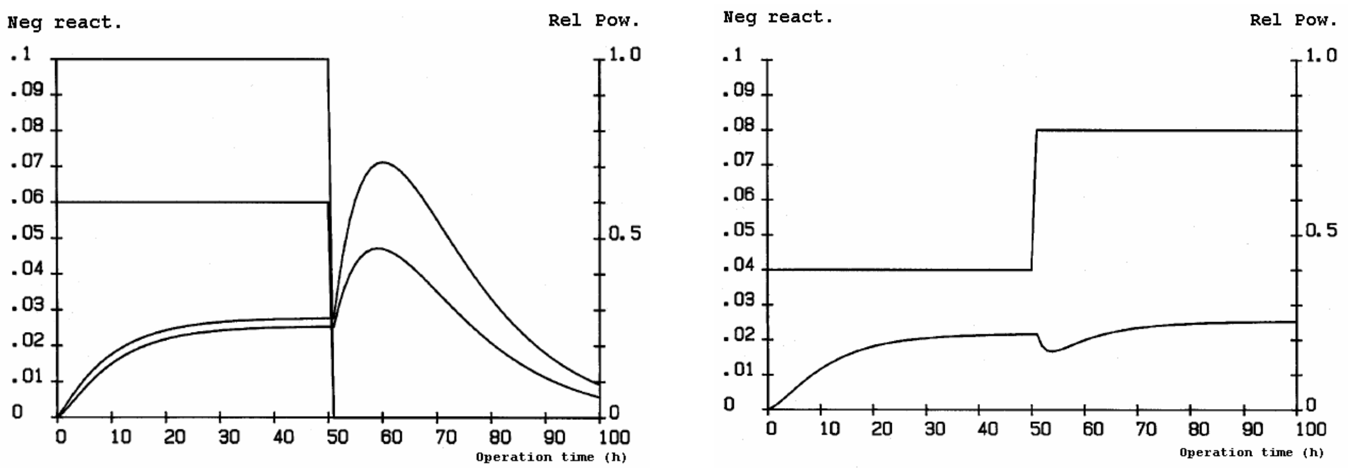

Figure 4.13. Influence of core power on Xenon poisoning. [20]

4.4.2.3 Calculation steps

Two different steps were required to perform depletion and Xenon calculations prior to the tests:

1. The first step calculated only the burnup from data set 37 in 24 hour steps, and assumed equilibrium Xenon for all burnup steps. This is far from the truth since assuming equilibrium Xenon means that the reactor has been operating in steady state for at least 72 hours, which was not the case at any moment during this time period (see Figure 4.12). This step was necessary however in order to be able to perform step 2.

2. In step 2, the exposure and distributions of isotopes for the state prior to TT2 that was calculated by step 1 were used. Xenon transient calculations were then performed by going back in time 72 hours, updating only the Xenon distributions, and keeping all other distributions constant. The Xenon transient was calculated in 6 hour steps, using average flow and subcooling conditions for the time period. The CR insertion was modeled using the CR sequence groups. The Xenon non-equilibrium distributions were saved at the end of the transient calculations for further use in the next step in the 3D transient analysis methodology; initialization of the core model.

The two steps are illustrated in Figure 4.14 for the last 180 hours prior to the TT2, where firstly the burnup is calculated, and secondly the Xenon transient is calculated. The core thermal power was given only as daily average values in [24], and the power was assumed to change linearly between each daily average value in step 2. For step 1 the power was assumed to be constant during each 24 hour step. This is visualized in Figure 4.14.

4.4.2.4 Result of depletion and Xenon calculations prior to Turbine Trip 2

Two sets of calculations were performed with the PHOENIX CD, assuming equilibrium and non-equilibrium xenon distributions respectively. The results of the depletion and xenon transient calculations are presented in Table 4.8. The core average axial relative power is plotted in Figure 4.15 and compared to the P1 edit from PB2 [1] and to POLCA7 calculations using PSU CD.

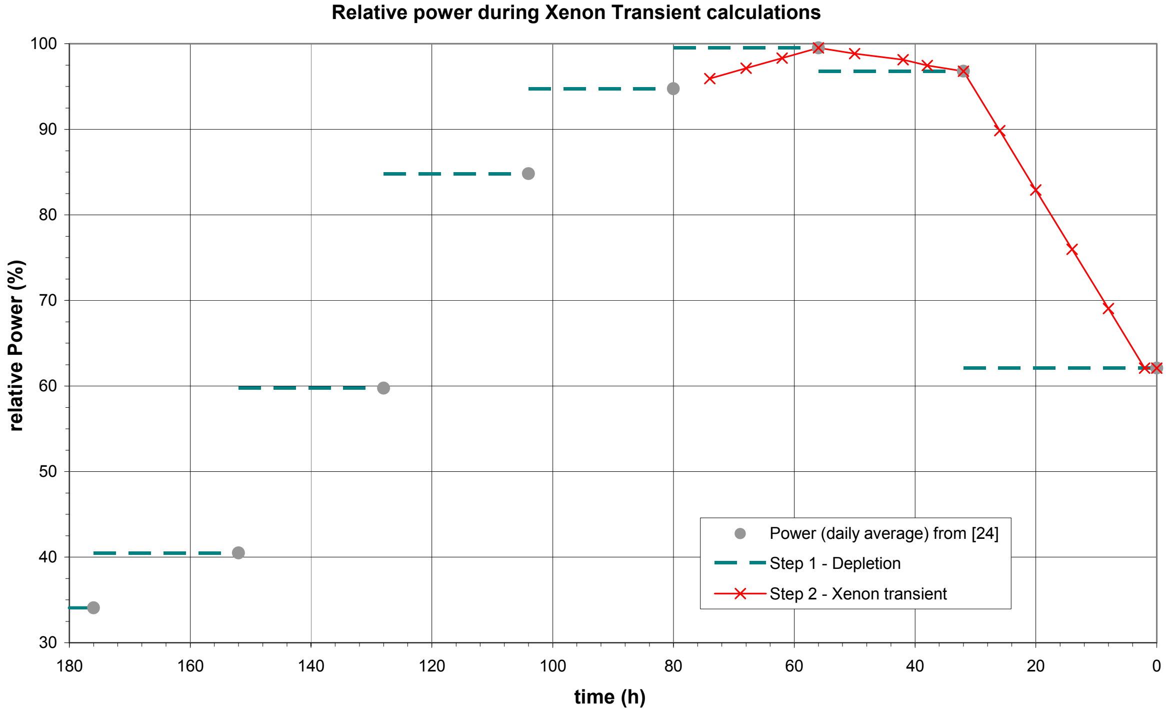

Figure 4.14. Methodology for calculating Xenon non-equilibrium distributions prior to TT2

Table 4.8. Results of depletion and xenon calculations for TT2 initial state

Cell data	PHOENIX	PHOENIX	PSU
Xenon	non-equilib.	equilibrium	equilibrium
k-effective	0.98957	0.99360	1.00787
Power peaking factor total	2.151	2.102	2.349
Power peaking factor radial	1.417	1.417	1.460
Power peaking factor axial	1.447	1.417	1.538
Axial Offset (%)	4.91	5.69	12.74
Core avg void (%)	30.67	30.53	28.72
Bypass flow (kg/s)	736.20	735.53	737.09
Bypass outlet void (%)	0.89	1.01	0.61

The results in Figure 4.15 show that the calculated core average axial relative power calculated with PHOENIX CD has a much better agreement with the P1 edit than the results using PSU CD. The xenon equilibrium and non-equilibrium calculations with PHOENIX CD show small differences in the axial relative power. The calculations assuming equilibrium xenon show best agreement with the P1 edit. This does not necessarily mean that these results are the best. The axial power shape produced by the P1 edit process computer is based on signals from a number of in-core power range monitors and is processed assuming equilibrium xenon. Further 3D analysis must be performed where the calculated LPRM signals are compared with the measured LPRM signals from the raw data to see which of the equilibrium or non-equilibrium xenon distributions give the best results. This however was not performed due to time limitation, and further investigation is required before drawing final conclusions.

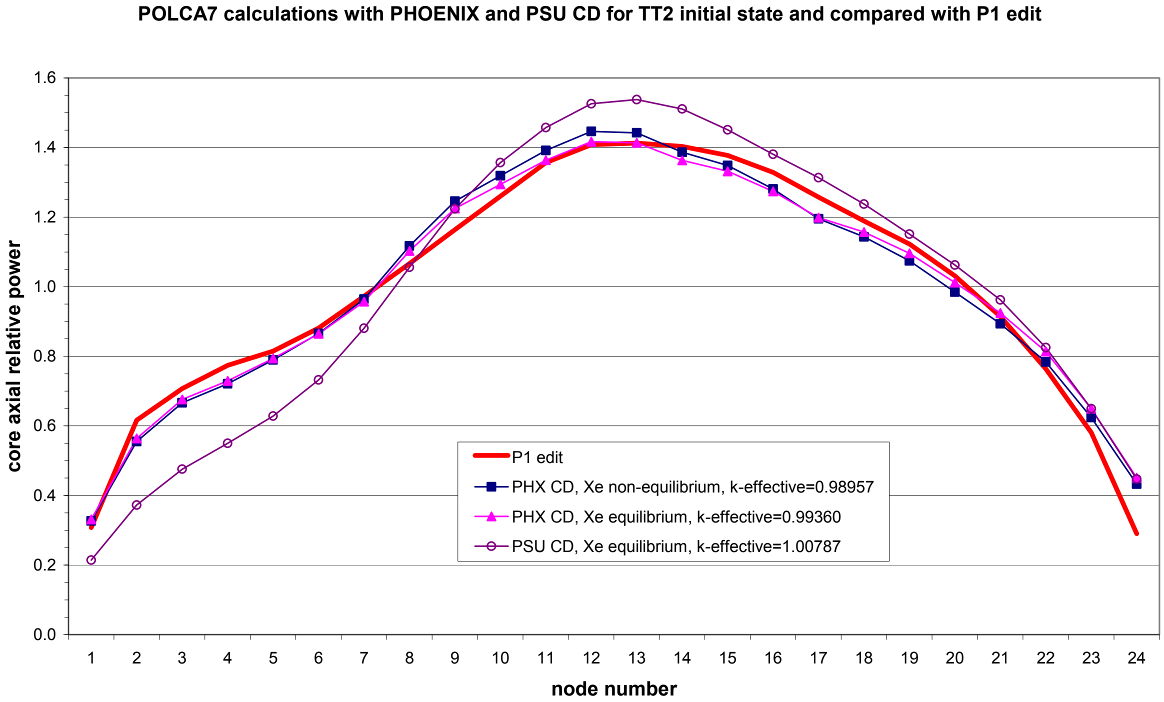

Figure 4.15. Comparison between calculated core average axial relative power and P1 edit at TT2 initial state.

The calculated effective multiplication factor (k-effective) is considerably lower for the PHOENIX CD compared to the PSU CD, as seen in Table 4.8. By comparing the two cases where equilibrium xenon is assumed, the difference is 1427 pcm. The difference in k-effective is 403 pcm between the equilibrium and non-equilibrium xenon distributions calculated with the PHOENIX CD. The influence of assuming non-equilibrium xenon for the TT2 initial state is thus a decrease in k-effective of approximately 400 pcm, and a small change in core average axial relative power shape.

The results in Table 4.8 and Figure 4.15 show that the results with PHOENIX CD can be trusted to use for further calculations. The non-equilibrium xenon distributions will be used in the future calculations where the core model is initialized and in the transient calculations.

4.5 Conclusions

The depletion calculations were performed using 43 depletion steps for cycle 1 and 22 steps for cycle 2 up to data set 37. During all these calculations equilibrium xenon was assumed in the core. During each burnup step the process parameters total power, flow, subcooling and number of inserted control rod notches were averaged, and kept constant during the entire burnup step.

During cycle 1, the correct burnup was difficult to model due to the many startup tests performed (see Figure 4.1). During the first six calendar months of cycle 1, many process parameters were missing in the data summaries of [24], and the parameters were estimated for these days.

The first sets of depletion calculations performed for cycle 1 predicted high outlet void in the bypass channel for some depletion steps. A sensitivity study was performed and the high bypass void was derived from setting the POLCA7 input parameter `SPLFIX` > 0 and using a leakage path 1 area and a loss coefficient that were too large.

The conclusion was made that the POLCA7 option `SPLFIX` > 0 must never be used.

When the input parameter was changed to `SPLFIX` = 0, no bypass void or very small bypass void was predicted in the calculation steps.

The calculated core average axial TIP signal at the end of cycle 1 was more bottom peaked than the measured core average axial TIP signal. The deviation was mainly due to the difficulties of modeling the burnup during the startup tests, and to model the amount of bypass flow.

The calculated core average TIP signal at data set 37, prior to the test performed at the end of cycle 2 showed very good agreement with the measured core average TIP signal. When looking at the 3D distribution of the TIP signals for case 7 it is shown that the largest underestimations in the calculated TIP response occurs in node 1 and 16 most frequently. The largest overestimations in the calculated TIP response occur most frequently in node 22. The overall RMS difference in the core is 7.2% between the measured and calculated TIP signals. The radial RMS difference is 4.5% and the axial RMS difference is 4.3%.

The RMS deviations are acceptable and the results of the depletion calculations for case 7 show good agreements with the measured data from PB2.

It was also concluded that varying the leakage path 1 area between 5000 and 7000 cm^2, and varying the leakage path 1 loss coefficient between 100 and 240 have a small influence on the results, hence any number within this range can be used.

Calculations for the TT2 initial state were performed assuming both equilibrium and non-equilibrium xenon distribution in the core respectively. The difference in the core average axial relative power shape was very small between the respective cases. The k-effective was 400 pcm smaller when calculating the non-equilibrium xenon case compared to the case assuming equilibrium xenon. Further 3D analysis must be performed where calculated LPRM signals are compared to measured LPRM signals to see if assuming non-equilibrium give better results or not before making final conclusions.

The core average axial relative power shape showed better agreement using the PHOENIX generated cross sections with the P1 edit compared to when using the PSU cross sections.

The distributions calculated by case 7 and assuming non-equilibrium xenon distributions will be used in further calculation steps of the 3D transient analysis, when the core model is initialized and in the transient calculations.

5 INITIALIZATION OF THE CORE MODEL

The initialization of the core model is the fourth step of the 3D transient analysis methodology. The reason for initializing the core model and performing steady state calculations is to test the response of the 3D core model only.

The first part of initializing the core model was performing Hot Zero Power calculations and is described in section 5.1. When the neutronics input model was initialized, Hot Full Power calculations were performed, and this is described in section 5.2.

5.1 Hot Zero Power

The Hot Zero Power (HZP) is an artificial state where the core neutronics model is initialized. The thermal hydraulic parameters are fixed in each node which means that the thermal hydraulic feedback is turned off; thus only the neutronics model is tested. The power is set to 1 % of rated power for the HZP calculations.

The control rod setting and HZP initial conditions are given in Table 5.2.3 and Figure 5.2.1 of [2], and should according to the reference produce a very near critical reactor. The control rod setting for the HZP state is shown in Appendix 3.

Three different cases were calculated to see the influence of the Xenon distributions on the HZP calculations and are described below:

1. Xenon non-equilibrium at 61.65% power as calculated in the depletion and Xenon transient calculations

2. Xenon equilibrium at 61.65% power

3. Xenon equilibrium at 1% power

The Power level was 61.65% of rated power for the state prior to the TT2 test, hence the reason for calculating the distributions at this power level. The PSU CD was generated by CASMO/SIMULATE assuming equilibrium xenon at 61.65% power [35]. The HZP state was calculated for both non-equilibrium and equilibrium xenon with PHOENIX CD and compared to the PSU CD for two reasons: to see the difference in results between the two sets of CD using equilibrium xenon, and to see the influence of the non-equilibrium xenon on the results.

The results of the HZP calculation are shown in Figure 5.1 and Figure 5.2, and are compared to previous POLCA7 calculations using PSU CD, and also to the average value of all participants' results in the benchmark [36].

The results are presented in three different graphs. In Figure 5.1 the core average relative axial power is shown. In Figure 5.2 the normalized axial relative power for fuel assemblies 75 and 367 are shown. These fuel assemblies were selected in [2] to show the differences for rodded and un-rodded fuel assemblies in the Hot Full Power (HFP) calculations. However, for the HZP calculations, both fuel assemblies are next to a fully inserted control rod. The locations of fuel assemblies 75 and 367 in the core are shown in Appendix 4.

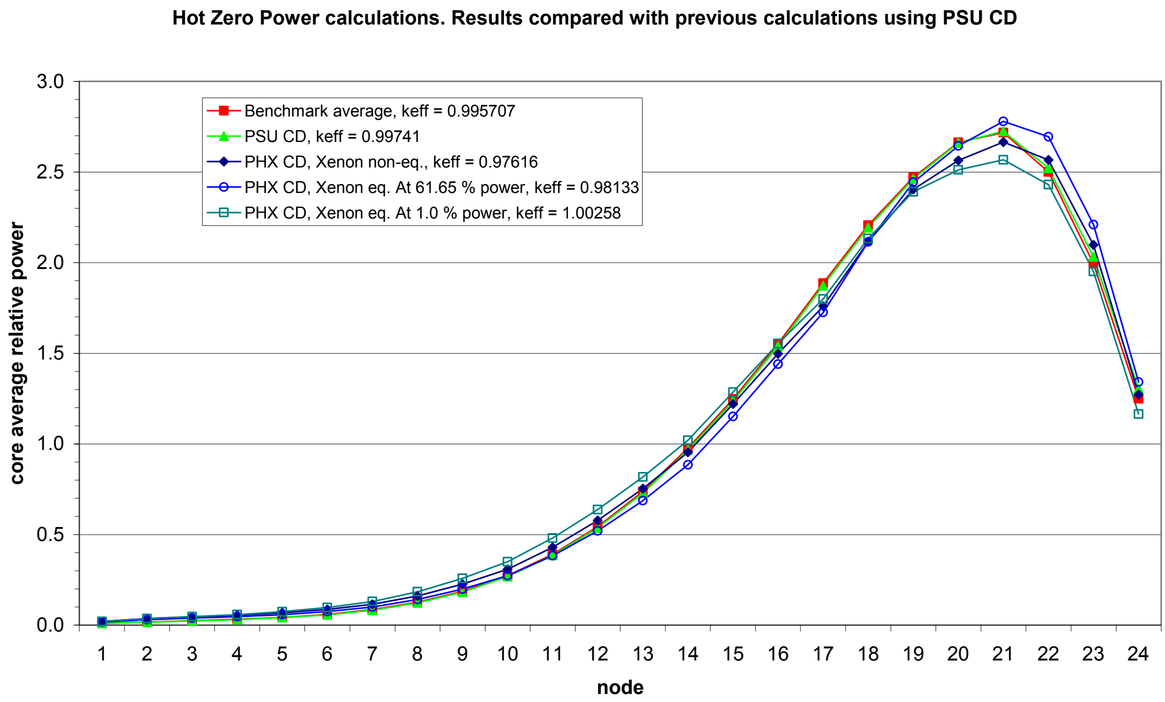

Figure 5.1. POLCA7 Hot Zero Power calculations. Comparison between Phoenix CD and previous calculations with PSU CD

The HZP core average relative power show good agreement with previous HZP calculations using PSU CD. The PSU CD is generated assuming equilibrium xenon at 61.65% power [35] so the results in the HZP calculations verify that the CD generated by PHOENIX and the depletion calculations can be used for further calculations. There is a difference in k-effective of 2125 pcm between the PSU data and the PHOENIX data assuming non-equilibrium Xenon distributions. The Xenon is a large contributor for the difference in k-effective. The difference in k-effective is 517 pcm between the cases when assuming non-equilibrium and equilibrium xenon with the PHOENIX CD at a power level of 61.65%.

For the HZP calculations, fuel assemblies 75 and 367 are next to fully inserted control rods. For fuel assembly (FA) 75, the POLCA7 result with PHOENIX CD show very good agreement with the results of the benchmark participants (see Figure 5.2). For FA 367, there is a deviation between the benchmark average calculated with PSU CD and the POLCA7 results with PHOENIX CD.

The radial power distributions for the POLCA7 HZP calculations are shown in Appendix 5 using both PHOENIX and PSU CD. In the HZP case there are significant differences in the radial power distributions between PHOENIX and PSU CD calculations.

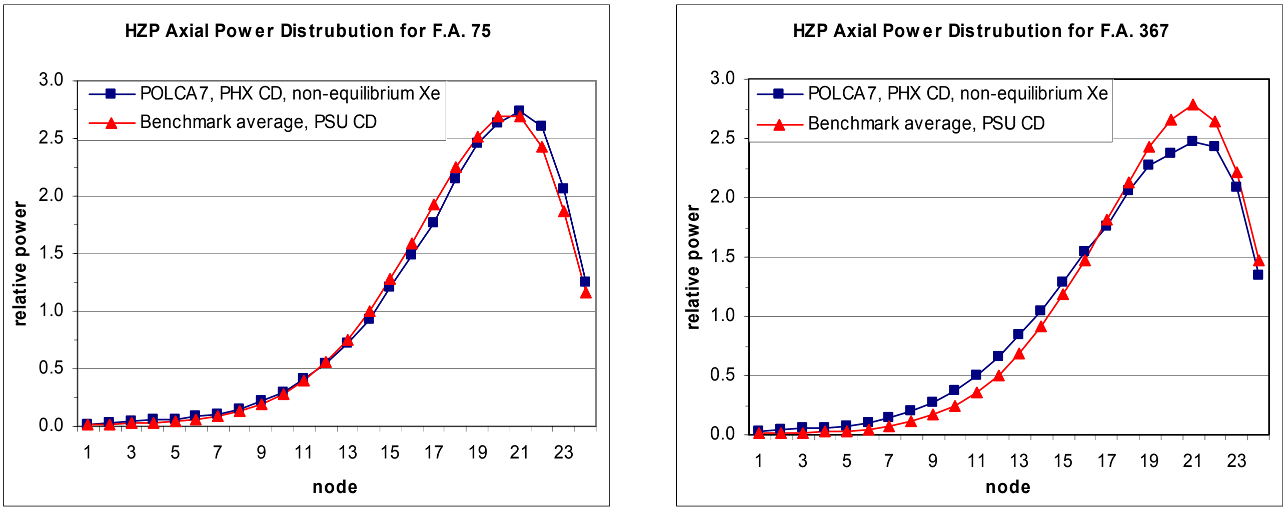

Figure 5.2. Hot Zero Power Axial Power distributions for Fuel Assemblies 75 and 367

The calculated core average axial relative power shape show good agreement with previous calculations using PSU CD. The calculated radial power distributions show significant differences for the two different sets of CD. The differences in the radial power distribution originate from the generation of the cell data and/or the depletion calculations. The methodology and codes used differ in between the PHOENIX and PSU data. Further investigations of the differences must be performed before final conclusions are made.

The results of the HFP calculations are presented in the next section.

5.2 Hot Full Power

When the core model was initialized, Hot Full Power (HFP) steady state calculations were performed for the state prior to the TT2 test. In these calculations, the full 3D core model was tested with thermal hydraulic feedback.

The TT benchmark consisted of three different exercises. These exercises are explained in detail in [2]. Steady state calculations were performed for exercise 2 and exercise 3, which are described briefly below.

For exercise 2, steady state calculations were performed with coupled 3-D core kinetics and thermal hydraulics using core inlet and outlet boundary conditions provided by PSU.

For exercise 3, calculations were performed with coupled 3-D core kinetics and thermal hydraulics, and a 1D plant thermal hydraulics model.

The Turbine Trip 2 initial conditions are shown in Table 5.1 below. The values are taken from Table 5.2.1 in [2].

Table 5.1. TT2 Initial conditions.

Parameter	Value
Core Thermal Power (MWt)	2030
Initial power level (% of rated)	61.65
Gross power output (MWe)	625.1
Feedwater flow (kg/s)	980.26
Reactor pressure (Pa)	6798470
Total core flow (kg/s)	10445
Core inlet subcooling (kJ/kg)	48.005
Feedwater temperature (°C)	169.16
Core pressure drop, measured (Pa)	113560.7
Core pressure drop, calculated (Pa)	83567.4
Jet pump driving flow (kg/s)	2871.24
Core average exit quality	0.097
Core average void fraction	0.304

Steady state calculations were performed for the state shown in Table 5.1 with POLCA7, and with POLCA-T input models for exercise 2 and 3. The difference between the codes is that POLCA-T uses a more advanced thermal-hydraulic model than POLCA7, based on the RIGEL code [5]. POLCA-T is a transient analysis code, but performs a static calculation before the transient calculations starts. POLCA-T performs only a steady state calculation if the end time for the transient calculation is set to zero. The differences between the POLCA-T input models for exercise 2 and 3 is that in exercise 2 core inlet and outlet boundary conditions are used, and in exercise 3 a plant model that includes the reactor pressure vessel, recirculation loop, main steam line and steam bypass lines is used (see chapter 6). The POLCA-T reactor pressure vessel model nodalization of PB2 is shown in Appendix 6 [5].

The HFP core average relative power results are presented in Figure 5.3 for POLCA7 and POLCA-T exercise 2 and 3 using both PHOENIX and PSU CD. The results are compared with the P1 edit.

The calculated axial power show better agreement with the P1 edit for the Phoenix generated CD as compared to the PSU CD. All POLCA7 inputs for the core geometries are the same for all cases; it is only the CD that is different.

It is clearly shown in Figure 5.3 that the CD generated with PHOENIX gives better agreement with the P1 edit than the results with PSU CD.

The calculated values for the steady state calculations with POLCA7 and POLCA-T using both PHOENIX and PSU Cell Data are presented in Table 5.2.

One difference that is shown from the results of POLCA7 and POLCA-T is the amount of flow that goes into the bypass. The difference is approximately 180 kg/s. According to Figure 4.8 the bypass flow should be 780 kg/s. However, in the benchmark, a bypass flow of 841 kg/s was used (table 3.1.3.3 in [2]). The reason for the difference in bypass flow between the two codes is that POLCA-T models the flow through the CR guide tubes, while POLCA7 does not do it for GE reactors.

In order to see the influence of the bypass flow rate, a sensitivity study was performed where the leakage path 1 area was modified in order to get the correct bypass flow.

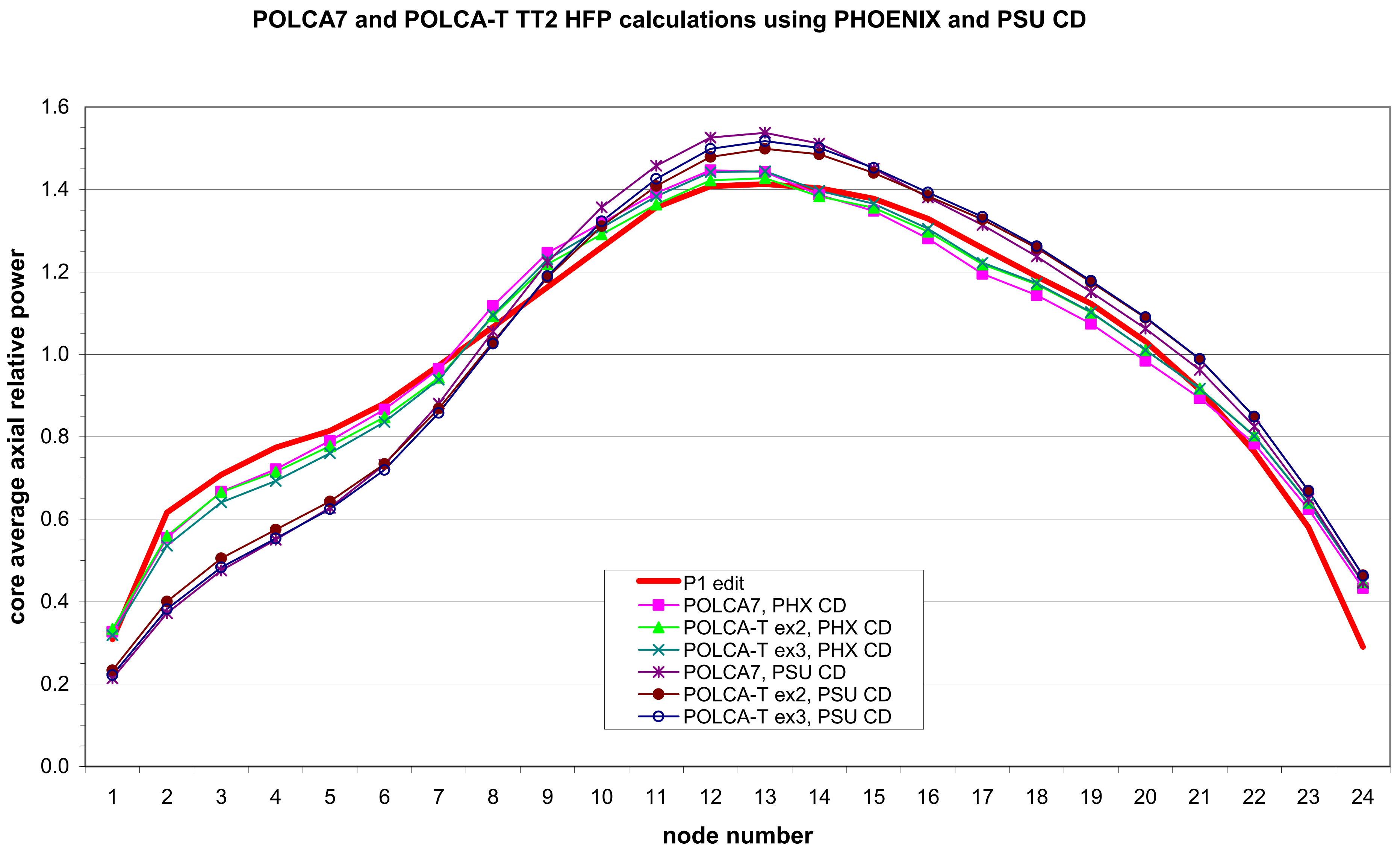

Figure 5.3. TT2 steady state HFP calculations with POLCA7 and POLCA-T

Table 5.2. TT2 steady state calculated data with POLCA7 and POLCA-T using Phoenix and PSU Cell Data

Code/exercise	POLCA7	POLCA-T ex2	POLCA-T ex3	POLCA7	POLCA-T ex2	POLCA-T ex3
Cell data	PHOENIX	PHOENIX	PHOENIX	PSU	PSU	PSU
L1AREA	5215	5215	5215	5215	5215	5215
Bypass flow (kg/s)	736.20	921.02	914.51	737.09	910.61	904.29
Bypass outlet void (%)	0.89	3.63	2.46	0.61	3.71	2.76
k-effective	0.98957	0.98704	0.98809	1.00787	1.00419	1.00524
PPF total	2.151	2.107	2.132	2.349	2.280	2.305
PPF radial	1.417	1.416	1.415	1.460	1.456	1.454
PPF axial	1.447	1.427	1.444	1.538	1.499	1.517
Axial Offset (%)	4.91	6.42	6.83	12.74	13.56	14.13
Core avg void (%)	30.67	32.80	31.99	28.72	30.88	30.10
Total core flow (kg/s)	10445.0	10445.0	10445.0	10445.0	10445.0	10444.5
Steam dome pressure (Pa)	6798470	-	6798470	6798470	-	6798470
lower plenum temperature (°C)	274.6	276.5	276.9	274.6	276.5	276.9

5.2.1 Sensitivity study of bypass flow rate

In order to compare POLCA7 and POLCA-T results with the same flow in the bypass, the leakage area A_{leak1} (called `L1AREA` in the POLCA7 input) was changed. Changing the leakage area (or any parameter in the input model) is only allowed when the input model is set up. The values used in previous validations cannot be used because other options and cross section model were used. The results of the sensitivity studies described in chapter 4 showed that changing the value of the leakage path 1 area within a certain range does not affect the results. The leakage path 1 area was changed to achieve a bypass flow about 840 kg/s, as it was stated in [2].

The results are shown in Figure 5.4 for POLCA-T exercise 2 as core average axial relative power and in Table 5.3 for all cases.

In Figure 5.4 it is shown that changing the leakage path 1 area to get the benchmark specified bypass flow does not change the shape of the axial relative power significantly. Hence the influence of the bypass flow rate is not significant for the static solution. This is further emphasized by looking at more calculated values in Table 5.3 and comparing them with the results obtained using the previous investigated bypass area presented in Table 5.2. The core average axial power shape for the cases with corrected `L1AREA` is plotted in Figure 5.5.

By comparing the results in Table 5.2 and Table 5.3 it is seen that for exercise 2, changing the bypass area by approximately 30%, changes the bypass flow rate by about 10%; this in turn gives a change in k-effective of only 37 pcm. This shows that the bypass flow does not significantly affect the results of the static calculations. The axial power shapes with the corrected `L1AREA` is shown in Figure 5.5.

The static calculations performed by the codes POLCA7 and POLCA-T show good agreement with the P1 edit core average axial relative power in Figure 5.5, where the corrected `L1AREA` is used.

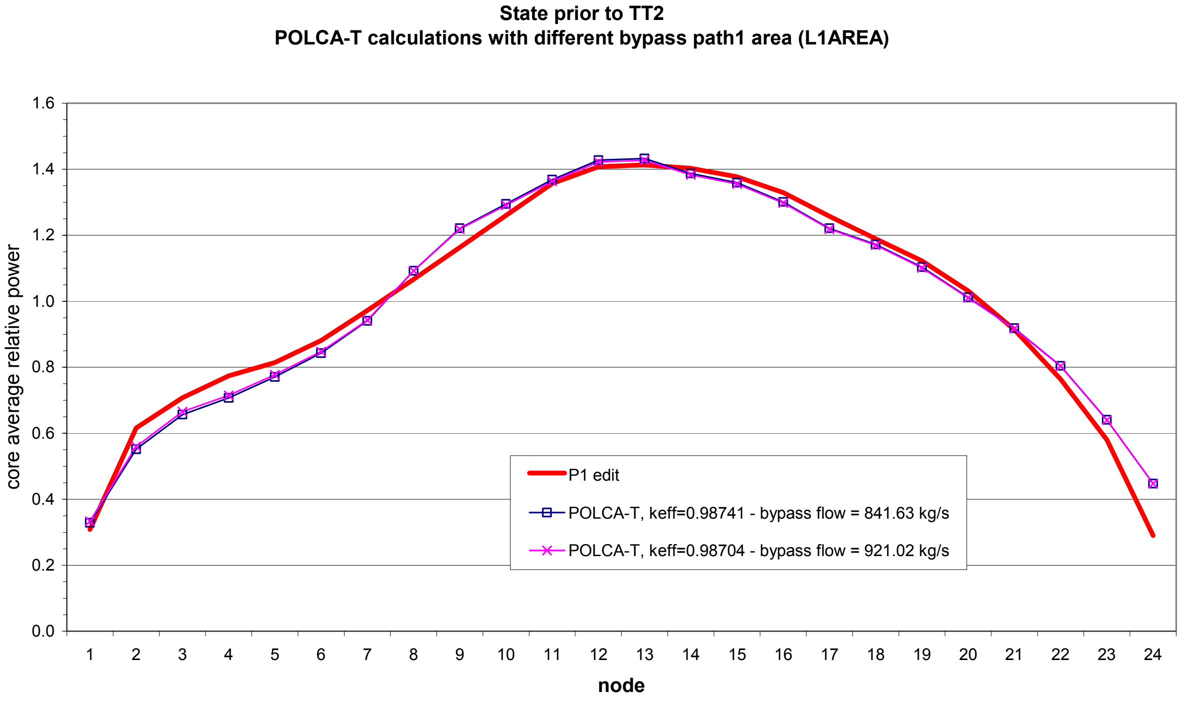

Figure 5.4. Bypass flow sensitivity study with POLCA-T exercise 2 input model

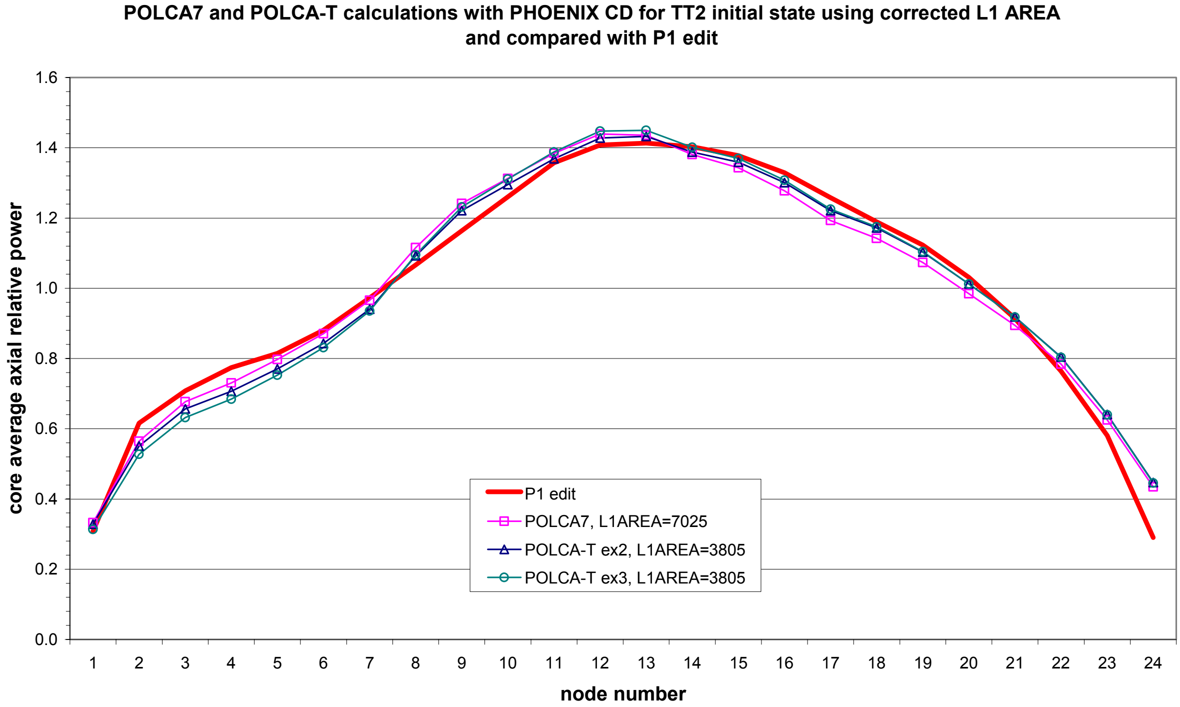

Figure 5.5. Core average axial power shape using corrected L1AREA

Table 5.3. TT2 steady state calculations with corrected L1AREA

Code/exercise	POLCA7	POLCA-T ex2	POLCA-T ex3
Cell data	PHOENIX	PHOENIX	PHOENIX
L1AREA	7025	3805	3805
Bypass flow (kg/s)	841.59	841.63	835.10
Bypass outlet void (%)	0.00	5.95	4.83
k-effective	0.98918	0.98741	0.98847
PPF total	2.140	2.114	2.140
PPF radial	1.417	1.416	1.415
PPF axial	1.439	1.432	1.450
Axial Offset (%)	4.73	6.66	7.09
Core avg void (%)	30.98	32.54	31.73
Total core flow (kg/s)	10445.0	10445.0	10445.3
Steam dome pressure (Pa)	6798470	-	6798470
lower plenum temperature (°C)	274.6	276.5	276.9

5.2.2 Relative power for fuel assemblies 75 and 367

In the benchmark specifications [2] the relative power for fuel assembly (FA) number 75 and 367 were requested in order to compare different codes results for rodded and un-rodded fuel bundles. For the TT2 initial state, FA 75 is next to a fully inserted control rod, and FA 367 is next to a fully withdrawn control rod (see Appendices 3 and 4 for control rod positions and FA numbers). The relative power calculated with POLCA-T using PHOENIX CD is compared with the average value of the benchmark participants' relative power [36] using PSU CD in Figure 5.6.

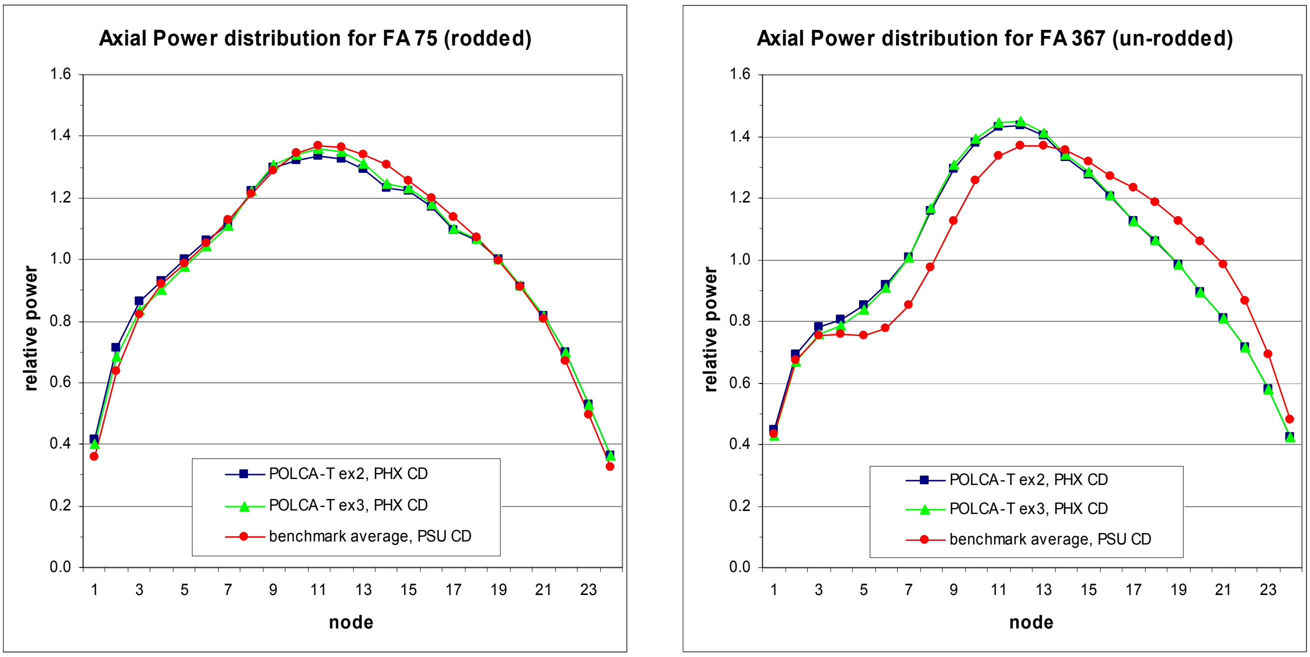

Figure 5.6. Axial power distributions for fuel assemblies 75 and 367

In Figure 5.6 it is seen that for FA 75, which is next to a fully inserted control rod, the normalized relative powers are very similar. For FA 367 however, which is next to a fully withdrawn control rod, there is a difference in the normalized relative power. It has to be noted that the deviations between the POLCA-T results and the benchmark participants' average axial power for FA 367 are inside the range of the spread of the results obtained by different codes in [36]. In order to perform a complete 3D study, the radial distributions of the power must be analyzed also and this is done in the next section.

5.2.3 Radial power distributions

For the radial powers in Appendix 5, it is shown that the normalized radial powers are similar between the PHOENIX and PSU data in the HFP case. The main differences are on the core periphery where the normalized power with PHOENIX data is larger than with the PSU data.

Further analysis is required of the radial power distributions before final conclusions can be made, the time limitation of the present project does not allow such analysis to be performed. The full 3D analysis will be future work.

5.2.4 Core averaged axial void distribution

The core averaged axial void distribution for POLCA7 and POLCA-T calculations are shown in Figure 5.7 and are compared to the average values of the participants in the benchmark [36].

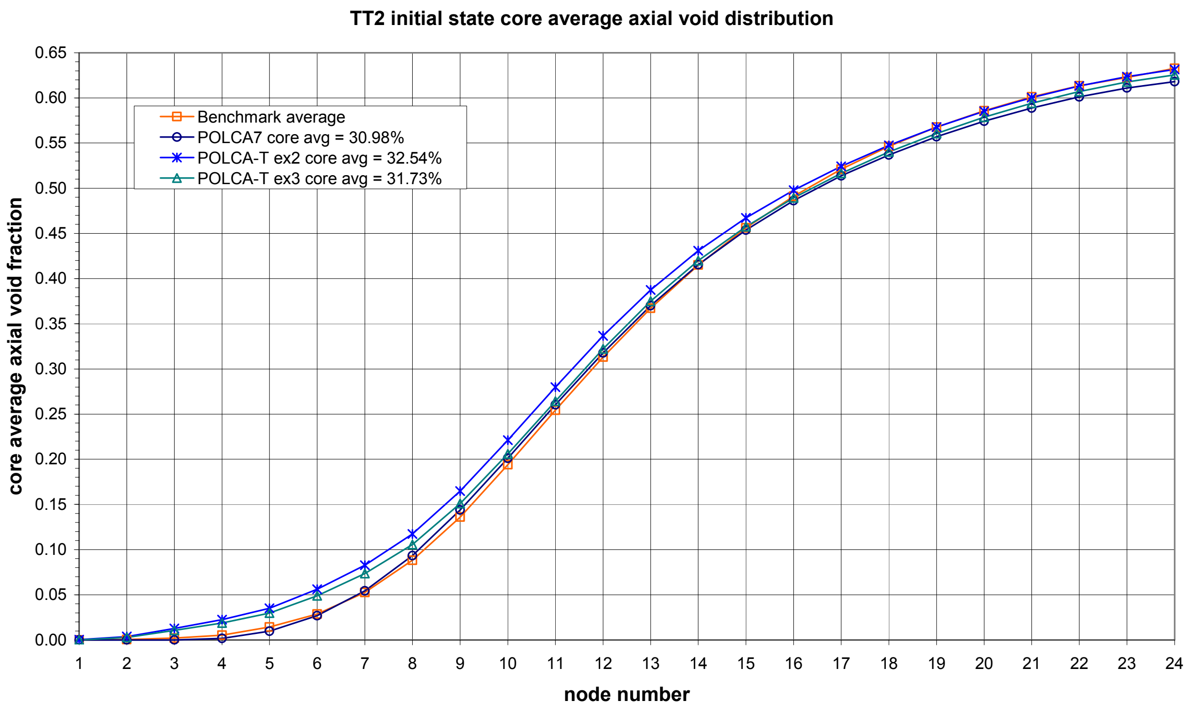

Figure 5.7. TT2 initial state core average axial void distribution

The void fraction between the different runs and cross sections are very similar, except at the bottom of the core where the POLCA-T calculated void is larger than the POLCA7 void and the benchmark average. The higher void at the bottom of the core is caused by the higher core inlet coolant temperature in the POLCA-T case (see Table 5.3). In the POLCA7 case, the core inlet subcooling is set as a boundary condition, while in the PB2 POLCA-T model the feed water temperature and feed water flow is a boundary condition. The larger void at the bottom of the core is the reason for the small discrepancies in axial power shape between the results of the POLCA7 and POLCA-T codes. The axial power shape calculated by POLCA-T (Figure 5.5) has a lower relative power at the bottom of the core. The higher temperature and/or void at the bottom gives lower moderator density, and hence a lower power.

5.3 Conclusions

The Hot Zero Power calculations are performed in order to initialize the neutronics model. The HZP calculations with PHOENIX CD show good agreement with the PSU data for the core average axial relative power. The value of the effective multiplication factor (k-effective) is smaller when using the PHOENIX CD with 2125 pcm. The lower k-effective is partly due to using non-equilibrium Xenon distributions in the calculations with the PHOENIX data. The radial normalized power distributions show differences in all parts of the core when using the two different sets of CD for the HZP calculations. Further analysis of the obtained radial power distributions is required.

In the Hot Full Power calculations the core average axial relative power calculated with PHOENIX CD show better agreement with the P1 edit than the results calculated with PSU CD. Also in this case, the k-effective is lower with PHOENIX CD with 1830 pcm using POLCA7 and 1715 pcm using POLCA-T, both compared to PSU CD. For the HFP calculations, the normalized radial power distributions show good agreement between the two different sets of CD. The main difference is on the core periphery where the relative power with the PHOENIX CD is larger than with PSU CD. More analysis is required for the HFP radial distributions in order to draw conclusions. These analysis will be performed in future work.

A sensitivity study on the bypass flow rate showed that varying the leakage path 1 area by 30%, which changed the bypass flow rate with 10% had a negligible effect on the overall results when using both POLCA7 and POLCA-T.

The core average axial void distributions showed good agreement with the average results of the benchmarks participants. When using POLCA-T, there is a slightly higher void at the bottom of the core. POLCA-T does also calculate a higher bypass void than POLCA7. The reason is partly due to higher core inlet temperature in the POLCA-T calculations and the modeling of the CR guide tube flow in POLCA-T.

The results from the HFP calculations with PHOENIX data show good agreement with the P1 edit for the core average relative power and better agreement than with PSU data. The results prove that the generation of the cross section data, the core depletion, the thermal hydraulic plant model and the neutronics model can be used in the final step of the transient analysis; the coupled 3D core neutron kinetics and plant systems thermal hydraulics transient analysis.

6 COUPLED 3D CORE AND PLANT SYSTEMS TRANSIENT ANALYSIS

The final step in the 3D transient analysis is to perform coupled 3D core neutron kinetics and plant systems thermal hydraulic analysis.

The scenario of the TT2 transient was modeled using the Westinghouse 3D transient code POLCA-T.

The transient analysis is performed in two steps. Firstly a 10 second zero transient calculation is run. A zero transient is a transient calculation without perturbations of any parameters. This step is made to confirm that the coupling of the core and plant models provides a stable transient solution. The second step is to perform transient calculations for the first 5 seconds of the TT2 scenario. The TT transient calculations are followed immediately after the zero transient calculations, in the same run. This means that the TT transient starts after 10.0 seconds zero transient calculations.

In the next section the POLCA-T plant model of PB2 is explained. The model was developed in previous validations ([5],[21]). The TT simulation cases that were run are explained in section 6.2. In section 6.3 the calculation procedure of the zero transient is explained along with the results. In section 6.4 the TT2 transient simulation and results are explained.

6.1 POLCA-T PB2 plant model

The POLCA-T Reactor Pressure Vessel (RPV) and plant systems model was developed in exercise 1 of the BWR TT benchmark [2]. The development and details of the RPV and plant systems are described in [5] and [21], along with results obtained of the response of the RPV and plant model. The POLCA-T RPV nodalization of PB2 is shown in Appendix 6.

No changes were made in the POLCA-T RPV and plant model for the present study. Only required changes in the POLCA7 3D core model were made to be able to use the cell data generated by PHOENIX. The core model in the present study includes the following: 764 fuel channels and 122 radial reflector channels (divided in 24 axial nodes), top and bottom reflector albedo boundary conditions.

The PB2 plant is described by: reactor pressure vessel (RPV), recirculation loop, main steam lines, and steam bypass lines models. The RPV model includes: down comer with feed water inlet and jet pump, lower plenum with control rods guide tubes, core with bypass channel, upper plenum, standpipes, steam separators and dryers, and steam dome. The recirculation loop consists of suction and discharge coolant legs, and main circulation pump. The main steam lines consist of: steam lines, safety and relieve valves, turbine stop valves (TSV) and steam head. The steam bypass system model covers the bypass chest, valves, lines and orifice, and steam condenser [5],[21].

The balance of plant is simplified to reactor pressure controller, control rods speed and position controller, SAFIR scram controller, jet pump drive flow controller, feed water controller, RPV water level controller, four groups SAFIR safety and relief valves controller, turbine control and stop valve controller and steam bypass valve controller [5],[21].

The PB2 plant model was validated ([5],[21]) using the following boundary conditions: power vs. time table, turbine controller set-point vs. time, steam bypass valve position vs. time, and feed water mass flow vs. time. The results in [5] and [21] show good agreement with measured data for steam dome and core exit pressures, RPV water level, main steam line and turbine inlet pressures.

In the next sections, the cases run for the simulation, the zero transient and TT transient simulation using POLCA-T are explained.

6.2 Description of Turbine Trip simulation cases run

Several cases were run for the transient calculations. The tested models in the study were the simplified transient cross section model vs. the full static cross section model [37], and the influence of using the spectrum interaction (SI) model or not [38]. Five cases were finally calculated and the results are presented in section 6.3.2. The cases were the following:

Case 1: PSU cell data was used. In this case all models in POLCA7/POLCA-T for cross section corrections are disabled. The cross sections are calculated by look-up in the cross section tables using a special routine that links the PSU tables to the POLCA7/POLCA-T interpolation method.

Case 2: PHOENIX cell data was used along with the model for spectrum interaction correction. This case was calculated with the transient cross section model.

Case 3: PHOENIX cell data was used. The cross section correction model for spectrum interaction was disabled and the transient cross section model was used.

Case 4: PHOENIX cell data was used along with the model for spectrum interaction correction. This case was calculated using the static cross section model.

Case 5: PHOENIX cell data was used. The cross section correction model for spectrum interaction correction was disabled. As for case 5, the full static cross section model was used.

A summary of the cases is found in Table 6.1 below.

Table 6.1. Summary of transient calculation cases

Case	Cell Data	Spectrum Interaction	Cross section model
1	PSU	not available	special routine
2	PHOENIX	yes	transient
3	PHOENIX	no	transient
4	PHOENIX	yes	static
5	PHOENIX	no	static

The results of the different cases are presented in the next section for the zero transient calculations. The results of the TT transient simulation are presented in section 6.4.

6.3 Zero transient calculations

Before performing TT transient analysis, zero transient calculations must be performed in order to ensure that the code's solution is stable before perturbing it to simulate the "real" transient [37]. Performing a zero transient calculation means performing a transient calculation without any intentional perturbations to the system. A small perturbation normally occurs at the transition from the static to transient calculation and the system stabilizes quickly. The sources of the initial perturbations in the transition from static to transient calculation are descried in detail in [37]. A summary of [37] which is based on results from this present study is presented in the next section.

6.3.1 Static and transient cross section models

The perturbations in static to transient transition are common for all system thermal hydraulic codes, even for codes without coupled neutron kinetics. The source of the perturbations comes from the fact that in order to obtain the steady state solution, one must assume a state of mass and energy balance in the system. The balance is reached by manipulating some inlet/outlet system parameters, often fluid flows/temperatures. After making such a manipulation in the code for the first static calculation, adjustment to the input must be made in order to avoid large perturbations when going from static to transient calculations. Although adjusting the input, one cannot avoid the numerical noise which always occurs between the static and transient solution. In order to deal with this problem, zero transient calculations without perturbations must be run, to let the transient solution stabilize, before the system is perturbed by the required action in order to simulate the "real" transient. [37]

In previous versions of POLCA-T a simplified cross section model for the transient calculations was used. The transient cross section model preserves dependencies of the parameters that are important for the transient simulation (moderator density, CR positions etc.). All other cross section terms are lumped into one residual term which dependency on moderator density is tabulated [37]. The residual cross section data is then calculated by linearly interpolating (and extrapolating) in this table.

This transient cross section model works well with previous versions of POLCA-T. In the mean time the POLCA7 static cross section model was further developed and improved to deal with isotopes tracking and spectrum interaction effects. These improvements created a gap between the static and transient cross section models. When the new POLCA7 version was merged with POLCA-T, significant power oscillations occurred in the zero transient calculations when going from the static to transient calculations when using the transient cross section model. A new test version was created where the transient cross section model was replaced by the full static cross section model of POLCA7 [38]. The results are presented in the next section.

6.3.2 Results of Zero transient

The initial fission power perturbation was caused by reasons described in the previous section by the simplified transient cross section model. It is seen in Figure 6.1 that using the spectrum interaction (SI) model or not using it (NoSI) significantly influences the initial perturbation when the transient cross section model is used. The power perturbation in these two cases is significant and the powers stabilize after 6-8 seconds at power levels different from the static one. In these two cases the steam dome pressure does not stabilize at all, as seen in Figure 6.2. These results cannot be used when simulating the “real” TT transient.

The transient cross section model was replaced by the full static cross section model and the results show much more stable behavior in the transition from static to transient calculations as seen in Figure 6.1. Using the static cross section model, a very small initial perturbation occurs when the SI model is used, and the system stabilizes quickly. No initial perturbation is observed when the spectrum interaction model is not used, (NoSI). The perturbation when SI is used is caused by the sensitivity of the spectrum to changes in coolant density [37]. In these two cases, the steam dome pressure is stable during the 10 second zero transient (Figure 6.2). These results can be used when simulating the TT transient, when the TT transient calculation would start from the initial, or very close to the initial values of the test.

In the case when PSU cell data is used, the transient cross section routine is not used by POLCA-T, and the same tables are used in the static and transient calculations [37]. In this case no initial perturbation is observed in the fission power, as seen in Figure 6.1.

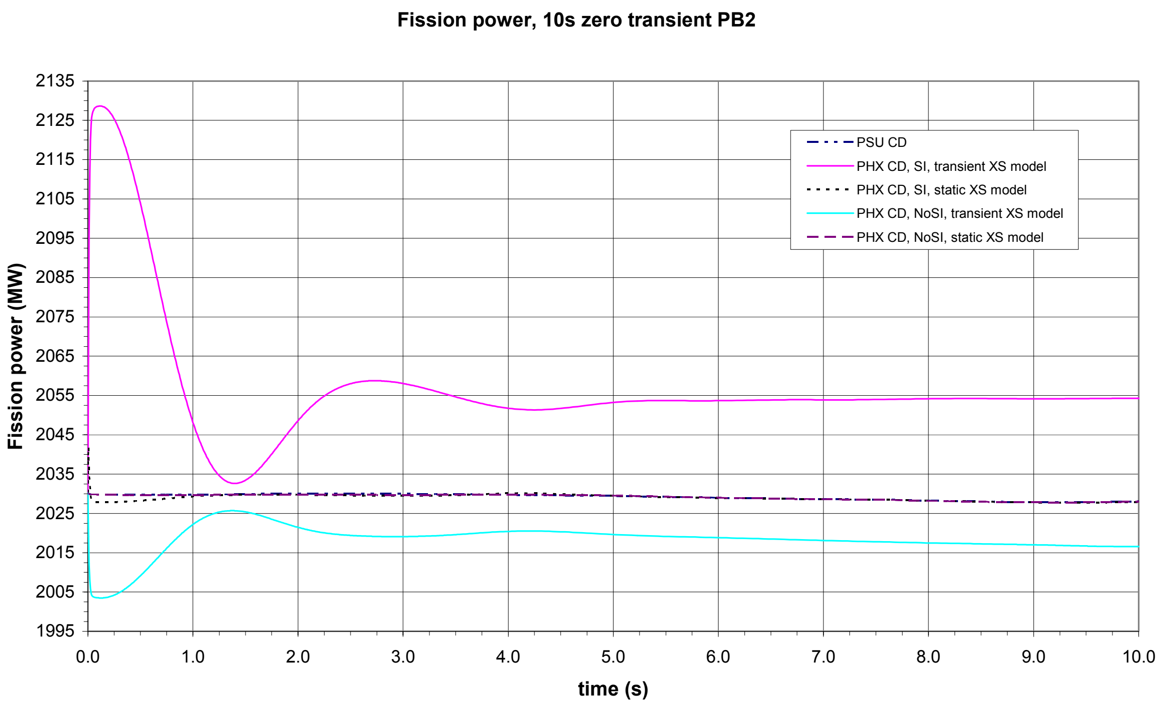

Figure 6.1. Fission power during 10 second zero transient calculations

It is observed in Figure 6.1 and Figure 6.2 that in the calculations using the simplified transient cross section model the power stabilizes at levels different from the static one, and the pressure does not stabilize at all.

For the cases with the static cross section model and the case using PSU data, the calculations have stabilized and have after 10 seconds values very close to the static ones.

The results from these three latter cases can be used for further calculations, when the TT2 transient is calculated.

In the TT transient simulation only cases 1 and 4 were calculated for the five first seconds of the transient. The reason for selecting case 4 was to be consistent with previous calculation steps, where the spectrum interaction model was used in POLCA7. The other three cases were calculated only through the power peak of the TT transient to see their influence on the results.

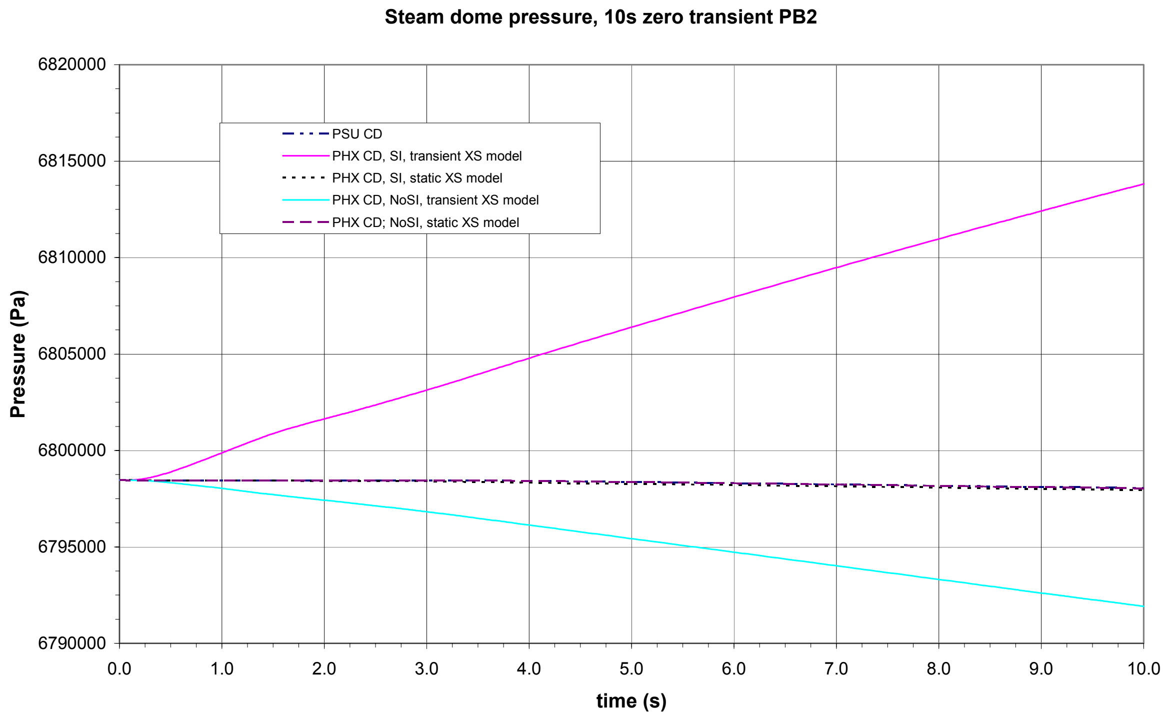

Figure 6.2. Steam dome pressure during 10 second zero transient calculations

6.4 Turbine Trip transient simulation

The TT transient experiment was initiated by a manual closure of the turbine stop valve (TSV) by the operator. The TSV closure caused a pressure wave in the main steam line that propagated into the reactor pressure vessel and the core. The TSV closure was followed by an opening of the turbine bypass valve, causing a pressure relief in the reactor system. Normally, the reactor protection scram system would be initiated immediately from the TSV position input signal. However, for the transient experiment the reactor scram system was intentionally delayed to allow a small neutron flux transient to occur. The pressure increase in the core caused a collapse of the void, which in turn provided higher moderation of neutrons and a transient increase of neutron flux. The power increase in turn provided significant changes in void and flow distributions in the core. [2]

The TT2 scenario was simulated using POLCA-T. In the simulation, the following boundary conditions were used: turbine controller set-point vs. time, bypass valve position vs. time, and feed water mass flow vs. time. The reactor scram was initiated during the experiment when the power reached 95% (3128.35 MW) of the rated power [1]. The same scram set point was used in the simulation by POLCA-T using the SAFIR controlled scram model.

Sensitivity studies have been performed in previous validations on several input parameters [5],[6],[8]. In this study, only one case with PHOENIX CD was run for the first five seconds of the TT transient due to the time limitation of the project. One of the models that must be tested in future runs is the STAV7 burnup dependent gas gap heat conductance model. In the present study, a constant gas gap heat transfer coefficient specified in the benchmark [2] was used.

6.4.1 Results of TT2 transient simulation

Two cases were calculated, one using PSU CD, and one using PHOENIX CD with the spectrum interaction model and the full static cross section model. The sequence of the events is presented in Table 6.2 for cases 1 and 4. The calculated results are compared to measured data from PB2 [1]. The results of the TT2 simulation include fission power, steam dome, core exit, main steam line and turbine inlet pressures and are presented in Figure 6.3 through Figure 6.8.

The sequence of the events in Table 6.2 show good agreement with the measured data for the power peak. The power peak is delayed 6 ms for the cases with PHOENIX CD, and 12 ms for the case with PSU CD and is visualized in Figure 6.3. In Figure 6.4 a more detailed plot of the power peak is shown. The maximum power is underestimated with 6.2% for case 4 using PHOENIX CD, and overestimated with 6.7% using PSU CD. Case 5 using no spectrum interaction and the static cross section model show better agreement with measured data than case 4 with SI. Further investigation of the use of the SI model is required in order to make final conclusions. Gas gap heat conductance will also affect the time and value of the power peak and need to be investigated too.

The calculated pressure responses are faster than the measured for all pressures compared in Table 6.2. The calculated turbine inlet and main steam line pressure initial response is 54 ms faster than the measured steam line A. The largest deviation is in the RPV pressure response which is 96 ms faster in the calculated case. The differences in initial response are visualized in Figure 6.5 through Figure 6.8.

The calculated steam dome pressures in Figure 6.5 show that the initial pressure peak is underestimated by approximately 50 kPa. The second and third pressure peaks are closer to the measured steam dome pressure. The calculated main steam line and turbine inlet pressures follow the measured pressures well during the first five seconds of the transient as seen in Figure 6.7 and Figure 6.8.

It has to be noted that the time delay of the measurements are not considered in the results. Moreover, the initial time response in steam lines A and D of the turbine differs with 24 ms and in the main steam line with 36 ms so the uncertainty of the time responses in the measurements has not been taken into account.

The pressures with the PSU CD are higher than with PHOENIX CD in all cases. This is caused by the higher and wider power peak in the case with PSU CD, which adds more energy into the reactor system, more coolant is boiled off, and the pressure becomes higher. The calculated pressures show close agreement with measured data.

The steam bypass valve was fully open 846 ms into the transient, and it is shown in the calculated cases that the first reduction in steam dome pressure follows immediately after the opening of the bypass valve.

Table 6.2. TT2 sequence of events

Event*	**Measured** time (ms)	case 4 **PHOENIX** time (ms)	case 1 **PSU** time (ms)
TSV begin to close	0	0 (48)	0 (48)
TSV closed	96	90	90
Begin bypass opening	60	60	60
Bypass full open	846	846	846
Time of scram initiation	630	576	576
Time delay prior to rod motion	120	120	120
Initiates CR insertion	750	696	696
Turbine pressure initial response	102/126**	48	48
Steam line pressure initial response	348/378**	294	294
Vessel pressure initial response	432	336	336
Core exit pressure initial response	486	438	438
Time of Power peak	726	732	738
Power peak (MW)	9190.43	8619.93	9809.62

* - Time delays of the measurements are not considered in the analyses
** - Steam lines A and D respectively

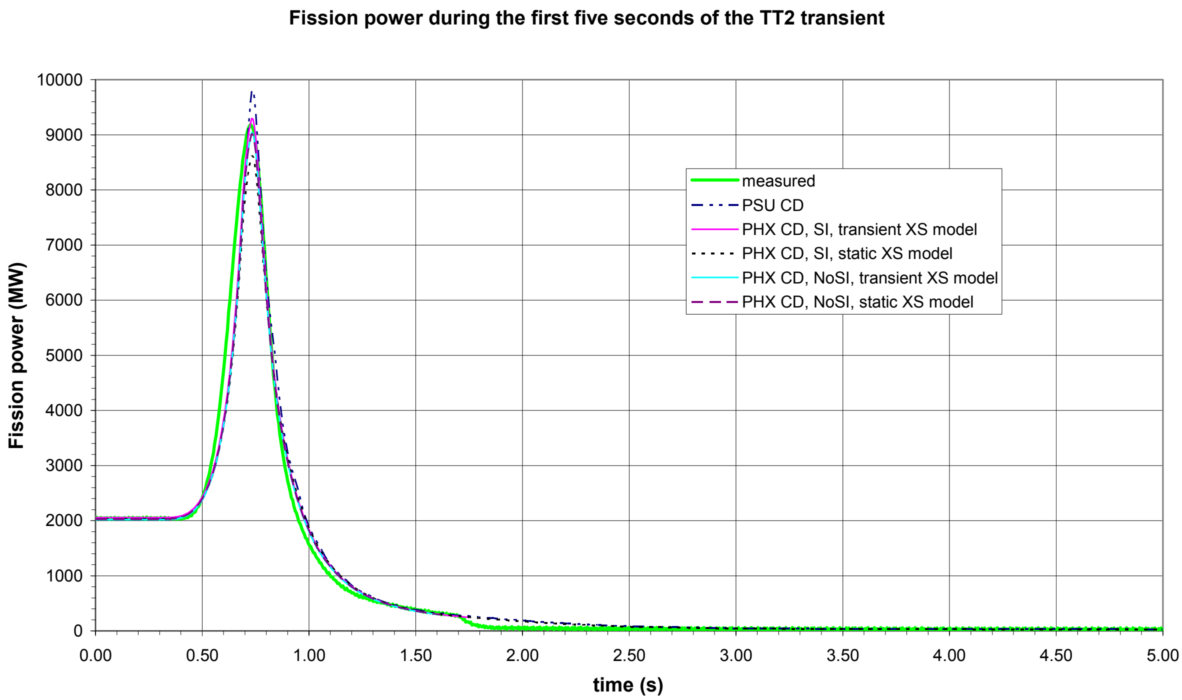

Figure 6.3. Fission power during the first five seconds of the TT2 transient

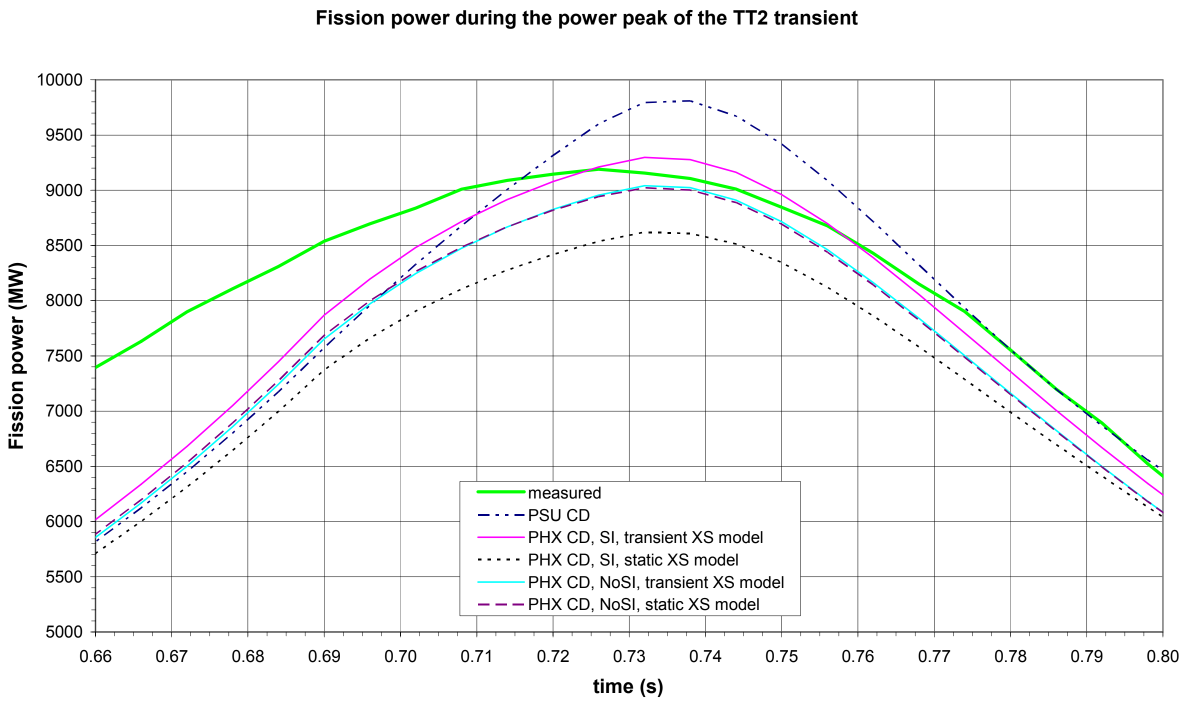

Figure 6.4. Fission power during the power peak of the TT2 transient

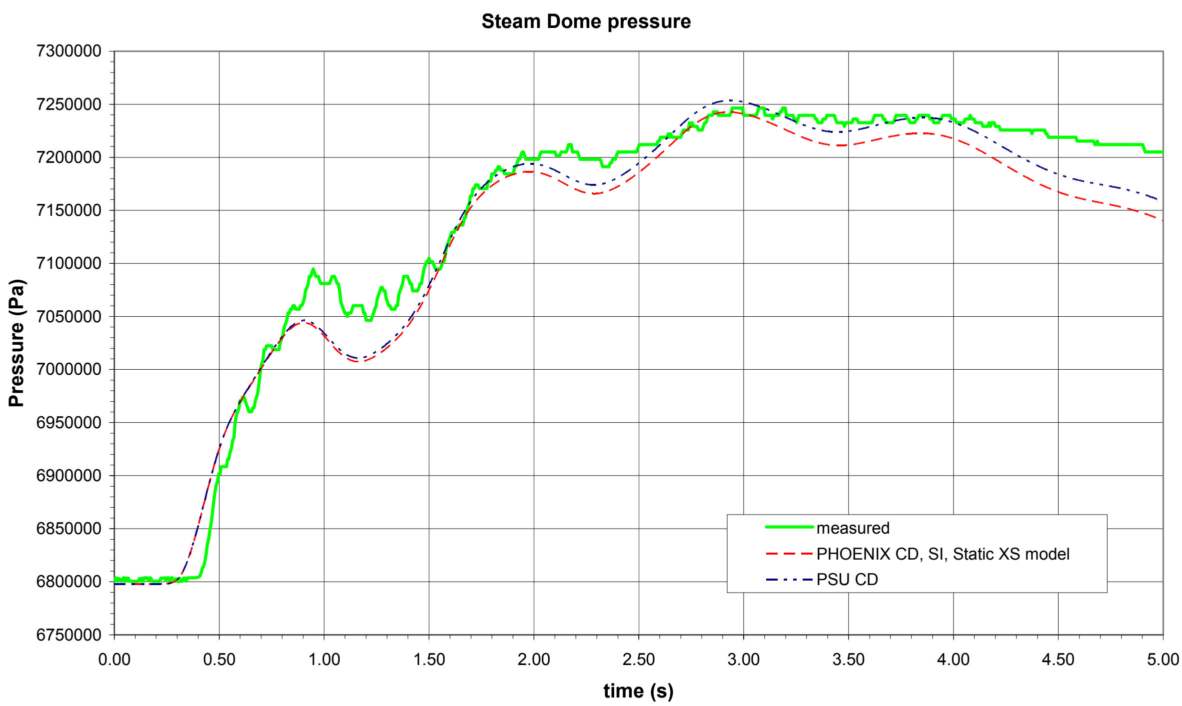

Figure 6.5. Steam dome pressure for the first five seconds of the TT2 transient

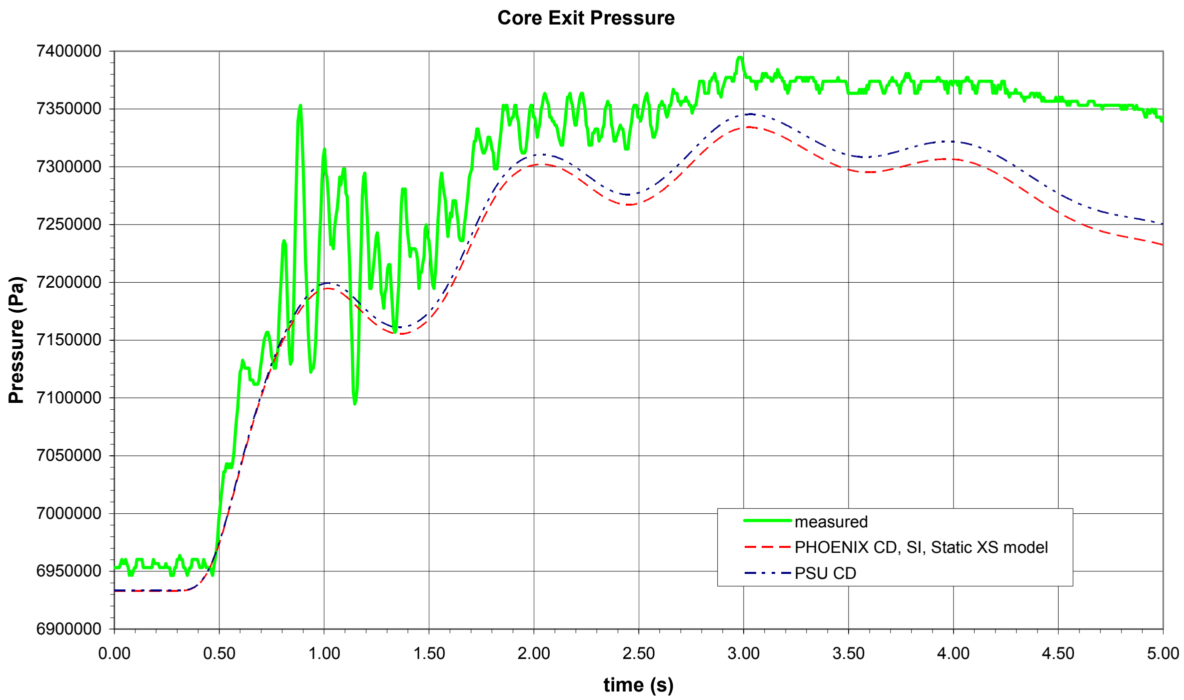

Figure 6.6. Core exit pressure for the first five seconds of the TT2 transient

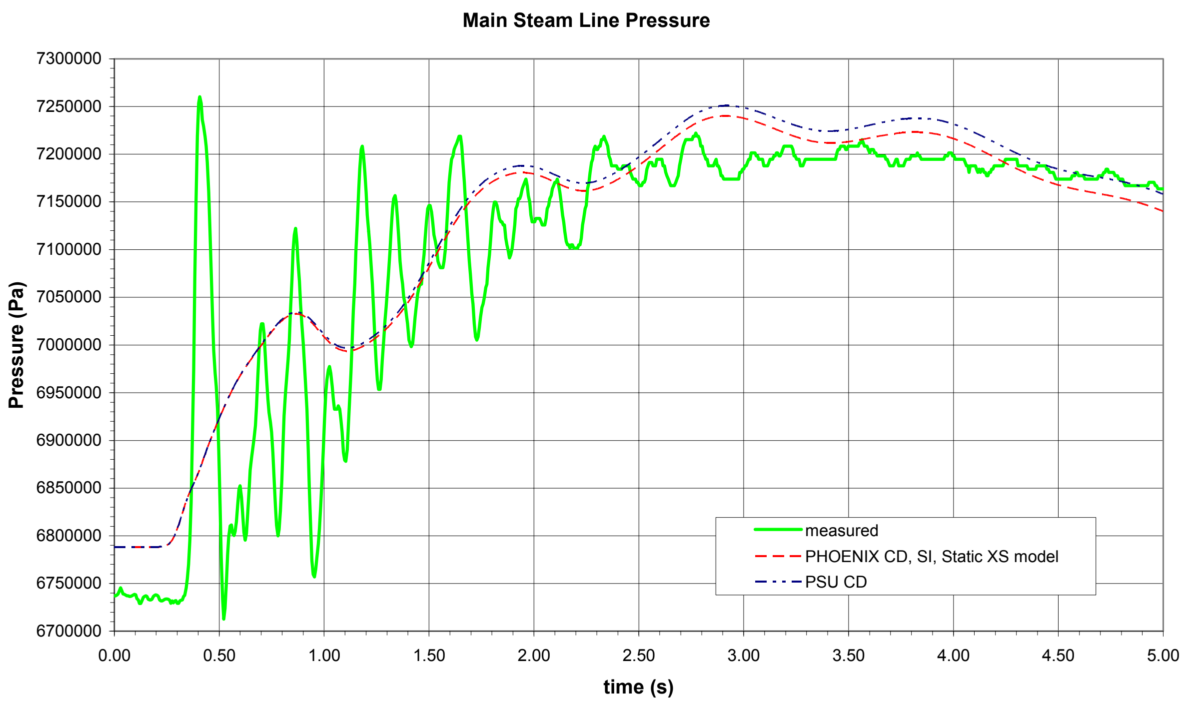

Figure 6.7. Main steam line pressure for the first five seconds of the TT2 transient

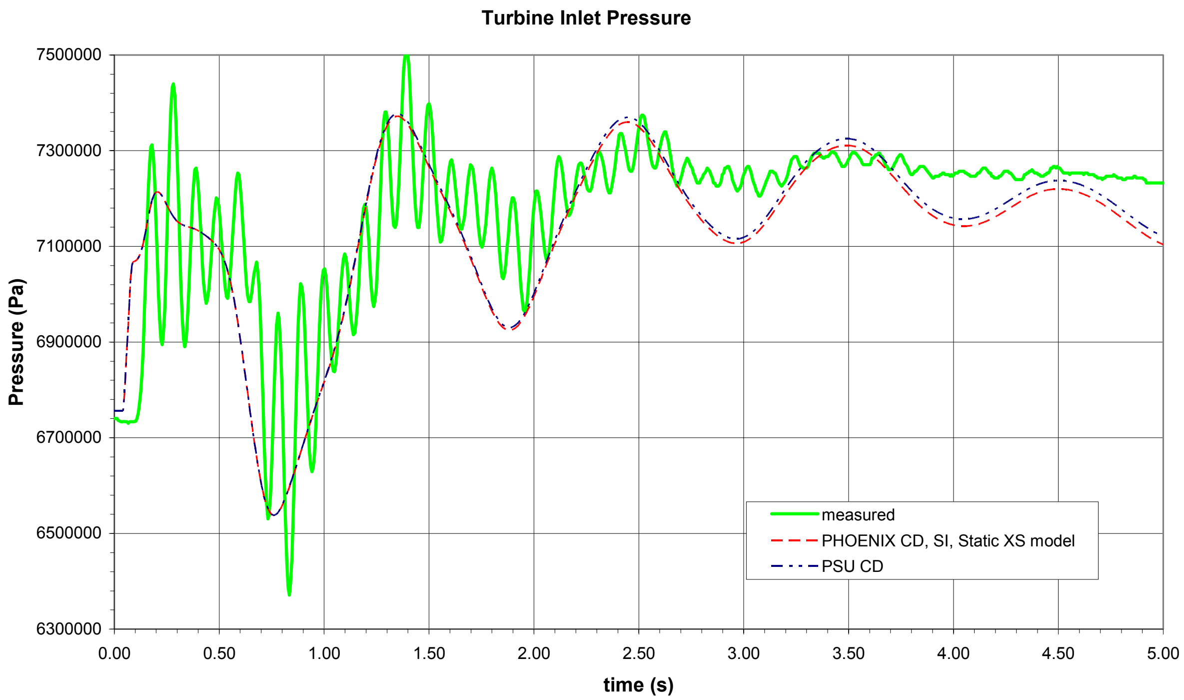

Figure 6.8. Turbine inlet pressure for the first five seconds of the TT2 transient

6.5 Conclusions

The results from the zero transient calculations show that the simplified transient cross section model in POLCA-T give large initial perturbations in the transition from static to transient calculations. The power stabilized at levels different than the initial, and the steam dome pressures did not stabilize at all when the transient cross section model was used.

When the full static cross section model was used in the zero transient calculations, very small or no initial perturbations were shown for the cases using spectrum interaction (SI), and no spectrum interaction respectively. In the case with SI the system stabilized quickly at a state very close to the initial static state.

The results of the POLCA-T Turbine Trip 2 transient simulations are in good agreement with measured results for the fission power, steam dome, core exit, main steam line and turbine inlet pressures. The results when using the cell data generated with PHOENIX (using static cross section model and SI model) showed better agreement with the measured power than the results obtained when using the PSU cell data. The power peak is slightly underestimated by POLCA-T when using PHOENIX cell data, and overestimated when using PSU cell data.

Further analysis is required of the sensitivity of the results to the SI model. The SI model was used in these calculations to be consistent with POLCA7 calculations in previous steps of the 3D transient methodology.

Further 3D analysis of the power redistribution in the core during the transient is also required. Future analysis will be performed of this phenomenon by comparing measured and calculated

LPRM signals during the transient. The time limitation of the present project did not allow such analysis.

Further analysis will also be performed where the Westinghouse STAV7 burnup dependent gas gap heat conductance model is used.

A summary of all steps and the results obtained during the 3D transient analysis are summarized in the next chapter.

7 SUMMARY

Westinghouse coupled 3D core neutron kinetics and plant systems thermal hydraulics transient code POLCA-T was validated against Peach Bottom 2 end of cycle 2 turbine trip test 2.

Five steps of 3D transient analysis were applied in this validation as follows:

- Cross section data generation
- Core depletion calculations
- Transient thermal hydraulics analysis only: initialization of plant model
- 3D core steady state analysis: initialization of 3D core model
- Coupled 3D core neutron kinetics and plant systems thermal hydraulics transient analysis.

The cross section data was generated using Westinghouse neutron transport theory and depletion code PHOENIX. Cross section data generated by PHOENIX are tabularized with dependencies in the three state parameters: exposure, coolant density, and coolant density history.

Core depletion calculations were performed for cycle 1 and cycle 2 using Westinghouse two group 3D nodal core simulator POLCA7. Core depletion calculations were performed in order to model the correct distributions of isotopes in the core for the state of the transient test.

Steady state calculations were performed with POLCA7 at the end of cycle 1 and cycle 2 in order to check the results of the depletion calculations. The calculated neutron TIP detector response was compared with measured neutron TIP detector response from Peach Bottom 2. When comparing the TIP distributions, a good overview of the neutron flux in the core is obtained. At the end of cycle 2 prior to the turbine trip tests, the calculated TIP response showed good agreement with the measured TIP response.

The plant systems model was developed in previous validations, and it is independent of the cross section model used. Hence this step was not repeated in the present validation. However, in order to study and understand the observed power perturbations in the zero transient calculations a case with thermal hydraulic plant analysis has been run too. Only required changes in the POLCA7 3D core model were made to be able to use the cell data generated by PHOENIX.

The core model was initialized by performing Hot Zero Power calculations. The results from the Hot Zero Power calculations showed good agreement with previous calculations using PSU cross section data for the core average axial power shape.

Hot Full Power calculations were performed using both POLCA7 and POLCA-T for the Turbine Trip 2 initial state. The results obtained with POLCA7 and POLCA-T showed better agreement with the P1 edit when using PHOENIX cross section data compared to when using PSU cross section data. Differences between POLCA7 and POLCA-T bypass flow rates were obtained, and the main reason was that POLCA-T models flow through the control rod guide tubes, while POLCA7 does not do it for GE reactors. The effects of these differences showed negligible effect on the obtained results. The radial power distributions showed better agreement than in the Hot Zero Power case between the two different cell data; further analysis of the radial power distributions are required however.

Transient analysis with POLCA-T was the final step, and different cases were run in order to see the influence of different cross section models and cross section correction options. The results from the zero transient calculations show that the simplified transient cross section model in POLCA-T give large initial perturbations in the transition from static to transient calculations, and it does not show consistency with the full static cross section model. The transient cross section model was replaced by the full static cross section model, and the perturbations caused in the transition from static to transient calculations were negligible in this case.

The results of the POLCA-T Turbine Trip 2 transient simulations are in good agreement with measured results for the fission power, steam dome, core exit, main steam line and turbine inlet pressures. The results with PHOENIX cell data showed better agreement with the measured power than with PSU cell data. The power peak is slightly underestimated by POLCA-T when using PHOENIX cell data, and overestimated when using PSU cell data.

Further 3D analysis of the power redistribution in the core during the transient will be performed by comparing measured and calculated LPRM signals. The time limitation of the present project did not allow such analysis.

Further analysis will also be performed where the Westinghouse STAV7 burnup dependent gas gap heat conductance model is used. In the present project a constant value for the gas gap heat conductance specified in the benchmark [2] was used.

8 REFERENCES

[1] EPRI NP-564, Research Project 1020-1, Topical Report, June 1978
Transient and Stability Tests at Peach Bottom Atomic Power Station Unit 2 at End of Cycle 2
L.A. Carmichael, R.O. Niemi

[2] OECD Nuclear Energy Agency Nuclear Science Committee DOC(2001)1
Boiling Water Reactor Turbine Trip Benchmark Vol. I: Final specifications, Revision.1 October 2001
J. Solis et. Al

[3] Westinghouse Atom AB Report BTU 02-038, Rev 0
POLCA-T: Validation against Peach Bottom 2 End of Cycle 2 Low-Flow Stability Tests
D. Panayotov

[4] Nuclear Mathematical and Computational Sciences: A Century in Review, A Century Anew; Gatlinburg, Tennessee, April 6-11, 2003
POLCA-T CODE VALIDATION AGAINST PEACH BOTTOM 2 END OF CYCLE 2 LOW-FLOW STABILITY TESTS
D. Panayotov, M. Thunman

[5] PHYSOR 2002; Seoul, Korea, October 7-10, 2002
OECD/NRC BWR TURBINE TRIP BENCHMARK: SIMULATION BY POLCA-T CODE
D. Panayotov

[6] TOP FUEL 2003
POLCA-T – Consistent BWR Core and Systems Modeling
D. Panayotov, U. Bredolt, P. Jerfsten

[7] PHYSOR 2004; Chicago, Illinois, April 25-29, 2004
POLCA-T Simulation of OECD/NRC BWR Turbine Trip Benchmark Exercise 3 Best Estimate Scenario TT2 Test and Four Extreme Scenarios
D. Panayotov

[8] Nuclear Science and Engineering, Vol. 148 pp. 247-255, October 2004
OECD/NRC BWR Turbine Trip Benchmark: Simulation by POLCA-T Code
D. Panayotov

[9] Westinghouse Atom AB Report BTU 01-149, Rev 0
Computer Code description, BWR application
F. Schliephacke

[10] Westinghouse Atom AB Report UR 90-323, Rev 8
IFIGEN – User's manual to the input generator for PHOENIX
Ö. Hammarström

[11] Westinghouse Electric Sweden AB Report BTF 01-157, Rev 1
Standardized BWR cell data generation for CM2
W. Linderoth

[12] Westinghouse Atom AB Report UR 90-216, Rev 6
Cell-data files – the service program TABBE
J. Bujak

[13] Westinghouse Electric Sweden AB Report BR 95-924, Rev 22
POLIN - Input Processor of POLCA7
S-Ö Lindahl

[14] Westinghouse Atom AB Report BR 94-1061, Rev 3
POLCA7 – Data and Calculational Flow
S-Ö Lindahl

[15] Westinghouse Atom AB Report BCM 97-246, Rev 6
POLDIS – Distribution file service program for POLCA7
K. Tammemäe

[16] Westinghouse Atom AB Report BCM 98-113 Rev. 2
SKYFFEL – Shuffling program for POLCA7
K. Tammemäe

[17] Westinghouse Atom AB Report SES 02-061, Rev 1
POLCA-T User Guide
U. Bredolt

[18] Westinghouse Atom AB Report SES 03-019, Rev 1
POLCA-T, Input Reference Manual
U. Bredolt

[19] Westinghouse Atom AB Report BCM 98-040
CoreLink Methodology
E. Müller

[20] Study material, Royal Institute of Technology (KTH), Stockholm, 2003/2004
Fission and Reactor Physics
P. Persson

[21] OECD/NRC BWR Turbine Trip Benchmark – Third Workshop, Dresden, Germany, May 28-29, 2002
OECD BWR TT Benchmark Exercise 1: Final Results obtained with POLCA-T code
D. Panayotov

[22] ABB Atom AB Report UR 85-194, Rev 5
PHOENIX – USER’s guide
R. Stamm’ler

[23] ABB Atom AB Report BR 92-054, Rev 1
Standardization of PHOENIX calculations
A. Larsson

[24] EPRI NP-563, Research Project 1020-1, Topical Report, June 1978
Core Design and Operating Data for Cycles 1 and 2 of Peach Bottom 2
N.H. Larsen

[25] ABB Atom AB Report BCM 97-166, Rev 0
Cell Data Block – Newsletter
W. Lipiec

[26] Private communication 2004
Dr. Waldemar Lipiec, BTU, Westinghouse Electric Sweden AB

[27] Private communication 2004
Dr. Dobromir Panayotov, BTU, Westinghouse Electric Sweden AB

[28] Private communication 2004
Dr. Erwin Müller, BTU, Westinghouse Electric Sweden AB

[29] Westinghouse Atom AB Report BTU 03-015 Rev 0
Generic BWR Nodal Reflector Data
E. Müller

[30] Westinghouse Atom AB Report BR 94-715, Rev 3
POLCA7 – Fuel Depletion
S-Ö Lindahl

[31] Study material, Royal Institute of Technology (KTH), Stockholm, 2004
Lectures on Applied Reactor Technology and Nuclear Power Safety
H. Anglart

[32] ABB Atom AB Report BCM 98-139, Rev 0
POLCA7 – Thermal Hydraulics Correlations
S-Ö Lindahl

[33] Westinghouse Atom AB Report BR 94-700, Rev 2
POLCA7 – BWR Thermal Hydraulics Model
S-Ö Lindahl

[34] Westinghouse Atom AB Report BTA 03-128, Rev 0
Thermal-Hydraulic input data to POLCA7 in the CM2 environment – general advises
P. Wiman

[35] Private Communication 2004
Prof. Kostadin N. Ivanov, Pennsylvania State University

[36] OECD/NRC BWR Turbine Trip Benchmark – Fifth Workshop, Barcelona, Spain
Content and Format of the Final Report on EXERCISE 2 & Comparative Analysis of the Final Results of EXERCISE 2
B. Akdeniz, J. Vedovi, Pennsylvania State University

[37] Westinghouse Electric Sweden AB Memorandum BTU 04-104, Rev 0
POLCA-T Transient XS Model: Problems and Solutions
D. Panayotov

[38] Westinghouse Atom AB Report BR 94-712, Rev 5
POLCA7 Cross Section Model
S-Ö Lindahl

APPENDIX 1 – PROCESS PARAMETERS FOR CYCLE 1 AND CYCLE 2

date	Power MWt	Flow (w) Mlb/hr	Flow (w) kg/s	subcooling Btu/lb	subcooling kJ/kg	# of notches inserted
740112	0	41	5166	15	34.89	> 4500
740114	546	41	5166	15	34.89	> 4500
740115	537	41	5166	15	34.89	> 4500
740116	557	41	5166	15	34.89	> 4500
740118	579	41	5166	15	34.89	> 4500
740119	0	41	5166	15	34.89	> 4500
740214	0	41	5166	15	34.89	> 4500
740215	156	41	5166	15	34.89	> 4500
740216	212	41	5166	15	34.89	> 4500
740217	222	41	5166	15	34.89	> 4500
740218	535	41	5166	15	34.89	> 4500
740219	757	51	6426	15	34.89	1910
740220	757	63	7938	12	27.912	1910
740221	757	40.5	5103	18	41.868	1910
740222	757	39.5	4977	17	39.542	1910
740223	902	63.5	8001	14	32.564	1844
740224	1023	76	9576	12.5	29.075	1844
740225	1023	80.5	10143	11.5	26.749	1844
740226	1023	87	10962	11	25.586	1844
740227	1136	94	11844	10.5	24.423	1834
740228	1136	101.5	12789	9.5	22.097	1844
740301	1101	102	12852	9	20.934	1866
740302	1118	99.5	12537	9.5	22.097	1528
740303	1129	58.5	7371	17.5	40.705	1194
740304	1002	71	8946	13.5	31.401	1844
740305	646	78	9828	11	25.586	1844
740306	0	78	9828	11	25.586	> 4500
740309	0	44	5544	18.5	43.031	> 4500
740310	238	44	5544	18.5	43.031	2244
740311	699	30.5	3843	16.5	38.379	2066
740312	218	38	4788	14	32.564	2378
740313	356	38	4788	12.5	29.075	2344
740314	56	38	4788	16.25	37.7975	> 4500
740315	735	41	5166	20	46.52	2022
740316	1122	67	8442	15	34.89	1867
740317	1325	42	5292	26	60.476	1018
740318	1269	73.5	9261	17.75	41.2865	1018
740319	0	73.5	9261	17.75	41.2865	> 4500
740328	0	69	8694	19	44.194	> 4500
740329	167	69	8694	19	44.194	> 4500
740330	958	69	8694	19	44.194	> 4500
740331	1301	69	8694	19	44.194	> 4500
740401	1556	69	8694	19	44.194	910
740402	1720	87.25	10993.5	16.5	38.379	910
740403	1862	105.5	13293	14.5	33.727	910
740404	1844	105.5	13293	13.5	31.401	910
740405	1733	105.5	13293	13.5	31.401	910
740406	1611	78	9828	15.5	36.053	910
740407	1544	75	9450	17.5	40.705	910
740408	0	75	9450	17.5	40.705	> 4500
740409	0	52	6552	8	18.608	> 4500
740410	284	52	6552	8	18.608	2422
740411	940	43	5418	22.5	52.335	1844
740412	1596	69	8694	21	48.846	930
740413	1698	86	10836	16.5	38.379	910
740414	1800	105	13230	14.5	33.727	930
740415	1433	97.5	12285	14	32.564	1033
740416	378	28.5	3591	27	62.802	1033
740417	31	28.5	3591	27	62.802	> 4500
740418	1133	53.5	6741	20.5	47.683	1549
740419	1655	31.5	3969	37.5	87.225	771
740420	1811	44.5	5607	34	79.084	642
740421	2022	83.5	10521	27.5	63.965	642
740422	2233	74.5	9387	23.5	54.661	642
740423	2411	90	11340	21.5	50.009	642
740424	2589	107	13482	18.5	43.031	642
740425	2256	107	13482	18.5	43.031	642
740426	2367	100	12600	19	44.194	642
740427	1933	27.5	3465	48	111.648	642
740428	633	80	10080	25	58.15	> 4500
740429	133	60.25	7591.5	21.625	50.29975	> 4500
740430	582	40.5	5103	18.25	42.4495	2150
740501	333	43	5418	25.5	59.313	> 4500
740502	189	43	5418	25.5	59.313	> 4500
740503	1111	43	5418	25.5	59.313	1878

date	Power MWt	Flow (w) Mlb/hr	Flow (w) kg/s	subcooling Btu/lb	subcooling kJ/kg	# of notches inserted
740504	1483.5	38	4788	32.5	75.595	1211
740505	1856	38	4788	45	104.67	684
740506	2111	53.5	6741	33	76.758	590
740507	2366	67	8442	28	65.128	590
740508	2600	88	11088	24.5	56.987	590
740509	2433	94	11844	22	51.172	590
740510	1944	43	5418	39.5	91.877	488
740511	2156	50	6300	37	86.062	488
740512	2388	66	8316	30.25	70.3615	488
740513	2611	72.5	9135	28.5	66.291	488
740514	2933	105.5	13293	22.5	52.335	488
740515	2679	109.5	13797	22	51.172	488
740516	2067	59.5	7497	28.5	66.291	488
740517	1656	58	7308	29	67.454	600
740518	422	41.5	5229	24	55.824	> 4500
740519	444	41.5	5229	24	55.824	2333
740520	1711	51	6426	31	72.106	1060
740521	2181	56.5	7119	33.75	78.5025	711
740522	2137	46	5796	39	90.714	578
740523	2455	59.5	7497	34.25	79.6655	560
740524	2810	80.6	10155.6	27.75	64.5465	544
740525	3110	98	12348	25	58.15	544
740526	3032	105	13230	23	53.498	544
740527	911	26.5	3339	54.5	126.767	544
740528	1422	66.5	8379	17.3	40.2398	1790
740529	711	66.5	8379	17.3	40.2398	> 4500
740530	0	66.5	8379	17.3	40.2398	> 4500
740604	0	42.4	5342.4	21.3	49.5438	> 4500
740605	144	42.4	5342.4	21.3	49.5438	2322
740606	1644	65.75	8284.5	22.5	52.335	1622
740607	2389	67	8442	30.4	70.7104	678
740608	2855	73	9198	30.4	70.7104	544
740609	3167	98	12348	23.75	55.2425	544
740610	1640	103.5	13041	23.25	54.0795	544
740611	1530	60	7560	30.5	70.943	800
740612	2190	63	7938	29.75	69.1985	778
740613	2567	66.25	8347.5	31.25	72.6875	555
740614	2877	80	10080	28	65.128	555
740615	2710	70.25	8851.5	28.5	66.291	555
740616	3209	103.5	13041	25	58.15	586
740617	3261	107	13482	23	53.498	586
740618	3255	107	13482	22.5	52.335	586
740619	3255	106.25	13387.5	22.5	52.335	586
740620	3133	99.5	12537	24.5	56.987	586
740621	2800	100	12600	24	55.824	> 4500
740622	0	41.5	5229	25.25	58.7315	> 4500
740623	867	41.5	5229	25.25	58.7315	2144
740624	2011	58.25	7339.5	30.25	70.3615	1144
740625	2555	59.5	7497	33.5	77.921	883
740626	2844	77.75	9796.5	29.5	68.617	622
740627	3156	93	11718	26.5	61.639	586
740628	3278	98.5	12411	25.6	59.5456	586
740629	3300	99.75	12568.5	25	58.15	586
740630	3293	101	12726	25	58.15	586
740701	3293	99	12474	24.5	56.987	586
740702	3190	97.75	12316.5	25	58.15	586
740703	2020	58.75	7402.5	30	69.78	860
740704	2790	75	9450	28.5	66.291	644
740705	3010	80.5	10143	28.5	66.291	600
740706	3263	96.25	12127.5	24.25	56.4055	611
740707	3276	97.75	12316.5	24.5	56.987	611
740708	3276	97.75	12316.5	24.5	56.987	611
740709	3283	97.5	12285	24.75	57.5685	611
740710	3283	96.5	12159	25.5	59.313	645
740711	3270	96.75	12190.5	25.5	59.313	645
740712	3278	96.25	12127.5	25.5	59.313	645
740713	3278	97.5	12285	25.25	58.7315	678
740714	3287	97.5	12285	25.25	58.7315	678
740715	3286	96.25	12127.5	25.25	58.7315	678
740716	3286	96.25	12127.5	25.25	58.7315	678
740717	3290	96.25	12127.5	25.25	58.7315	678
740718	3290	96.25	12127.5	25.25	58.7315	678
740719	3290	96.25	12127.5	25.25	58.7315	678
740720	3033	88.625	11166.75	28.5	66.291	678
740721	2871	81	10206	28.5	66.291	678

date	Power MWt	Flow (w) Mlb/hr	Flow (w) kg/s	subcooling Btu/lb	subcooling kJ/kg	# of notches inserted
740722	2867	93.5	11781	25.5	59.313	678
740723	1473	56.75	7150.5	21.25	49.4275	> 4500
740724	2167	56.75	7150.5	21.25	49.4275	1988
740725	2167	57.625	7260.75	29	67.454	1422
740726	2176	58.5	7371	32	74.432	910
740727	2176	82.5	10395	27	62.802	910
740728	2176	90	11340	25.5	59.313	910
740729	2789	103.75	13072.5	23.5	54.661	910
740730	2789	104.5	13167	22.5	52.335	910
740731	3290	105.5	13293	22.5	52.335	910
740801	3207	107	13482	22.25	51.7535	910
740802	3082	106.5	13419	22.25	51.7535	910
740803	2494	69	8694	34.25	79.6655	900
740804	2722	70	8820	34.25	79.6655	900
740805	2800	71	8946	34.25	79.6655	900
740806	3068	90.25	11371.5	29	67.454	910
740807	3238	99	12474	26	60.476	910
740808	3250	102	12852	25	58.15	910
740809	3274	101.5	12789	25	58.15	910
740810	3293	100.75	12694.5	25	58.15	910
740811	3293	100.75	12694.5	25.25	58.7315	910
740812	3293	102.75	12946.5	24.5	56.987	930
740813	3280	102	12852	24.5	56.987	930
740814	3290	103	12978	23.75	55.2425	930
740815	3293	103	12978	23.75	55.2425	930
740816	3293	102.5	12915	24	55.824	930
740817	3292	103.1	12990.6	23.8	55.3588	984
740818	3293	103.5	13041	23.75	55.2425	984
740819	3293	104.5	13167	23.75	55.2425	984
740820	3278	104	13104	23.75	55.2425	984
740821	3275	103.5	13041	23.75	55.2425	984
740822	3275	102	12852	23.75	55.2425	984
740823	3275	103.25	13009.5	23.75	55.2425	984
740824	3270	101.75	12820.5	24.5	56.987	984
740825	3221	98.25	12379.5	25.25	58.7315	984
740826	3238	98	12348	26	60.476	984
740827	2554	65.25	8221.5	36	83.736	1050
740828	2967	79.75	10048.5	32.25	75.0135	1070
740829	3178	94.5	11907	27.5	63.965	1070
740830	3202	102.75	12946.5	24.5	56.987	1070
740831	3269	103	12978	24.75	57.5685	1070
740901	3290	101.75	12820.5	24.75	57.5685	1080
740902	3290	100.75	12694.5	25	58.15	1080
740903	3293	100	12600	25	58.15	1080
740904	3293	100.25	12631.5	25	58.15	1115
740905	3290	100.5	12663	24.75	57.5685	1115
740906	3293	100.75	12694.5	25	58.15	1115
740907	3293	101	12726	25.5	59.313	1115
740908	3293	100.75	12694.5	25	58.15	1115
740909	3287	99.75	12568.5	25	58.15	1115
740910	3275	101	12726	24.5	56.987	1144
740911	3275	100.75	12694.5	24.5	56.987	1144
740912	3280	100.5	12663	24.75	57.5685	1144
740913	3212	100	12600	25	58.15	1144
740914	588	74.5	9387	25	58.15	> 4500
740915	311	74.5	9387	25	58.15	> 4500
740916	539	74.5	9387	13.25	30.8195	2617
740917	1845	63.25	7969.5	28.5	66.291	1592
740918	2340	62.5	7875	31	72.106	1447
740919	2611	77.75	9796.5	27	62.802	1441
740920	2723	83.25	10489.5	26	60.476	1347
740921	2725	87.25	10993.5	25.25	58.7315	1347
740922	2725	87	10962	25	58.15	1347
740923	1289	87.25	10993.5	25.25	58.7315	1347
740924	2133	63.25	7969.5	32	74.432	1547
740925	2667	73	9198	32	74.432	1470
740926	2800	85	10710	28.5	66.291	1481
740927	2800	89.5	11277	27	62.802	1481
740928	2511	59	7434	37	86.062	1470
740929	2527	61.5	7749	36	83.736	1414
740930	2778	74.75	9418.5	32.5	75.595	1440
741001	2788	74.5	9387	31.5	73.269	1440
741002	2822	77.5	9765	32.5	75.595	1440
741003	2716	79	9954	31	72.106	1440
741004	2756	78.5	9891	35	81.41	1440

date	Power MWt	Flow (w) Mlb/hr	Flow (w) kg/s	subcooling Btu/lb	subcooling kJ/kg	# of notches inserted
741005	1978	58.8	7408.8	31	72.106	1487
741006	2745	76.5	9639	31.5	73.269	1440
741007	2790	75	9450	32	74.432	1385
741008	3000	79	9954	32.5	75.595	1385
741009	3110	88.5	11151	29.5	68.617	1385
741010	3160	93	11718	29	67.454	1403
741011	3060	96	12096	28.5	66.291	1403
741012	2430	61	7686	33.75	78.5025	1403
741013	2910	78.5	9891	31.25	72.6875	1403
741014	3150	89.5	11277	29	67.454	1403
741015	1567	94.5	11907	29	67.454	1403
741016	1595	57.5	7245	29	67.454	1838
741017	0	57.5	7245	29	67.454	> 4500
741019	0	60	7560	37.5	87.225	> 4500
741020	1865	60	7560	37.5	87.225	2260
741021	2310	60	7560	32.5	75.595	1626
741022	2850	79.5	10017	27.75	64.5465	1560
741023	1865	99.5	12537	24	55.824	1560
741024	730	43.5	5481	24.5	56.987	2182
741025	2430	64.5	8127	28.5	66.291	1804
741026	2955	93	11718	24.5	56.987	1592
741027	2890	93.5	11781	24	55.824	1592
741028	2677	62	7812	32.5	75.595	1514
741029	2656	67.5	8505	31.5	73.269	1537
741030	2682	72	9072	30	69.78	1548
741031	3033	86.5	10899	27.5	63.965	1548
741101	3240	101	12726	23.5	54.661	1548
741102	3275	104	13104	23	53.498	1548
741103	3280	105.75	13324.5	23	53.498	1548
741104	3289	105.75	13324.5	23	53.498	> 4500
741105	0	60	7560	23	53.498	> 4500
741108	0	60	7560	19.75	45.9385	> 4500
741109	225	60	7560	19.75	45.9385	> 4500
741110	1378	60	7560	19.75	45.9385	2521
741111	1890	59.25	7465.5	27	62.802	2038
741112	2390	58	7308	30	69.78	1703
741113	2640	69.5	8757	30	69.78	1592
741114	3000	86	10836	26.5	61.639	1574
741115	3225	95.5	12033	25	58.15	1574
741116	1744	51.25	6457.5	34	79.084	1574
741117	1930	59.75	7528.5	27.5	63.965	1904
741118	2875	70.75	8914.5	30.75	71.5245	1574
741119	3120	86.75	10930.5	26.5	61.639	1574
741120	3240	99	12474	23.5	54.661	1574
741121	3266	102.5	12915	23.5	54.661	1574
741122	3278	104	13104	23.5	54.661	1574
741123	3278	104.5	13167	23.5	54.661	1574
741124	3280	104.25	13135.5	23.5	54.661	1574
741125	3280	104	13104	23.5	54.661	1574
741126	3280	103.25	13009.5	23.5	54.661	1574
741127	3285	103	12978	23.5	54.661	1574
741128	3290	102.5	12915	23.5	54.661	1574
741129	2922	102.5	12915	23.5	54.661	1574
741130	0	102.5	12915	23.5	54.661	> 4500
741201	0	49.75	6268.5	19	44.194	> 4500
741202	644	49.75	6268.5	19	44.194	2850
741203	2149	59.5	7497	23.5	54.661	2427
741204	2231	79	9954	23.25	54.0795	1971
741205	2313	89.5	11277	21.75	50.5905	1904
741206	1996	48.75	6142.5	35.5	82.573	1714
741207	1767	40	5040	37.5	87.225	1804
741208	1996	44.5	5607	37	86.062	1770
741209	2386	57.25	7213.5	32.5	75.595	1712
741210	2733	75.5	9513	28.5	66.291	1712
741211	3064	97.5	12285	24	55.824	1712
741212	3255	104.5	13167	22.75	52.9165	1712
741213	3255	106.5	13419	22.75	52.9165	1712
741214	3255	107	13482	22.75	52.9165	1712
741215	3250	106.25	13387.5	22.75	52.9165	1712
741216	3000	106.5	13419	22.75	52.9165	1712
741217	2900	92	11592	25.25	58.7315	1712
741218	3188	102.5	12915	23.5	54.661	1712
741219	2778	70.25	8851.5	28.5	66.291	1712
741220	3227	70.25	8851.5	28.5	66.291	n/a
741221	2889	70.25	8851.5	28.5	66.291	n/a

date	Power MWt	Flow (w) Mlb/hr	Flow (w) kg/s	subcooling Btu/lb	subcooling kJ/kg	# of notches inserted
741222	2322	70.25	8851.5	28.5	66.291	n/a
741223	3044	84.5	10647	27.75	64.5465	1712
741224	3236	98.5	12411	24.75	57.5685	1712
741225	3255	104	13104	23	53.498	1712
741226	3267	105	13230	23.25	54.0795	1712
741227	3267	104.5	13167	23.25	54.0795	1712
741228	3267	104.5	13167	23.5	54.661	1712
741229	3267	105	13230	23.5	54.661	1712
741230	3277	104	13104	23.5	54.661	1712
741231	3277	103.5	13041	24	55.824	1712
750101	3214	100.5	12663	24	55.824	1712
750102	3191	99	12474	23.75	55.2425	1712
750103	2735	91	11466	26	60.476	1712
750104	2568	53.25	6709.5	34.5	80.247	1712
750105	3202	98.5	12411	25.25	58.7315	1712
750106	3269	102.5	12915	23.75	55.2425	1712
750107	3280	103.5	13041	23.75	55.2425	1712
750108	3280	103	12978	23.75	55.2425	1712
750109	3280	102.25	12883.5	24	55.824	1712
750110	3280	101.5	12789	24	55.824	1712
750111	3270	101.75	12820.5	23.75	55.2425	1712
750112	3224	101	12726	24	55.824	1712
750113	3273	101.5	12789	24	55.824	1712
750114	2780	101	12726	24	55.824	1712
750115	0	44	5544	24	55.824	> 4500
750123	0	44	5544	17	39.542	> 4500
750124	978	44	5544	17	39.542	3496
750125	2035	60.25	7591.5	28.25	65.7095	2327
750126	2486	62.5	7875	32.5	75.595	1710
750127	2735	70	8820	31	72.106	1710
750128	3013	85	10710	27.25	63.3835	1680
750129	3224	101.5	12789	24	55.824	1710
750130	3247	101.5	12789	24	55.824	1710
750131	3224	101	12726	24.5	56.987	1710
750201	3275	101.75	12820.5	24	55.824	1710
750202	3275	104	13104	24	55.824	1710
750203	3275	103.5	13041	24	55.824	1710
750204	3275	104	13104	23.75	55.2425	1710
750205	3275	104.25	13135.5	23.75	55.2425	1710
750206	3275	104	13104	23.75	55.2425	1710
750207	3275	104	13104	24	55.824	1710
750208	3275	104	13104	24	55.824	1710
750209	3280	104	13104	24	55.824	1710
750210	3144	98.5	12411	24	55.824	n/a
750211	2982	93	11718	24	55.824	n/a
750212	0	46.25	5827.5	24	55.824	> 4500
750220	0	46.25	5827.5	25	58.15	> 4500
750221	756	46.25	5827.5	25	58.15	2951
750222	2011	56.75	7150.5	31	72.106	2171
750223	2471	66.5	8379	31	72.106	1737
750224	2922	76.5	9639	31	72.106	1637
750225	3200	92.5	11655	26.25	61.0575	1637
750226	3267	101.5	12789	24.5	56.987	1660
750227	3278	99.5	12537	24.5	56.987	1660
750228	3289	101.25	12757.5	24.5	56.987	1660
750301	3293	100.5	12663	24	55.824	1660
750302	3293	100.75	12694.5	24	55.824	1660
750303	3293	101	12726	24	55.824	1660
750304	3293	100.75	12694.5	24	55.824	1660
750305	3293	101.25	12757.5	24	55.824	1660
750306	3293	101.75	12820.5	24	55.824	1660
750307	3293	102.25	12883.5	24	55.824	1660
750308	3293	101.25	12757.5	24	55.824	1660
750309	3293	101.5	12789	24	55.824	1660
750310	3293	101.75	12820.5	24	55.824	1660
750311	3293	101.75	12820.5	24	55.824	1660
750312	3293	102.25	12883.5	24	55.824	1660
750313	3293	102.5	12915	24	55.824	1660
750314	3293	102.25	12883.5	24	55.824	1660
750315	3293	104	13104	24	55.824	1660
750316	3293	103	12978	24	55.824	1660
750317	3293	103.5	13041	24	55.824	1660
750318	1312	103.25	13009.5	24	55.824	1660
750319	1556	58.25	7339.5	26.5	61.639	3496
750320	2367	55.5	6993	34.5	80.247	1804

date	Power MWt	Flow (w) Mlb/hr	Flow (w) kg/s	subcooling Btu/lb	subcooling kJ/kg	# of notches inserted
750321	2628	63.75	8032.5	33.25	77.3395	1714
750322	2979	81.5	10269	28.5	66.291	1714
750323	3157	92.5	11655	25.75	59.8945	1714
750324	3250	102	12852	23.5	54.661	1726
750325	3300	103.5	13041	23.5	54.661	1737
750326	3295	104.5	13167	23.5	54.661	1737
750327	3293	104.5	13167	23.5	54.661	1740
750328	3293	104.5	13167	23.5	54.661	1740
750329	3293	104.5	13167	23.5	54.661	1740
750330	3293	104.5	13167	23.5	54.661	1740
750331	3293	104.5	13167	23.5	54.661	1740
750401	3293	104	13104	23.5	54.661	1740
750402	3270	105.5	13293	23.5	54.661	1740
750403	3256	105.5	13293	23.5	54.661	1740
750404	3256	105.5	13293	23.5	54.661	1740
750405	3256	105.5	13293	23.75	55.2425	1740
750406	3011	92.25	11623.5	25	58.15	1740
750407	3256	103	12978	23.75	55.2425	1728
750408	3293	104.75	13198.5	23.5	54.661	1728
750409	3293	105.5	13293	23.5	54.661	1728
750410	3293	105.5	13293	23.5	54.661	1728
750411	3293	105.5	13293	23.5	54.661	1728
750412	3293	105.5	13293	23.5	54.661	1728
750413	3260	105.5	13293	23.5	54.661	1728
750414	3260	105.5	13293	23.5	54.661	1728
750415	3260	105.5	13293	23.5	54.661	1728
750416	3260	105.5	13293	23.5	54.661	1728
750417	3233	105.5	13293	23.5	54.661	1728
750418	3233	105.5	13293	23.5	54.661	1728
750419	3233	106	13356	23	53.498	1728
750420	3233	106	13356	23	53.498	1728
750421	3222	106	13356	23	53.498	1728
750422	3222	106	13356	23	53.498	1728
750423	3222	106	13356	23	53.498	1728
750424	3215	106	13356	23	53.498	1728
750425	3131	105.5	13293	23	53.498	1728
750426	2356	58.5	7371	33.25	77.3395	1692
750427	2656	63	7938	33	76.758	1670
750428	2200	74.5	9387	29.25	68.0355	1670
750429	1211	60	7560	21	48.846	2840
750430	2723	67.5	8505	31.75	73.8505	1668
750501	2908	78	9828	29.25	68.0355	1668
750502	3187	97.5	12285	24.75	57.5685	1668
750503	3288	103	12978	24	55.824	1668
750504	3261	104.75	13198.5	23.5	54.661	1668
750505	3247	104.5	13167	23.5	54.661	1668
750506	3243	105.5	13293	23	53.498	1668
750507	3232	105.5	13293	23	53.498	1668
750508	3227	105.25	13261.5	23	53.498	1668
750509	3218	105.5	13293	23	53.498	1668
750510	3210	105.5	13293	23	53.498	1668
750511	3198	105.5	13293	23	53.498	1668
750512	3187	105.5	13293	23	53.498	1668
750513	3172	105.5	13293	23	53.498	1668
750514	3160	105	13230	23	53.498	1668
750515	3154	104.75	13198.5	23	53.498	1668
750516	3031	105	13230	23	53.498	1668
750517	0	67	8442	20.5	47.683	2238
750606	0	45	5670	25.75	59.8945	> 4500
750607	440	45	5670	25.75	59.8945	2906
750608	2044	62.25	7843.5	28	65.128	2049
750609	1889	94.5	11907	20	46.52	1982
750610	1833.5	43	5418	31	72.106	1826
750611	1778	62.625	7890.75	30.5	70.943	2020
750612	1256	82.25	10363.5	23	53.498	1926
750613	0	45.75	5764.5	23	53.498	> 4500
750614	0	45.75	5764.5	32.5	75.595	> 4500
750615	1067	45.75	5764.5	32.5	75.595	2356
750616	2289	75	9450	25	58.15	1893
750617	2010	46.5	5859	38.25	88.9695	1525
750618	2476	59	7434	33.75	78.5025	1525
750619	2422	71.5	9009	30.5	70.943	1503
750620	0	44.9	5657.4	30.5	70.943	> 4500
750624	0	44.9	5657.4	34.25	79.6655	> 4500
750625	1473	44.9	5657.4	34.25	79.6655	2372

date	Power MWt	Flow (w) Mlb/hr	Flow (w) kg/s	subcooling Btu/lb	subcooling kJ/kg	# of notches inserted
750626	2444	102.5	12915	20.5	47.683	1915
750627	1711	41.5	5229	29.5	68.617	1971
750628	2289	64.5	8127	34.25	79.6655	1470
750629	2678	69.25	8725.5	33	76.758	1470
750630	3022	77	9702	30.25	70.3615	1470
750701	3256	98.25	12379.5	24.75	57.5685	1470
750702	3271	98.25	12379.5	24.75	57.5685	n/a
750703	3267	98.25	12379.5	24.75	57.5685	n/a
750704	3156	86.19	10859.94	25.75	59.8945	n/a
750705	2722	74.13	9340.38	26.75	62.2205	n/a
750706	2256	62.06	7819.56	27.75	64.5465	n/a
750707	1656	50	6300	28.75	66.8725	n/a
750708	1642	50	6300	28.75	66.8725	1672
750709	1633	49.5	6237	29.75	69.1985	1688
750710	1627	49.5	6237	30	69.78	1706
750711	1624	48.5	6111	29.75	69.1985	1717
750712	1622	49.5	6237	29.75	69.1985	1740
750713	1622	50	6300	29.75	69.1985	1740
750714	1622	50	6300	29.75	69.1985	1740
750715	1622	50	6300	29.75	69.1985	1717
750716	1636	49.5	6237	29.25	68.0355	1717
750717	1636	50	6300	29.25	68.0355	1706
750718	1636	50	6300	29.75	69.1985	1706
750719	1636	50	6300	29.75	69.1985	1717
750720	1633	50.5	6363	29.75	69.1985	1717
750721	1633	50.5	6363	29.75	69.1985	1717
750722	1645	50	6300	29.75	69.1985	1706
750723	1620	50	6300	29.75	69.1985	1706
750724	1622	49	6174	29.75	69.1985	1706
750725	1589	49.75	6268.5	29.75	69.1985	1706
750726	1645	40.25	5071.5	37.75	87.8065	1605
750727	1722	40.5	5103	39.5	91.877	1550
750728	1800	40	5040	41	95.366	1539
750729	1800	39.5	4977	41	95.366	1522
750730	1800	39.5	4977	41.5	96.529	1522
750731	1800	39.5	4977	41.5	96.529	1522
750801	1805	40	5040	41	95.366	1522
750802	1805	40	5040	41	95.366	1522
750803	1805	40	5040	41	95.366	1522
750804	1844	40	5040	41	95.366	1470
750805	1889	40	5040	41	95.366	1883
750806	100	69	8694	31	72.106	1537
750807	1544	40	5040	38.5	89.551	1537
750808	1778	40	5040	41.25	95.9475	1515
750809	1793	40	5040	41.25	95.9475	1515
750810	1811	40	5040	41.25	95.9475	1515
750811	1804	40	5040	41.25	95.9475	1515
750812	1822	40	5040	41.25	95.9475	1515
750813	1838	40	5040	41.5	96.529	1515
750814	1858	40	5040	41.5	96.529	1493
750815	1851	40	5040	41.5	96.529	1472
750816	1578	40	5040	41.5	96.529	1472
750817	193	42.5	5355	17	39.542	3130
750818	1656	57.5	7245	21.5	50.009	> 4500
750819	2000	72.5	9135	21.5	50.009	> 4500
750820	2213	87.5	11025	21.5	50.009	> 4500
750821	2533	102.5	12915	21.5	50.009	1671
750822	2355	86.5	10899	25.5	59.313	1593
750823	1800	41.75	5260.5	39.5	91.877	1548
750824	1844	41.75	5260.5	41	95.366	1526
750825	1836	41.25	5197.5	40.25	93.6215	1504
750826	1860	41	5166	41.75	97.1105	1486
750827	1855	40.5	5103	41.75	97.1105	1448
750828	1855	40	5040	41.75	97.1105	1430
750829	1855	40.5	5103	41.75	97.1105	1448
750830	1855	40.5	5103	41.75	97.1105	1426
750831	1855	40.5	5103	41.75	97.1105	1426
750901	1855	40.5	5103	42	97.692	1426
750902	1855	40.5	5103	42	97.692	1426
750903	1855	40.5	5103	42	97.692	1426
750904	1855	40.5	5103	42	97.692	1426
750905	1733	40.5	5103	42	97.692	1415
750906	0	40.5	5103	39	90.714	> 4500
750907	1381	41	5166	39	90.714	1838
750908	1860	41	5166	41.75	97.1105	1470

date	Power MWt	Flow (w) Mlb/hr	Flow (w) kg/s	subcooling Btu/lb	subcooling kJ/kg	# of notches inserted
750909	1878	40.5	5103	42	97.692	1403
750910	1893	40.5	5103	41.75	97.1105	1403
750911	1910	40.5	5103	42	97.692	1403
750912	1910	40.5	5103	42	97.692	1380
750913	1910	40.5	5103	42	97.692	1380
750914	1910	40.5	5103	42	97.692	1388
750915	1910	40.5	5103	42	97.692	1388
750916	1910	40.5	5103	42	97.692	1370
750917	1910	40.5	5103	42	97.692	1330
750918	1910	40.5	5103	42	97.692	1330
750919	1910	40.5	5103	42	97.692	1330
750920	1910	40.5	5103	42	97.692	1330
750921	1910	40.5	5103	42	97.692	1330
750922	1910	40.5	5103	42	97.692	1330
750923	1910	40.5	5103	42	97.692	1330
750924	1910	40.5	5103	42	97.692	1330
750925	1875	40.5	5103	42	97.692	1330
750926	1893	40.5	5103	42	97.692	1330
750927	1742	40.5	5103	42	97.692	1330
750928	1514	40.5	5103	35	81.41	1871
750929	1525	40.5	5103	38.5	89.551	1671
750930	1715	40.5	5103	39.5	91.877	1582
751001	1820	40.5	5103	40.5	94.203	1489
751002	1822	40.5	5103	41.5	96.529	1378
751003	1867	40	5040	42.5	98.855	1344
751004	1893	40.5	5103	41.5	96.529	1344
751005	1884	40.5	5103	41.5	96.529	1344
751006	1867	40.5	5103	41.5	96.529	1344
751007	1822	40.5	5103	41.5	96.529	1344
751008	1842	40.5	5103	41.5	96.529	1333
751009	1867	40.5	5103	41.5	96.529	1289
751010	1867	40.5	5103	41.5	96.529	1289
751011	1867	40.5	5103	41.5	96.529	1289
751012	1867	40.5	5103	41.5	96.529	1289
751013	1844	40.5	5103	41.5	96.529	1289
751014	1833	40.5	5103	41	95.366	1289
751015	1838	40.5	5103	41.5	96.529	1277
751016	1844	40.5	5103	41.5	96.529	1267
751017	1844	40.5	5103	42	97.692	1233
751018	1844	40.5	5103	42	97.692	1226
751019	1822	40.5	5103	42	97.692	1226
751020	1822	40.5	5103	42	97.692	1212
751021	1822	40.5	5103	42	97.692	1212
751022	1830	40.5	5103	42	97.692	1212
751023	1840	40.5	5103	41.5	96.529	1212
751024	1866	40.5	5103	41.5	96.529	1212
751025	1855	40.5	5103	41.5	96.529	1212
751026	1855	40.5	5103	41.5	96.529	1212
751027	1855	40.5	5103	41.5	96.529	1212
751028	1855	40.5	5103	41.5	96.529	1212
751029	1855	40.5	5103	41.5	96.529	1212
751030	1850	40.5	5103	41	95.366	1212
751031	1858	41	5166	41	95.366	1212
751101	0	41	5166	41	95.366	> 4500
SHUTDOWN FOR CORE SUPPORT PLATE HOLE PLUGGING						
751130	0	44	5544	38.25	88.9695	> 4500
751201	1278	44	5544	38.25	88.9695	1536
751202	1778	41.75	5260.5	40	93.04	1336
751203	1944	46.5	5859	36.5	84.899	1214
751204	2322	60	7560	34.6	80.4796	n/a
751205	2673	77	9702	32.7	76.0602	n/a
751206	2711	78	9828	30.8	71.6408	n/a
751207	2167	65.5	8253	28.9	67.2214	n/a
751208	2433	81	10206	27	62.802	1158
751209	2860	90	11340	25.75	59.8945	1158
751210	2940	103	12978	23	53.498	1158
751211	2711	108.5	13671	22.5	52.335	1158
751212	0	43.25	5449.5	22.5	52.335	> 4500
751214	0	43.25	5449.5	33	76.758	> 4500
751215	900	43.25	5449.5	33	76.758	1804
751216	1700	44	5544	36	83.736	1325
751217	2022	42.5	5355	41	95.366	1024
751218	2467	61.75	7780.5	33.5	77.921	908
751219	2789	69	8694	31.75	73.8505	908
751220	3089	85	10710	27.25	63.3835	908

date	Power MWt	Flow (w) Mlb/hr	Flow (w) kg/s	subcooling Btu/lb	subcooling kJ/kg	# of notches inserted
751221	3256	105.5	13293	23.75	55.2425	908
751222	3278	105	13230	23.75	55.2425	908
751223	3284	108	13608	22.25	51.7535	908
751224	3293	107	13482	22	51.172	n/a
751225	3067	46.5	5859	38.5	89.551	> 4500
751226	280	46.5	5859	38.5	89.551	> 4500
751227	1467	46.5	5859	38.5	89.551	1170
751228	2450	50.5	6363	34.5	80.247	1013
751229	1400	44.5	5607	38	88.388	846
751230	2456	54.25	6835.5	37	86.062	835
751231	2778	75.5	9513	30.5	70.943	835
760101	3131	97	12222	24	55.824	796
760102	3245	105.75	13324.5	22.25	51.7535	796
760103	3232	106.5	13419	22	51.172	796
760104	3223	107	13482	22	51.172	796
760105	3210	107.5	13545	22	51.172	796
760106	3187	107	13482	22	51.172	796
760107	3176	107.5	13545	22	51.172	796
760108	0	42	5292	29.25	68.0355	> 4500
760109	1114	42	5292	29.25	68.0355	2331
760110	1895	45.25	5701.5	36.5	84.899	867
760111	2351	54.25	6835.5	34.5	80.247	712
760112	2786	68.67	8652.42	31.3	72.8038	n/a
760113	3165	83.1	10470.6	28.2	65.5932	n/a
760114	3293	97.5	12285	25	58.15	611
760115	3293	99.5	12537	24.75	57.5685	611
760116	3288	101	12726	24.5	56.987	611
760117	3221	103	12978	24	55.824	611
760118	1137	40.5	5103	20.75	48.2645	2436
760119	2340	48.75	6142.5	40.5	94.203	611
760120	2842	66	8316	34.5	80.247	611
760121	3221	91.5	11529	27.5	63.965	611
760122	3287	103.5	13041	25.5	59.313	611
760123	3272	105	13230	22.75	52.9165	611
760124	3259	103.75	13072.5	22.25	51.7535	611
760125	3259	107	13482	22	51.172	611
760126	3276	107	13482	22	51.172	611
760127	3254	107	13482	22	51.172	611
760128	3243	107	13482	22	51.172	611
760129	3225	107	13482	22	51.172	611
760130	3221	106	13356	22	51.172	611
760131	3216	107	13482	22	51.172	611
760201	3212	106.5	13419	22.5	52.335	611
760202	3208	106.75	13450.5	22.5	52.335	611
760203	3195	107	13482	22.5	52.335	611
760204	3189	107	13482	22	51.172	611
760205	3178	107	13482	22.5	52.335	611
760206	2978	107.25	13513.5	22.5	52.335	611
760207	1400	41.5	5229	32	74.432	950
760208	1871	40.75	5134.5	44	102.344	544
760209	2220	51.5	6489	38.5	89.551	494
760210	1967	40.75	5134.5	42.5	98.855	567
760211	2524	56.75	7150.5	36.25	84.3175	494
760212	2822	71.5	9009	30.5	70.943	494
760213	3156	89.25	11245.5	25.25	58.7315	494
760214	2822	107	13482	23	53.498	494
760215	3011	88.5	11151	26	60.476	510
760216	3238	106.75	13450.5	22.5	52.335	510
760217	3222	107	13482	22.5	52.335	510
760218	3187	107	13482	22.5	52.335	510
760219	3169	107	13482	22.5	52.335	510
760220	3153	107	13482	22	51.172	510
760221	2000	67	8442	25.5	59.313	811
760222	2233	42	5292	50	116.3	400
760223	2556	56	7056	44	102.344	400
760224	2878	63.75	8032.5	37.75	87.8065	400
760225	3207	91.25	11497.5	32	74.432	400
760226	3273	99.25	12505.5	30	69.78	400
760227	3293	100.5	12663	29.5	68.617	400
760228	3264	101.5	12789	28.75	66.8725	400
760229	3256	102.5	12915	28.5	66.291	400
760301	3267	102.5	12915	28.5	66.291	n/a
760302	3260	102.5	12915	28.5	66.291	n/a
760303	3270	102.5	12915	28.5	66.291	n/a
760304	3258	102.5	12915	28.5	66.291	n/a

date	Power MWt	Flow (w) Mlb/hr	Flow (w) kg/s	subcooling Btu/lb	subcooling kJ/kg	# of notches inserted
760305	3210	102.5	12915	28.5	66.291	n/a
760306	2826	80.5	10143	31.5	73.269	400
760307	2860	80.5	10143	31.25	72.6875	400
760308	3205	98.5	12411	28.25	65.7095	400
760309	3260	107.25	13513.5	26.25	61.0575	400
760310	3249	107.25	13513.5	26.5	61.639	400
760311	3236	106.5	13419	26.5	61.639	400
760312	3216	106.5	13419	26.5	61.639	400
760313	3194	107.25	13513.5	26.5	61.639	400
760314	3187	107.25	13513.5	26.5	61.639	400
760315	3171	107.25	13513.5	26.5	61.639	400
760316	3171	107.25	13513.5	26.5	61.639	400
760317	3164	107.25	13513.5	26.25	61.0575	400
760318	3142	107.25	13513.5	26	60.476	400
760319	3127	107	13482	25.5	59.313	400
760320	3111	108	13608	25.5	59.313	400
760321	3105	108	13608	25.25	58.7315	400
760322	3100	108	13608	25	58.15	400
760323	3086	108	13608	24.75	57.5685	400
760324	3082	108	13608	24.75	57.5685	400
760325	3071	108	13608	24.75	57.5685	400
760326	3001	108	13608	24.75	57.5685	400
760327	0	108	13608	24.75	57.5685	> 4500
SHUTDOWN FOR REFUELING BETWEEN CYCLE 1 AND 2						
760623	0	44.75	5638.5	31	72.106	> 4500
760624	604	44.75	5638.5	31	72.106	> 4500
760625	1211	44.75	5638.5	31	72.106	1889
760626	2127	51.5	6489	36.5	84.899	1444
760627	2411	71	8946	28.75	66.8725	1432
760628	2633	85	10710	25.25	58.7315	1432
760629	1878	89.5	11277	24	55.824	1432
760630	0	44.75	5638.5	24	55.824	> 4500
760702	0	43	5418	26.5	61.639	> 4500
760703	1222	43	5418	26.5	61.639	2667
760704	2022	57.25	7213.5	30.5	70.943	1533
760705	2598	69	8694	30.5	70.943	1333
760706	2878	96.5	12159	24.5	56.987	1333
760707	3089	104	13104	22.25	51.7535	1333
760708	3078	107	13482	21	48.846	1333
760709	2978	107	13482	21.75	50.5905	1333
760710	2311	54.25	6835.5	35	81.41	1211
760711	2522	61.25	7717.5	33.75	78.5025	1200
760712	2947	78.75	9922.5	28.5	66.291	1200
760713	3211	93.25	11749.5	25.75	59.8945	1200
760714	3289	101.5	12789	24	55.824	1200
760715	3289	102.5	12915	24	55.824	1200
760716	3289	103.5	13041	23.5	54.661	1200
760717	3300	104	13104	24	55.824	1200
760718	3211	103	12978	24	55.824	1200
760719	3256	101	12726	24	55.824	1200
760720	3291	103.5	13041	23.5	54.661	1200
760721	3278	103.5	13041	23.5	54.661	1200
760722	3293	105.25	13261.5	23.5	54.661	1200
760723	3293	105.75	13324.5	23.5	54.661	1200
760724	3293	104.5	13167	23.5	54.661	1200
760725	3293	105.5	13293	23.5	54.661	1200
760726	3293	105.5	13293	24	55.824	1200
760727	3293	105.75	13324.5	24	55.824	1200
760728	3293	106	13356	24	55.824	1200
760729	3293	106.5	13419	24	55.824	1200
760730	3293	106.5	13419	24	55.824	1200
760731	3293	107	13482	24	55.824	1200
760801	3293	107	13482	22	51.172	1200
760802	3293	107	13482	23	53.498	1200
760803	3293	107	13482	22.5	52.335	1200
760804	3293	107	13482	22	51.172	1200
760805	1633	107.5	13545	22	51.172	1200
760806	1211	42.25	5323.5	28	65.128	1844
760807	1967	43.5	5481	39.5	91.877	1277
760808	2411	60	7560	33	76.758	1133
760809	1589	65.75	8284.5	32	74.432	1067
760810	1689	43	5418	31.5	73.269	1644
760811	2200	47	5922	39.5	91.877	1111
760812	2584	67.5	8505	31	72.106	1067
760813	2910	77.75	9796.5	28.5	66.291	1067

date	Power MWt	Flow (w) Mlb/hr	Flow (w) kg/s	subcooling Btu/lb	subcooling kJ/kg	# of notches inserted
760814	3153	93.5	11781	24.25	56.4055	1100
760815	3278	101	12726	23	53.498	1133
760816	3145	105	13230	22.25	51.7535	1178
760817	3145	96.5	12159	24	55.824	1178
760818	982	42.25	5323.5	24	55.824	> 4500
760819	0	42.25	5323.5	24	55.824	> 4500
760820	400	42.25	5323.5	28.5	66.291	2333
760821	1493	43	5418	35	81.41	1756
760822	1933	51.5	6489	37.75	87.8065	1544
760823	2522	70.25	8851.5	38.75	90.1325	1300
760824	0	42.25	5323.5	24	55.824	> 4500
760826	0	42.5	5355	27.5	63.965	> 4500
760827	1000	42.5	5355	27.5	63.965	2388
760828	2200	53	6678	41.75	97.1105	1356
760829	2744	72.25	9103.5	38.25	88.9695	1306
760830	3044	83.5	10521	28	65.128	1178
760831	3100	99.5	12537	24	55.824	1230
760901	3270	104	13104	23.5	54.661	1230
760902	3280	104	13104	23.5	54.661	1230
760903	3280	105	13230	23.5	54.661	1230
760904	3270	105	13230	23.5	54.661	1230
760905	3238	105	13230	23.5	54.661	1230
760906	3280	106	13356	23.5	54.661	1230
760907	3240	106.25	13387.5	23.5	54.661	1230
760908	3240	106.25	13387.5	23.5	54.661	1230
760909	3280	106.5	13419	23.5	54.661	1230
760910	3225	106.5	13419	23.5	54.661	1230
760911	3268	106.5	13419	23.5	54.661	1230
760912	3230	106.5	13419	23.5	54.661	1230
760913	3248	106.5	13419	23.5	54.661	1230
760914	3225	106.5	13419	23.5	54.661	1230
760915	3270	105.5	13293	23.5	54.661	1230
760916	3252	106.5	13419	23.5	54.661	1230
760917	3252	106.5	13419	23.5	54.661	1230
760918	3252	106.5	13419	23.5	54.661	1230
760919	3252	106.5	13419	23.5	54.661	1230
760920	3252	106.5	13419	23.5	54.661	1230
760921	2995	106.5	13419	23.5	54.661	1230
760922	3036	93	11718	24	55.824	1230
760923	3267	106	13356	23.5	54.661	1230
760924	2122	106	13356	23.5	54.661	1230
760925	0	42.25	5323.5	23.5	54.661	> 4500
760926	1271	42.25	5323.5	29.25	68.0355	2071
760927	2233	53.25	6709.5	35.5	82.573	1325
760928	2611	62	7812	34	79.084	1198
760929	2989	81.5	10269	29	67.454	1198
760930	2467	50.25	6331.5	35	81.41	1198
761001	2831	73	9198	30.8	71.6408	1198
761002	3200	91	11466	26	60.476	1198
761003	3278	99.75	12568.5	24.5	56.987	1198
761004	3238	98.25	12379.5	24.5	56.987	1198
761005	3278	100	12600	24.5	56.987	1198
761006	3280	101.5	12789	24.5	56.987	1198
761007	3280	101.5	12789	24.5	56.987	1198
761008	3280	101.5	12789	24.5	56.987	1198
761009	1807	42.25	5323.5	38.25	88.9695	1198
761010	1622	41.75	5260.5	36	83.736	1589
761011	2011	45	5670	38.5	89.551	1193
761012	2322	52.5	6615	37	86.062	1100
761013	2633	68.5	8631	31.5	73.269	1077
761014	2967	82.5	10395	29.25	68.0355	1056
761015	3252	93.5	11781	26.5	61.639	1044
761016	3298	68.25	8599.5	26.5	61.639	n/a
761017	2767	43	5418	26.5	61.639	> 4500
761018	163	43	5418	26.5	61.639	> 4500
761019	933	43	5418	29.75	69.1985	2348
761020	1951	47	5922	37.75	87.8065	1178
761021	2436	57.25	7213.5	35	81.41	1078
761022	2789	68.5	8631	32	74.432	1056
761023	3133	87.5	11025	27.75	64.5465	1032
761024	3289	97.75	12316.5	25.75	59.8945	1032
761025	3293	97.75	12316.5	25.75	59.8945	1032
761026	3293	100.5	12663	24.75	57.5685	1032
761027	3293	100.5	12663	24.75	57.5685	1032
761028	3293	100.5	12663	24.75	57.5685	1032

date	Power MWt	Flow (w) Mlb/hr	Flow (w) kg/s	subcooling Btu/lb	subcooling kJ/kg	# of notches inserted
761029	3293	101	12726	24.75	57.5685	1032
761030	3293	100.5	12663	24.75	57.5685	1032
761031	3289	100.25	12631.5	24.75	57.5685	1032
761101	3272	99.5	12537	24.75	57.5685	1032
761102	3270	99.5	12537	24.75	57.5685	1032
761103	3270	99.5	12537	24.75	57.5685	1032
761104	3260	99.5	12537	24.75	57.5685	1032
761105	3218	99.5	12537	24.75	57.5685	1032
761106	3238	101	12726	24.75	57.5685	1032
761107	3260	100	12600	24.75	57.5685	1032
761108	3240	99.5	12537	24.75	57.5685	1032
761109	3285	99.5	12537	24.75	57.5685	1032
761110	3285	102.5	12915	24.5	56.987	1032
761111	3263	101.5	12789	24.25	56.4055	1032
761112	3293	102.25	12883.5	23.5	54.661	1032
761113	3293	102.25	12883.5	24	55.824	1032
761114	1558	102.25	12883.5	23.5	54.661	1032
761115	0	51	6426	23.5	54.661	> 4500
761125	0	38.25	4819.5	13.25	30.8195	> 4500
761126	334	38.25	4819.5	13.25	30.8195	3322
761127	1547	41.25	5197.5	33	76.758	1744
761128	1860	41.5	5229	30.25	70.3615	1167
761129	2173	49.25	6205.5	39.5	91.877	986
761130	2486	59.5	7497	34.5	80.247	986
761201	2858	76	9576	30.5	70.943	986
761202	3156	87	10962	27.5	63.965	986
761203	3182	95.5	12033	26.5	61.639	986
761204	3078	92.4	11642.4	27	62.802	986
761205	2878	80	10080	28	65.128	986
761206	2573	59.5	7497	31	72.106	986
761207	2268	52.25	6583.5	37	86.062	986
761208	2967	75	9450	31	72.106	1011
761209	3256	97.5	12285	25	58.15	986
761210	3287	100.25	12631.5	24	55.824	986
761211	3289	101.5	12789	23.5	54.661	986
761212	3267	100.5	12663	23.5	54.661	986
761213	3229	100.25	12631.5	23.5	54.661	986
761214	3278	101.5	12789	23.5	54.661	986
761215	3300	102.5	12915	23.5	54.661	986
761216	3280	101.5	12789	23.5	54.661	986
761217	3293	103.75	13072.5	23.5	54.661	986
761218	3213	96.75	12190.5	23.5	54.661	986
761219	3253	101	12726	23.5	54.661	986
761220	3293	103.5	13041	23.5	54.661	986
761221	3278	104	13104	23.5	54.661	986
761222	3293	104	13104	23.5	54.661	986
761223	3293	104.5	13167	23.5	54.661	986
761224	3267	104.5	13167	23	53.498	986
761225	3280	105	13230	23	53.498	986
761226	3293	106	13356	23	53.498	986
761227	3270	104.5	13167	23	53.498	986
761228	3293	105	13230	23	53.498	986
761229	3273	106	13356	23.5	54.661	986
761230	3189	100.5	12663	23.5	54.661	986
761231	3207	99.75	12568.5	23.5	54.661	986
770101	3218	99.75	12568.5	23.5	54.661	986
770102	0	50	6300	23.5	54.661	> 4500
770109	0	40.25	5071.5	28.75	66.8725	> 4500
770110	702	40.25	5071.5	28.75	66.8725	3260
770111	1738	43.5	5481	35.5	82.573	1422
770112	2028	43	5418	42.25	98.2735	1228
770113	2318	56.5	7119	34.5	80.247	1033
770114	2653	65.75	8284.5	33	76.758	978
770115	2988	76	9576	30.25	70.3615	948
770116	3244	94.5	11907	26	60.476	948
770117	3277	97.75	12316.5	25.5	59.313	955
770118	3280	100	12600	24.5	56.987	1000
770119	3280	101.5	12789	24.5	56.987	948
770120	3280	101.75	12820.5	24.5	56.987	948
770121	3280	102	12852	24.5	56.987	948
770122	3280	102	12852	24.5	56.987	948
770123	3280	102.5	12915	24.5	56.987	948
770124	3256	103.5	13041	24.5	56.987	948
770125	3280	103.75	13072.5	24	55.824	948
770126	3280	104	13104	23.5	54.661	948

date	Power MWt	Flow (w) Mlb/hr	Flow (w) kg/s	subcooling Btu/lb	subcooling kJ/kg	# of notches inserted
770127	3256	104.5	13167	23	53.498	948
770128	3280	105	13230	23	53.498	948
770129	3271	105	13230	23	53.498	948
770130	3268	105	13230	23	53.498	948
770131	3265	105.25	13261.5	23	53.498	948
770201	3267	106	13356	23	53.498	948
770202	3270	106	13356	23	53.498	948
770203	3275	107.75	13576.5	23	53.498	948
770204	3076	103.5	13041	23	53.498	948
770205	0	43	5418	22	51.172	> 4500
770206	144	43	5418	22	51.172	3155
770207	1578	44	5544	34	79.084	1622
770208	1489	44.5	5607	31.5	73.269	1711
770209	1045	44	5544	35	81.41	1200
770210	1223	43	5418	31	72.106	2333
770211	1867	42	5292	40.25	93.6215	1067
770212	2211	50	6300	37.25	86.6435	978
770213	2500	60.75	7654.5	34.25	79.6655	933
770214	2856	72.5	9135	31.25	72.6875	908
770215	3189	94	11844	24.75	57.5685	908
770216	3277	102	12852	23.5	54.661	908
770217	3277	102.25	12883.5	23.25	54.0795	908
770218	3270	102.5	12915	23.5	54.661	908
770219	3265	103	12978	23.75	55.2425	908
770220	3238	103	12978	23.75	55.2425	908
770221	3256	103.25	13009.5	23.5	54.661	908
770222	3284	104.75	13198.5	23.25	54.0795	908
770223	3265	105	13230	23.25	54.0795	908
770224	3256	105	13230	23	53.498	908
770225	3267	107	13482	23	53.498	908
770226	3267	106.5	13419	23	53.498	908
770227	3260	107	13482	23.25	54.0795	908
770228	3231	106.5	13419	23.25	54.0795	908
770301	3256	106.75	13450.5	23.25	54.0795	908
770302	3244	107	13482	23.25	54.0795	908
770303	2100	106.5	13419	23.25	54.0795	908
770304	856	38.75	4882.5	43.5	101.181	1911
770305	1689	41.5	5229	39	90.714	1211
770306	2056	42.75	5386.5	41	95.366	862
770307	2311	53.75	6772.5	37.25	86.6435	824
770308	2500	62.25	7843.5	34.5	80.247	824
770309	2660	69.25	8725.5	32.5	75.595	824
770310	2867	77.75	9796.5	30.25	70.3615	824
770311	2856	78.5	9891	29.5	68.617	824
770312	2833	78.75	9922.5	29.5	68.617	824
770313	778	78.5	9891	29.5	68.617	824
770314	0	41.5	5229	29.5	68.617	> 4500
770316	0	41.5	5229	21	48.846	> 4500
770317	422	41.5	5229	21	48.846	2733
770318	1611	42.5	5355	34.5	80.247	1288
770319	2012	43.5	5481	41	95.366	811
770320	2295	49.5	6237	39	90.714	756
770321	2578	52	6552	38.5	89.551	732
770322	2904	79	9954	30	69.78	732
770323	3211	90.5	11403	26.25	61.0575	732
770324	3278	97.25	12253.5	25.75	59.8945	732
770325	3278	99	12474	25.5	59.313	732
770326	3267	99.5	12537	25	58.15	732
770327	3267	101	12726	24.75	57.5685	732
770328	3250	100	12600	24.5	56.987	732
770329	3271	102.75	12946.5	24	55.824	732
770330	3250	102.5	12915	23.5	54.661	732
770331	3258	103.5	13041	23.5	54.661	732
770401	3278	103.25	13009.5	23.5	54.661	732
770402	3278	104.5	13167	23.5	54.661	732
770403	3265	104.25	13135.5	23.5	54.661	732
SHUTDOWN PRIOR TO TT AND PT TESTS						

APPENDIX 2 – INPUT DATA FOR DEPLETION CALCULATIONS

CYCLE 1

Number of notches withdrawn for each CR sequence group (A and A2) (48 = fully out, 0 = fully in)

burn step time period	Explanation	Power (MWt)	EFPH	Accumulated EFPH	core flow (kg/s)	subcooling (kJ/kg)	1	2	3	4	5	6	7	8	9	10	11	12	13	14	15	16	17	18	19	20	21
740112-740405	burn step 1, data set 1	772.10	253.22	253.22	7695.1	35.19	48	48	48	48	48	48	48	48	36	36	36	36	36	8	20	20	20	4	4	20	4
740405-740417	burn step 2	1106.00	88.67	341.89	8757.0	40.07	48	48	48	48	48	48	48	48	48	48	48	48	48	8	24	24	24	4	4	20	2
740417-740425	burn step 3, data set 2	1874.69	109.30	451.20	8697.9	59.82	48	48	48	48	48	48	48	48	48	48	48	48	48	36	32	36	30	10	8	30	12
740425-740508	burn step 4	1348.12	127.73	578.93	7087.5	65.91	48	48	48	48	48	48	48	48	48	48	48	48	48	34	30	34	28	6	8	26	10
740508-740512	burn step 5, data set 3	2256.75	65.79	644.72	8316.0	73.20	Figure A.2.1.a																				
740512-740518	burn step 6	2225.17	97.30	742.02	9633.8	61.11	Figure A.2.1.a																				
740518-740526	burn step 7, data set 4	2071.88	120.80	862.82	7975.0	69.27	48	48	48	48	48	48	48	48	48	48	48	48	48	26	36	30	26	26	6	26	6
740526-740530	burn step 8	1140.00	33.23	896.06	7725.4	63.53	48	48	48	48	48	48	48	48	48	48	48	40	40	20	26	24	20	20	6	20	4
740604-740619	burn step 9, data set 5	2337.70	255.56	1151.62	9920.2	60.79	Figure A.2.1.b																				
740619-740622	burn step 10	2520.17	55.10	1206.72	11481.8	56.11	CR map for burnup step 10 in Appendix 2																				
740622-740715	burn step 11, data set 6	2901.91	486.44	1693.17	10862.7	61.42	48	48	48	48	48	48	48	48	48	48	48	48	48	32	40	40	32	20	6	34	10
740715-740723	burn step 12	3038.31	177.15	1870.32	11412.8	60.11	48	48	48	48	48	48	48	48	48	48	48	48	48	32	40	40	32	20	8	36	10
740723-740817	burn step 13, data set 7	2891.30	526.81	2397.12	11441.1	60.36	Figure A.2.1.c																				
740817-740827	burn step 14	3234.10	235.71	2632.83	12636.9	57.72	Figure A.2.1.d																				
740827-740910	burn step 15, data set 8	3225.18	329.08	2961.91	12317.6	60.52	Figure A.2.1.e																				
740910-740915	burn step 16	2429.60	88.54	3050.45	11680.2	57.68	Figure A.2.1.f																				
740915-741004	burn step 17, data set 9	2361.71	327.04	3377.49	9524.6	67.48	48	48	48	48	48	48	48	48	40	44	48	38	36	20	12	12	16	6	4	16	8
741004-741017	burn step 18	2528.69	239.58	3617.07	9845.4	71.21	48	48	48	48	48	48	48	48	40	44	48	38	36	20	14	14	18	8	4	22	4
741019-741121	burn step 19, data set 10	2377.23	519.77	4136.84	9639.0	62.75	48	48	48	48	48	48	48	48	34	38	34	36	32	28	12	12	10	6	6	10	4
741121-741130	burn step 20	3058.44	200.61	4337.46	13027.0	54.66	48	48	48	48	48	48	48	48	36	38	36	38	34	30	14	14	12	8	6	12	10
741201-750106	burn step 21, data set 11	2786.10	731.00	5068.46	10777.8	60.11	Figure A.2.1.g																				
750106-750115	burn step 22	3033.50	198.98	5267.44	12442.5	55.60	Figure A.2.1.h																				
750123-750203	burn step 23, data set 12	2648.14	212.30	5479.74	10369.2	58.57	48	48	48	48	48	48	48	48	34	36	28	32	32	16	12	8	8	4	4	6	4
750203-750212	burn step 24	3046.50	199.83	5679.57	12468.8	55.63	48	48	48	48	48	48	48	48	36	38	32	34	34	24	14	12	10	6	6	10	10
750220-750313	burn step 25, data set 13	2969.36	454.47	6134.04	11591.3	58.73	48	48	48	48	48	48	48	48	36	38	32	38	32	22	10	10	8	8	6	8	6
750313-750318	burn step 26	3094.90	112.78	6246.82	12993.8	55.82	48	48	48	48	48	48	48	48	36	38	34	38	34	24	14	12	10	8	6	10	12
750318-750402	burn step 27, data set 14	2972.07	324.91	6571.73	11696.0	59.51	Figure A.2.1.i																				
750402-750406	burn step 28	3227.13	94.08	6665.81	13084.3	55.24	Figure A.2.1.j																				
750406-750424	burn step 29, data set 15	3248.44	426.15	7091.97	13243.1	54.43	Figure A.2.1.k																				
750424-750425	burn step 30	3173.00	23.13	7115.09	13324.5	53.50	Figure A.2.1.k																				
750425-750513	burn step 31, data set 16	2927.97	384.11	7499.21	11585.0	59.09	Figure A.2.1.l																				
750513-750517	burn step 32	2732.75	79.67	7578.87	12631.5	52.77	Figure A.2.1.m																				
750606-750725	burn step 33, data set 17	1845.70	591.88	8170.75	7556.2	67.41	48	48	48	48	48	48	48	48	38	44	44	38	38	10	10	6	6	4	0	4	8
750725-750816	burn step 34, data set 18	1704.43	273.29	8444.04	5229.7	93.37	48	48	48	48	48	48	48	48	42	44	44	40	40	16	22	18	8	4	6	8	8
750816-750927	burn step 35, data set 19	1807.10	553.16	8997.20	5733.0	90.10	48	48	48	48	48	48	48	48	44	44	44	44	38	16	22	22	8	4	4	10	18
750927-751031	burn step 36, data set 20	1823.91	451.96	9449.16	5102.1	95.88	Figure A.2.1.n																				
		core support plate hole plugging																									

Number of notches withdrawn for each CR sequence group (A and A2)
(48 = fully out, 0 = fully in)

CYCLE 1

burn step time period	Explanation	Power (MWt)	EFPH	accumulated EFPH	core flow (kg/s)	subcooling (kJ/kg)	1	2	3	4	5	6	7	8	9	10	11	12	13	14	15	16	17	18	19	20	21
		core support plate hole plugging																									
751130-751224	burn step 37, data set 21	2284.02	366.22	9815.38	9037.6	70.85	Figure A.2.1.o																				
751224-760108	burn step 38	2529.90	276.58	10091.96	9886.8	67.82	Figure A.2.1.p																				
760108-760115	burn step 39, data set 22	2321.50	118.44	10210.40	8307.4	70.36	Figure A.2.1.q																				
760115-760207	burn step 40	3037.72	509.21	10719.60	12178.2	56.54	Figure A.2.1.r																				
760207-760214	burn step 41, data set 23	2381.57	121.50	10841.11	7645.5	81.24	48	48	48	48	48	48	48	48	48	48	48	48	48	38	38	40	36	36	30	18	24
760214-760221	burn step 42	3055.86	155.90	10997.01	12784.5	53.91	48	48	48	48	48	48	48	48	48	48	48	48	48	38	38	40	34	34	28	16	22
760221-760326	burn step 43, data set 24	3096.72	767.36	11764.37	12386.0	66.95	48	48	48	48	48	48	48	48	48	48	48	48	48	40	40	42	36	40	36	26	32
CYCLE 2																											
760623-760628	burn step 1, data set 25	1533.90	55.90	55.90	6977.3	72.28	48	48	48	48	48	48	48	48	18	10	6	4	2	40	40	42	38	32	44	48	26
760628-760709	burn step 2	2221.50	161.91	217.80	9913.1	59.63	48	48	48	48	48	48	48	48	18	10	6	4	2	40	40	42	38	34	44	48	28
760709-760714	burn step 3, data set 26	2870.00	83.67	301.47	9800.4	68.33	Figure A.2.2.a																				
760714-760806	burn step 4	3169.52	531.30	832.77	13074.6	54.81	Figure A.2.2.b																				
760806-760901	burn step 5, data set 27	2072.06	362.44	1195.21	8180.8	70.51	48	48	48	48	48	48	48	48	24	18	8	8	10	34	40	40	40	34	48	48	42
760901-760925	burn step 6	3120.38	545.81	1741.02	13120.4	54.71	48	48	48	48	48	48	48	48	28	20	10	10	14	38	40	40	40	38	48	48	42
760925-761008	burn step 7, data set 28	2738.15	259.43	2000.45	9945.5	65.49	48	48	48	48	48	48	48	48	26	16	8	10	16	38	40	40	40	38	48	48	42
761008-761010	burn step 8	2129.00	31.03	2031.48	7174.1	79.67	48	48	48	48	48	48	48	48	22	12	6	8	16	36	40	40	40	36	48	48	42
761010-761028	burn step 9, data set 29	2571.14	337.30	2368.78	8869.9	69.25	Figure A.2.2.c																				
761028-761115	burn step 10	3084.81	404.69	2773.47	12500.3	56.97	Figure A.2.2.d																				
761125-761216	burn step 11, data set 30	2662.19	407.45	3180.92	9727.7	63.56	48	48	48	48	48	48	48	48	36	44	48	48	48	24	32	32	10	6	24	26	10
761216-761228	burn step 12, data set 31	3276.04	286.52	3467.44	13027.9	54.22	48	48	48	48	48	48	48	48	40	44	48	48	48	28	36	36	12	10	28	28	14
761228-770102	burn step 13	2906.70	105.92	3573.36	12184.2	54.54	48	48	48	48	48	48	48	48	40	44	48	48	48	28	36	36	12	10	28	28	14
770109-770119	burn step 14, data set 32	2386.80	173.95	3747.32	8670.4	71.38	Figure A.2.2.e																				
770119-770126	burn step 15, data set 33	3276.57	167.16	3914.48	12928.5	56.65	Figure A.2.2.f																				
770126-770202	burn step 16, data set 34	3268.86	166.77	4081.25	13243.5	53.58	Figure A.2.2.f																				
770202-770205	burn step 17	2662.00	58.20	4139.45	12001.5	53.11	Figure A.2.2.f																				
770205-770223	burn step 18, data set 35	2366.75	310.49	4449.94	9327.5	65.69	Figure A.2.2.g																				
770223-770304	burn step 19	2993.50	196.35	4646.29	12937.8	56.50	Figure A.2.2.h																				
770304-770311	burn step 20, data set 36	2277.00	116.17	4762.46	7305.8	83.40	48	48	48	48	48	48	48	48	30	34	36	10	20	38	40	42	44	48	48	48	48
770311-770314	burn step 21	1679.67	36.73	4799.18	9124.5	68.62	48	48	48	48	48	48	48	48	32	34	36	14	24	38	40	42	44	48	48	48	48
770316-770403	burn step 22, data set 37	2741.14	359.60	5158.79	10392.4	64.09	48	48	48	48	48	48	48	48	30	30	34	14	32	36	36	42	44	48	48	48	48

LEGEND: - = fully withdrawn, 0 = fully inserted. (Maximum withdrawal = 48 notches)

Figure A.2.1.a

				-	-	-	-	-	-	-				
			-	42	-	40	-	40	-	42	-			
		-	-	-	-	-	-	-	-	-	-	-		
	-	-	-	38	-	32	-	32	-	38	-	-	-	
-	-	-	-	-	-	-	-	-	-	-	-	-	-	-
-	-	38	-	12	-	38	-	38	-	12	-	38	-	-
-	-	-	-	-	-	-	-	-	-	-	-	-	-	-
-	-	30	-	38	-	12	-	12	-	38	-	30	-	-
-	-	-	-	-	-	-	-	-	-	-	-	-	-	-
-	-	38	-	12	-	38	-	38	-	12	-	38	-	-
-	-	-	-	-	-	-	-	-	-	-	-	-	-	-
	-	-	-	38	-	32	-	32	-	38	-	-	-	
		-	-	-	-	-	-	-	-	-	-	-		
			-	42	-	40	-	40	-	42	-			
				-	-	-	-	-	-	-				

Figure A.2.1.b

				-	-	-	-	-	-	-				
			-	-	28	-	38	-	28	-	-			
		-	-	-	-	-	-	-	-	-	-	-		
	-	-	36	-	28	-	20	-	28	-	36	-	-	
-	-	-	-	-	-	-	-	-	-	-	-	-	-	-
-	28	-	28	-	12	-	28	-	12	-	28	-	28	-
-	-	-	-	-	-	-	-	-	-	-	-	-	-	-
-	38	-	20	-	28	-	6	-	28	-	20	-	38	-
-	-	-	-	-	-	-	-	-	-	-	-	-	-	-
-	28	-	28	-	12	-	28	-	12	-	28	-	28	-
-	-	-	-	-	-	-	-	-	-	-	-	-	-	-
	-	-	36	-	28	-	20	-	28	-	36	-	-	
		-	-	-	-	-	-	-	-	-	-	-		
			-	-	28	-	38	-	28	-	-			
				-	-	-	-	-	-	-				

Figure A.2.1.c

				-	-	-	-	-	-	-				
			-	-	32	-	40	-	32	-	-			
		-	-	-	-	-	-	-	-	-	-	-		
	-	-	40	-	34	-	28	-	38	-	40	-	-	
-	-	-	-	-	-	-	-	-	-	-	-	-	-	-
-	32	-	38	-	12	-	38	-	12	-	34	-	32	-
-	-	-	-	-	-	-	-	-	-	-	-	-	-	-
-	40	-	28	-	38	-	14	-	38	-	28	-	40	-
-	-	-	-	-	-	-	-	-	-	-	-	-	-	-
-	32	-	34	-	12	-	38	-	12	-	38	-	32	-
-	-	-	-	-	-	-	-	-	-	-	-	-	-	-
	-	-	40	-	38	-	28	-	34	-	40	-	-	
		-	-	-	-	-	-	-	-	-	-	-		
			-	-	32	-	40	-	32	-	-			
				-	-	-	-	-	-	-				

Figure A.2.1.d

				-	-	-	-	-	-	-				
			-	42	-	26	-	26	-	42	-			
		-	-	-	-	-	-	-	-	-	-	-		
	-	34	-	30	-	8	-	8	-	30	-	34	-	
-	-	-	44	-	42	-	-	-	42	-	44	-	-	-
-	-	32	-	8	-	28	-	28	-	8	-	32	-	-
-	-	-	44	-	40	-	44	-	40	-	44	-	-	-
-	-	14	-	32	-	8	-	8	-	32	-	14	-	-
-	-	-	44	-	40	-	44	-	40	-	44	-	-	-
-	-	32	-	8	-	28	-	28	-	8	-	32	-	-
-	-	-	44	-	42	-	-	-	42	-	44	-	-	-
	-	34	-	30	-	8	-	8	-	30	-	34	-	
		-	-	-	-	-	-	-	-	-	-	-		
			-	42	-	26	-	26	-	42	-			
				-	-	-	-	-	-	-				

Figure A.2.1.e

				-	-	-	-	-	-	-				
			-	42	-	26	-	26	-	42	-			
		-	-	-	-	-	-	-	-	-	-	-		
	-	34	-	30	-	8	-	8	-	30	-	34	-	
-	-	-	44	-	42	-	-	-	42	-	44	-	-	-
-	-	32	-	8	-	26	-	26	-	8	-	32	-	-
-	-	-	44	-	40	-	44	-	40	-	44	-	-	-
-	-	14	-	32	-	6	-	6	-	32	-	14	-	-
-	-	-	44	-	40	-	44	-	40	-	44	-	-	-
-	-	32	-	8	-	26	-	26	-	8	-	32	-	-
-	-	-	44	-	42	-	-	-	42	-	44	-	-	-
	-	34	-	30	-	8	-	8	-	30	-	34	-	
		-	-	-	-	-	-	-	-	-	-	-		
			-	42	-	26	-	26	-	42	-			
				-	-	-	-	-	-	-				

Figure A.2.1.f

				-	-	-	-	-	-	-				
			-	38	-	28	-	28	-	38	-			
		-	-	-	-	-	-	-	-	-	-	-		
	-	34	-	20	-	8	-	8	-	20	-	34	-	
-	-	-	38	-	42	-	-	-	42	-	38	-	-	-
-	-	26	-	8	-	26	-	26	-	8	-	26	-	-
-	-	-	44	-	40	-	40	-	40	-	44	-	-	-
-	-	12	-	32	-	8	-	8	-	32	-	12	-	-
-	-	-	44	-	40	-	40	-	40	-	44	-	-	-
-	-	26	-	8	-	26	-	26	-	8	-	26	-	-
-	-	-	38	-	42	-	-	-	42	-	38	-	-	-
	-	34	-	20	-	8	-	8	-	20	-	34	-	
		-	-	-	-	-	-	-	-	-	-	-		
			-	38	-	28	-	28	-	38	-			
					-	-	-	-	-	-				

Figure A.2.1.g

				-	-	-	-	-	-	-				
			-	38	-	26	-	26	-	38	-			
		-	-	-	-	-	-	-	-	-	-	-		
	-	34	-	20	-	6	-	6	-	20	-	34	-	
-	-	-	38	-	42	-	-	-	42	-	38	-	-	-
-	-	26	-	4	-	24	-	24	-	4	-	26	-	-
-	-	-	44	-	40	-	40	-	40	-	44	-	-	-
-	-	10	-	32	-	6	-	6	-	32	-	10	-	-
-	-	-	44	-	40	-	40	-	40	-	44	-	-	-
-	-	26	-	4	-	24	-	24	-	4	-	26	-	-
-	-	-	38	-	42	-	-	-	42	-	38	-	-	-
	-	34	-	20	-	6	-	6	-	20	-	34	-	
		-	-	-	-	-	-	-	-	-	-	-		
			-	38	-	26	-	26	-	38	-			
				-	-	-	-	-	-	-				

Figure A.2.1.h

				-	-	-	-	-	-	-				
			-	36	-	28	-	28	-	36	-			
		-	36	-	16	-	4	-	16	-	36	-		
	-	-	-	26	-	38	-	38	-	26	-	-	-	
-	36	-	8	-	4	-	16	-	4	-	8	-	36	-
-	-	20	-	36	-	34	-	34	-	36	-	20	-	-
-	30	-	6	-	12	-	8	-	12	-	6	-	30	-
-	-	8	-	36	-	32	-	32	-	36	-	8	-	-
-	30	-	6	-	12	-	8	-	12	-	6	-	30	-
-	-	20	-	36	-	34	-	34	-	36	-	20	-	-
-	36	-	8	-	4	-	16	-	4	-	8	-	36	-
	-	-	-	26	-	38	-	38	-	26	-	-	-	
		-	36	-	16	-	4	-	16	-	36	-		
			-	36	-	28	-	28	-	36	-			
				-	-	-	-	-	-	-				

Figure A.2.1.i

				-	-	-	-	-	-	-				
			-	38	-	28	-	28	-	38	-			
		-	36	-	16	-	6	-	16	-	36	-		
	-	-	-	30	-	38	-	38	-	30	-	-	-	
-	36	-	8	-	6	-	16	-	6	-	8	-	36	-
-	-	24	-	36	-	34	-	34	-	36	-	24	-	-
-	32	-	6	-	10	-	12	-	10	-	6	-	32	-
-	-	10	-	36	-	36	-	36	-	36	-	10	-	-
-	32	-	6	-	10	-	12	-	10	-	6	-	32	-
-	-	24	-	36	-	34	-	34	-	36	-	24	-	-
-	36	-	8	-	6	-	16	-	6	-	8	-	36	-
	-	-	-	30	-	38	-	38	-	30	-	-	-	
		-	36	-	16	-	6	-	16	-	36	-		
			-	38	-	28	-	28	-	38	-			
				-	-	-	-	-	-	-				

Figure A.2.1.j

				-	-	-	-	-	-	-				
			-	34	-	28	-	28	-	34	-			
		-	36	-	14	-	8	-	14	-	36	-		
	-	-	-	24	-	34	-	34	-	24	-	-	-	
-	34	-	8	-	6	-	18	-	6	-	8	-	34	-
-	-	16	-	36	-	32	-	32	-	36	-	16	-	-
-	32	-	4	-	6	-	8	-	6	-	4	-	32	-
-	-	10	-	36	-	32	-	32	-	36	-	10	-	-
-	32	-	4	-	6	-	8	-	6	-	4	-	32	-
-	-	16	-	36	-	32	-	32	-	36	-	16	-	-
-	34	-	8	-	6	-	18	-	6	-	8	-	34	-
	-	-	-	24	-	34	-	34	-	24	-	-	-	
		-	36	-	14	-	8	-	14	-	36	-		
			-	34	-	28	-	28	-	34	-			
				-	-	-	-	-	-	-				

Figure A.2.1.j

				-	-	-	-	-	-	-				
			-	38	-	28	-	28	-	38	-			
		-	36	-	14	-	8	-	14	-	36	-		
	-	-	-	28	-	38	-	38	-	28	-	-	-	
-	36	-	8	-	8	-	18	-	8	-	8	-	36	-
-	-	20	-	36	-	34	-	34	-	36	-	20	-	-
-	30	-	6	-	8	-	12	-	8	-	6	-	30	-
-	-	10	-	38	-	36	-	36	-	38	-	10	-	-
-	30	-	6	-	8	-	12	-	8	-	6	-	30	-
-	-	20	-	36	-	34	-	34	-	36	-	20	-	-
-	36	-	8	-	8	-	18	-	8	-	8	-	36	-
	-	-	-	28	-	38	-	38	-	28	-	-	-	
		-	36	-	14	-	8	-	14	-	36	-		
			-	38	-	28	-	28	-	36	-			
				-	-	-	-	-	-	-				

Figure A.2.1.k

				-	-	-	-	-	-	-				
			-	38	-	28	-	28	-	38	-			
		-	36	-	14	-	8	-	14	-	36	-		
	-	-	-	28	-	38	-	38	-	28	-	-	-	
-	36	-	10	-	8	-	18	-	8	-	10	-	36	-
-	-	20	-	36	-	34	-	34	-	36	-	20	-	-
-	30	-	6	-	8	-	12	-	8	-	6	-	30	-
-	-	12	-	38	-	36	-	36	-	38	-	12	-	-
-	30	-	6	-	8	-	12	-	8	-	6	-	30	-
-	-	20	-	36	-	34	-	34	-	36	-	20	-	-
-	36	-	10	-	8	-	18	-	8	-	10	-	36	-
	-	-	-	28	-	38	-	38	-	28	-	-	-	
		-	36	-	14	-	8	-	14	-	36	-		
			-	38	-	28	-	28	-	38	-			
				-	-	-	-	-	-	-				

Figure A.2.1.l

				-	-	-	-	-	-	-				
			-	38	-	30	-	30	-	38	-			
		-	36	-	14	-	8	-	14	-	36	-		
	-	-	-	32	-	38	-	38	-	32	-	-	-	
-	36	-	12	-	10	-	20	-	10	-	12	-	36	-
-	-	20	-	36	-	36	-	36	-	36	-	20	-	-
-	34	-	6	-	10	-	14	-	10	-	6	-	34	-
-	-	14	-	40	-	36	-	36	-	40	-	14	-	-
-	34	-	6	-	10	-	14	-	10	-	6	-	34	-
-	-	20	-	36	-	36	-	36	-	36	-	20	-	-
-	36	-	12	-	10	-	20	-	10	-	12	-	36	-
	-	-	-	32	-	38	-	38	-	32	-	-	-	
		-	36	-	14	-	8	-	14	-	36	-		
			-	38	-	30	-	30	-	36	-			
				-	-	-	-	-	-	-				

Figure A.2.1.m

				-	-	-	-	-	-	-				
			-	38	-	26	-	26	-	38	-			
		-	32	-	10	-	6	-	10	-	32	-		
	-	-	-	32	-	38	-	38	-	32	-	-	-	
-	36	-	8	-	8	-	16	-	8	-	8	-	36	-
-	-	16	-	36	-	32	-	32	-	36	-	16	-	-
-	30	-	6	-	8	-	12	-	8	-	6	-	30	-
-	-	10	-	38	-	30	-	30	-	38	-	10	-	-
-	30	-	6	-	8	-	12	-	8	-	6	-	30	-
-	-	16	-	36	-	32	-	32	-	36	-	16	-	-
-	36	-	8	-	8	-	16	-	8	-	8	-	36	-
	-	-	-	32	-	38	-	38	-	32	-	-	-	
		-	32	-	10	-	6	-	10	-	32	-		
			-	38	-	26	-	26	-	36	-			
				-	-	-	-	-	-	-				

Figure A.2.1.n

				-	-	-	-	-	-	-				
			-	-	-	38	-	38	-	-	-			
		-	34	-	20	-	8	-	20	-	34	-		
	-	-	-	46	-	-	-	-	-	46	-	-	-	
-	34	-	10	-	10	-	8	-	10	-	10	-	34	-
-	-	-	-	42	-	42	-	42	-	42	-	-	-	-
-	20	-	4	-	12	-	8	-	12	-	4	-	20	-
-	-	-	-	-	-	42	-	42	-	-	-	-	-	-
-	20	-	4	-	12	-	8	-	12	-	4	-	20	-
-	-	-	-	42	-	42	-	42	-	42	-	-	-	-
-	34	-	10	-	10	-	8	-	10	-	10	-	34	-
	-	-	-	46	-	-	-	-	-	46	-	-	-	
		-	34	-	20	-	8	-	20	-	34	-		
			-	-	-	38	-	38	-	-	-			
				-	-	-	-	-	-	-				

Figure A.2.1.o

				-	-	-	-	-	-	-				
			-	-	-	38	-	38	-	-	-			
		-	38	-	36	-	20	-	36	-	38	-		
	-	-	-	-	-	-	-	-	-	-	-	-	-	
-	36	-	30	-	14	-	32	-	14	-	30	-	36	-
-	-	-	-	44	-	44	-	44	-	44	-	-	-	-
-	36	-	12	-	22	-	20	-	22	-	12	-	36	-
-	-	-	-	-	-	-	-	-	-	-	-	-	-	-
-	36	-	12	-	22	-	20	-	22	-	12	-	36	-
-	-	-	-	44	-	44	-	44	-	44	-	-	-	-
-	36	-	30	-	14	-	32	-	14	-	30	-	36	-
	-	-	-	-	-	-	-	-	-	-	-	-	-	
		-	38	-	36	-	20	-	36	-	38	-		
			-	-	-	38	-	38	-	-	-			
				-	-	-	-	-	-	-				

Figure A.2.1.p

				-	-	-	-	-	-	-				
			-	-	-	38	-	38	-	-	-			
		-	34	-	28	-	16	-	28	-	34	-		
	-	-	-	-	-	-	-	-	-	-	-	-	-	
-	34	-	30	-	8	-	32	-	8	-	30	-	34	-
-	-	-	-	44	-	44	-	44	-	44	-	-	-	-
-	28	-	8	-	18	-	12	-	18	-	8	-	28	-
-	-	-	-	-	-	-	-	-	-	-	-	-	-	-
-	28	-	8	-	18	-	12	-	18	-	8	-	28	-
-	-	-	-	44	-	44	-	44	-	44	-	-	-	-
-	34	-	30	-	8	-	32	-	8	-	30	-	34	-
	-	-	-	-	-	-	-	-	-	-	-	-	-	
		-	34	-	28	-	16	-	28	-	34	-		
			-	-	-	38	-	38	-	-	-			
				-	-	-	-	-	-	-				

Figure A.2.1.q

				-	-	-	-	-	-	-				
			-	-	-	34	-	34	-	-	-			
		-	36	-	24	-	28	-	24	-	36	-		
	-	-	-	-	-	-	-	-	-	-	-	-	-	
-	36	-	32	-	8	-	26	-	8	-	32	-	36	-
-	-	-	-	44	-	44	-	44	-	44	-	-	-	-
-	24	-	12	-	20	-	6	-	20	-	12	-	24	-
-	-	-	-	-	-	-	-	-	-	-	-	-	-	-
-	24	-	12	-	20	-	6	-	20	-	12	-	24	-
-	-	-	-	44	-	44	-	44	-	44	-	-	-	-
-	36	-	32	-	8	-	26	-	8	-	32	-	36	-
	-	-	-	-	-	-	-	-	-	-	-	-	-	
		-	36	-	24	-	28	-	24	-	36	-		
			-	-	-	34	-	34	-	-	-			
				-	-	-	-	-	-	-				

Figure A.2.1.r

				-	-	-	-	-	-	-				
			-	-	-	44	-	44	-	-	-			
		-	42	-	30	-	34	-	30	-	42	-		
	-	-	-	-	-	-	-	-	-	-	-	-	-	
-	42	-	38	-	12	-	38	-	12	-	38	-	42	-
-	-	-	-	-	-	-	-	-	-	-	-	-	-	-
-	32	-	16	-	32	-	8	-	32	-	16	-	32	-
-	-	-	-	-	-	-	-	-	-	-	-	-	-	-
-	32	-	16	-	32	-	8	-	32	-	16	-	32	-
-	-	-	-	-	-	-	-	-	-	-	-	-	-	-
-	42	-	38	-	12	-	38	-	12	-	38	-	42	-
	-	-	-	-	-	-	-	-	-	-	-	-	-	
		-	42	-	30	-	34	-	30	-	42	-		
			-	-	-	44	-	44	-	-	-			
				-	-	-	-	-	-	-				

CYCLE 2

Figure A.2.2.a

				-	-	-	-	-	-	-				
			-	-	-	34	-	34	-	-	-			
		-	38	-	38	-	42	-	38	-	38	-		
	-	-	-	22	-	12	-	12	-	22	-	-	-	
-	38	-	38	-	38	-	40	-	38	-	38	-	38	-
-	-	22	-	10	-	10	-	10	-	10	-	22	-	-
-	40	-	40	-	-	-	44	-	-	-	40	-	40	-
-	-	24	-	10	-	14	-	14	-	10	-	24	-	-
-	40	-	40	-	-	-	44	-	-	-	40	-	40	-
-	-	22	-	10	-	10	-	10	-	10	-	22	-	-
-	38	-	38	-	38	-	40	-	38	-	38	-	38	-
	-	-	-	22	-	12	-	12	-	22	-	-	-	
		-	38	-	38	-	42	-	38	-	38	-		
			-	-	-	34	-	34	-	-	-			
				-	-	-	-	-	-	-				

Figure A.2.2.b

				-	-	-	-	-	-	-				
			-	-	-	34	-	34	-	-	-			
		-	38	-	38	-	42	-	38	-	38	-		
	-	-	-	22	-	10	-	10	-	22	-	-	-	
-	38	-	38	-	38	-	40	-	38	-	38	-	38	-
-	-	22	-	8	-	10	-	10	-	8	-	22	-	-
-	40	-	40	-	-	-	44	-	-	-	40	-	40	-
-	-	22	-	10	-	12	-	12	-	10	-	22	-	-
-	40	-	40	-	-	-	44	-	-	-	40	-	40	-
-	-	22	-	8	-	10	-	10	-	8	-	22	-	-
-	38	-	38	-	38	-	40	-	38	-	38	-	38	-
	-	-	-	22	-	10	-	10	-	22	-	-	-	
		-	38	-	38	-	42	-	38	-	38	-		
			-	-	-	34	-	34	-	-	-			
				-	-	-	-	-	-	-				

Figure A.2.2.c

				-	-	-	-	-	-	-				
			-	40	-	34	-	34	-	40	-			
		-	32	-	24	-	8	-	24	-	32	-		
	-	-	-	-	-	-	-	-	-	-	-	-	-	
-	34	-	16	-	8	-	32	-	8	-	16	-	34	-
-	-	40	-	-	-	-	-	-	-	-	-	40	-	-
-	30	-	6	-	26	-	8	-	26	-	6	-	30	-
-	-	-	-	42	-	-	-	-	-	42	-	-	-	-
-	30	-	6	-	26	-	8	-	26	-	6	-	30	-
-	-	40	-	-	-	-	-	-	-	-	-	40	-	-
-	34	-	16	-	8	-	32	-	8	-	16	-	34	-
	-	-	-	-	-	-	-	-	-	-	-	-	-	
		-	32	-	24	-	8	-	24	-	32	-		
			-	40	-	34	-	34	-	40	-			
				-	-	-	-	-	-	-				

Figure A.2.2.d

				-	-	-	-	-	-	-				
			-	42	-	36	-	36	-	42	-			
		-	34	-	26	-	12	-	26	-	34	-		
	-	-	-	-	-	-	-	-	-	-	-	-	-	
-	36	-	18	-	12	-	32	-	12	-	18	-	36	-
-	-	40	-	-	-	-	-	-	-	-	-	40	-	-
-	32	-	10	-	30	-	12	-	30	-	10	-	32	-
-	-	-	-	44	-	-	-	-	-	44	-	-	-	-
-	32	-	10	-	30	-	12	-	30	-	10	-	32	-
-	-	40	-	-	-	-	-	-	-	-	-	40	-	-
-	36	-	18	-	12	-	32	-	12	-	18	-	36	-
	-	-	-	-	-	-	-	-	-	-	-	-	-	
		-	34	-	26	-	12	-	26	-	34	-		
			-	42	-	36	-	36	-	42	-			
				-	-	-	-	-	-	-				

Figure A.2.2.e

				-	-	-	-	-	-	-				
			-	32	-	28	-	28	-	32	-			
		-	40	-	40	-	40	-	40	-	40	-		
	-	38	-	8	-	16	-	16	-	8	-	38	-	
-	40	-	40	-	40	-	-	-	40	-	40	-	40	-
-	-	18	-	2	-	32	-	32	-	2	-	18	-	-
-	36	-	-	-	44	-	44	-	44	-	-	-	36	-
-	-	18	-	30	-	2	-	2	-	30	-	18	-	-
-	36	-	-	-	44	-	44	-	44	-	-	-	36	-
-	-	18	-	2	-	32	-	32	-	2	-	18	-	-
-	40	-	40	-	40	-	-	-	40	-	40	-	40	-
	-	38	-	8	-	16	-	16	-	8	-	38	-	
		-	40	-	40	-	40	-	40	-	40	-		
			-	32	-	28	-	28	-	32	-			
				-	-	-	-	-	-	-				

Figure A.2.2.f

				-	-	-	-	-	-	-				
			-	36	-	32	-	32	-	36	-			
		-	44	-	44	-	44	-	44	-	44	-		
	-	38	-	16	-	26	-	26	-	16	-	38	-	
-	40	-	44	-	44	-	-	-	44	-	44	-	40	-
-	-	28	-	8	-	36	-	36	-	8	-	28	-	-
-	38	-	-	-	-	-	-	-	-	-	-	-	38	-
-	-	28	-	36	-	6	-	6	-	36	-	28	-	-
-	38	-	-	-	-	-	-	-	-	-	-	-	38	-
-	-	28	-	8	-	36	-	36	-	8	-	28	-	-
-	40	-	44	-	44	-	-	-	44	-	44	-	40	-
	-	38	-	16	-	26	-	26	-	16	-	38	-	
		-	44	-	44	-	44	-	44	-	44	-		
			-	36	-	32	-	32	-	36	-			
				-	-	-	-	-	-	-				

Figure A.2.2.g

				-	-	-	-	-	-	-				
			-	30	-	26	-	26	-	30	-			
		-	44	-	44	-	44	-	44	-	44	-		
	-	32	-	8	-	20	-	20	-	8	-	32	-	
-	34	-	44	-	44	-	-	-	44	-	44	-	34	-
-	-	20	-	2	-	30	-	30	-	2	-	20	-	-
-	32	-	-	-	46	-	-	-	46	-	-	-	32	-
-	-	28	-	30	-	4	-	4	-	30	-	28	-	-
-	32	-	-	-	46	-	-	-	46	-	-	-	32	-
-	-	20	-	2	-	30	-	30	-	2	-	20	-	-
-	34	-	44	-	44	-	-	-	44	-	44	-	34	-
	-	32	-	8	-	20	-	20	-	8	-	32	-	
		-	44	-	44	-	44	-	44	-	44	-		
			-	30	-	26	-	26	-	30	-			
				-	-	-	-	-	-	-				

Figure A.2.2.h

				-	-	-	-	-	-	-				
			-	34	-	28	-	28	-	34	-			
		-	44	-	44	-	44	-	44	-	44	-		
	-	36	-	12	-	24	-	24	-	12	-	36	-	
-	40	-	44	-	44	-	-	-	44	-	44	-	40	-
-	-	24	-	6	-	36	-	36	-	6	-	24	-	-
-	36	-	-	-	-	-	-	-	-	-	-	-	36	-
-	-	34	-	36	-	8	-	8	-	36	-	34	-	-
-	36	-	-	-	-	-	-	-	-	-	-	-	36	-
-	-	24	-	6	-	36	-	36	-	6	-	24	-	-
-	40	-	44	-	44	-	-	-	44	-	44	-	40	-
	-	36	-	12	-	24	-	24	-	12	-	36	-	
		-	44	-	44	-	44	-	44	-	44	-		
			-	34	-	28	-	28	-	34	-			
				-	-	-	-	-	-	-				

APPENDIX 3 – CONTROL ROD CONFIGURATIONS FOR TT2 INITIAL STATE AND HOT ZERO POWER STATE

Legend:48 – Fully withdrawn control rod
0 – Fully inserted control rod

Control Rod configuration for Turbine Trip 2 Initial State

Y/X	02	06	10	14	18	22	26	30	34	38	42	46	50	54	58
59					48	48	48	48	48	48	48				
55				48	48	34	48	36	48	34	48	48			
51			48	48	0	48	26	48	26	48	0	48	48		
47		48	48	40	48	36	48	32	48	36	48	40	48	48	
43	48	48	0	48	26	48	4	48	4	48	26	48	0	48	48
39	48	34	48	36	48	48	48	48	48	48	48	36	48	34	48
35	48	48	26	48	4	48	32	48	32	48	4	48	26	48	48
31	48	36	48	32	48	48	48	48	48	48	48	32	48	36	48
27	48	48	26	48	4	48	32	48	32	48	4	48	26	48	48
23	48	34	48	36	48	48	48	48	48	48	48	36	48	34	48
19	48	48	0	48	26	48	4	48	4	48	26	48	0	48	48
15		48	48	40	48	36	48	32	48	36	48	40	48	48	
11			48	48	0	48	26	48	26	48	0	48	48		
07				48	48	34	48	36	48	34	48	48			
03					48	48	48	48	48	48	48				

Control Rod configuration for Hot Zero Power artificial state

Y/X	02	06	10	14	18	22	26	30	34	38	42	46	50	54	58
59					0	48	0	48	0	48	0				
55				0	48	0	48	0	48	0	48	0			
51			0	48	0	48	0	48	0	48	0	48	0		
47		0	48	0	48	0	48	0	48	0	48	0	48	0	
43	0	48	0	48	0	48	0	48	0	48	0	48	0	48	0
39	48	0	48	0	48	0	48	0	48	0	48	0	48	0	48
35	0	48	0	48	0	48	0	48	0	48	0	48	0	48	0
31	48	0	48	0	48	0	48	0	48	0	48	0	48	0	48
27	0	48	0	48	0	48	0	48	0	48	0	48	0	48	0
23	48	0	48	0	48	0	48	0	48	0	48	0	48	0	48
19	0	48	0	48	0	48	0	48	0	48	0	48	0	48	0
15		0	48	0	48	0	48	0	48	0	48	0	48	0	
11			0	48	0	48	0	48	0	48	0	48	0		
07				0	48	0	48	0	48	0	48	0			
03					0	48	0	48	0	48	0				

APPENDIX 4 – ASSEMBLY NUMBERS MAP FOR PEACH BOTTOM 2 IN POLCA7

Radial reflector regions are labeled with zeros.
Fuel assemblies are numbered from 1 to 764 with coordinates according to [24]

Y/X	..	01	03	05	07	09	11	13	15	17	19	21	23	25	27	29	31	33	35	37	39	41	43	45	47	49	51	53	55	57	59	..
..									0	0	0	0	0	0	0	0	0	0	0	0	0	0	0	0								
60								0	0	1	2	3	4	5	6	7	8	9	10	11	12	13	14	0	0							
58						0	0	0	15	16	17	18	19	20	21	22	23	24	25	26	27	28	29	30	0	0	0					
56						0	31	32	33	34	35	36	37	38	39	40	41	42	43	44	45	46	47	48	49	50	0					
54					0	0	51	52	53	54	55	56	57	58	59	60	61	62	63	64	65	66	67	68	69	70	0	0				
52			0	0	0	71	72	73	74	75	76	77	78	79	80	81	82	83	84	85	86	87	88	89	90	91	92	0	0	0		
50			0	93	94	95	96	97	98	99	100	101	102	103	104	105	106	107	108	109	110	111	112	113	114	115	116	117	118	0		
48		0	0	119	120	121	122	123	124	125	126	127	128	129	130	131	132	133	134	135	136	137	138	139	140	141	142	143	144	0	0	
46	0	0	145	146	147	148	149	150	151	152	153	154	155	156	157	158	159	160	161	162	163	164	165	166	167	168	169	170	171	172	0	0
44	0	173	174	175	176	177	178	179	180	181	182	183	184	185	186	187	188	189	190	191	192	193	194	195	196	197	198	199	200	201	202	0
42	0	203	204	205	206	207	208	209	210	211	212	213	214	215	216	217	218	219	220	221	222	223	224	225	226	227	228	229	230	231	232	0
40	0	233	234	235	236	237	238	239	240	241	242	243	244	245	246	247	248	249	250	251	252	253	254	255	256	257	258	259	260	261	262	0
38	0	263	264	265	266	267	268	269	270	271	272	273	274	275	276	277	278	279	280	281	282	283	284	285	286	287	288	289	290	291	292	0
36	0	293	294	295	296	297	298	299	300	301	302	303	304	305	306	307	308	309	310	311	312	313	314	315	316	317	318	319	320	321	322	0
34	0	323	324	325	326	327	328	329	330	331	332	333	334	335	336	337	338	339	340	341	342	343	344	345	346	347	348	349	350	351	352	0
32	0	353	354	355	356	357	358	359	360	361	362	363	364	365	366	367	368	369	370	371	372	373	374	375	376	377	378	379	380	381	382	0
30	0	383	384	385	386	387	388	389	390	391	392	393	394	395	396	397	398	399	400	401	402	403	404	405	406	407	408	409	410	411	412	0
28	0	413	414	415	416	417	418	419	420	421	422	423	424	425	426	427	428	429	430	431	432	433	434	435	436	437	438	439	440	441	442	0
26	0	443	444	445	446	447	448	449	450	451	452	453	454	455	456	457	458	459	460	461	462	463	464	465	466	467	468	469	470	471	472	0
24	0	473	474	475	476	477	478	479	480	481	482	483	484	485	486	487	488	489	490	491	492	493	494	495	496	497	498	499	500	501	502	0
22	0	503	504	505	506	507	508	509	510	511	512	513	514	515	516	517	518	519	520	521	522	523	524	525	526	527	528	529	530	531	532	0
20	0	533	534	535	536	537	538	539	540	541	542	543	544	545	546	547	548	549	550	551	552	553	554	555	556	557	558	559	560	561	562	0
18	0	563	564	565	566	567	568	569	570	571	572	573	574	575	576	577	578	579	580	581	582	583	584	585	586	587	588	589	590	591	592	0
16	0	0	593	594	595	596	597	598	599	600	601	602	603	604	605	606	607	608	609	610	611	612	613	614	615	616	617	618	619	620	0	0
14		0	0	621	622	623	624	625	626	627	628	629	630	631	632	633	634	635	636	637	638	639	640	641	642	643	644	645	646	0	0	
12			0	647	648	649	650	651	652	653	654	655	656	657	658	659	660	661	662	663	664	665	666	667	668	669	670	671	672	0		
10			0	0	0	673	674	675	676	677	678	679	680	681	682	683	684	685	686	687	688	689	690	691	692	693	694	0	0	0		
08					0	0	695	696	697	698	699	700	701	702	703	704	705	706	707	708	709	710	711	712	713	714	0	0				
06						0	715	716	717	718	719	720	721	722	723	724	725	726	727	728	729	730	731	732	733	734	0					
04						0	0	0	735	736	737	738	739	740	741	742	743	744	745	746	747	748	749	750	0	0	0					
02								0	0	751	752	753	754	755	756	757	758	759	760	761	762	763	764	0	0							
..									0	0	0	0	0	0	0	0	0	0	0	0	0	0	0	0								

APPENDIX 5 – RADIAL POWER DISTRIBUTIONS PRIOR TO TT2

HZP calculations with POLCA7 using PSU Cell Data

```
************
* POWER    *       Assembly avg distribution     Unit= -          Scal power = -3
************       --------------------------    -------------    ---------------
                            Avg value = 1000.00
                            Max value = 2011.19    Assy = 26/29
                            Min value =  127.44    Assy = 60/43
```

Y/X	..	01	03	05	07	09	11	13	15	17	19	21	23	25	27	29	31	33	35	37	39	41	43	45	47	49	51	53	55	57	59	..
..									0	0	0	0	0	0	0	0	0	0	0	0	0	0	0	0								
60								0	0	127	217	396	431	291	303	478	477	303	290	427	399	217	127	0	0							
58						0	0	0	242	330	472	698	808	573	623	880	878	622	575	809	694	473	330	242	0	0	0					
56						0	151	207	359	772	794	694	682	1111	980	705	700	975	1108	689	696	797	772	354	207	151	0					
54					0	0	312	406	588	832	911	742	776	1052	1050	812	805	1037	1048	772	745	928	826	588	409	316	0	0				
52			0	0	0	198	393	856	865	788	779	1296	1141	951	870	1397	1395	861	948	1146	1305	787	795	873	867	399	201	0	0	0		
50			0	153	317	400	610	877	995	808	859	1192	1212	923	927	1225	1223	909	922	1220	1208	876	822	1015	895	623	404	323	156	0		
48		0	0	211	414	868	885	821	820	1367	1213	1042	964	1517	1295	959	957	1281	1520	976	1065	1251	1414	842	845	907	887	422	216	0	0	
46	0	0	250	369	602	882	1010	824	884	1222	1248	988	1010	1350	1367	1040	1037	1349	1367	1029	1012	1322	1274	923	855	1040	902	614	377	253	0	0
44	0	132	342	799	851	810	827	1394	1240	1064	999	1601	1395	1165	1076	1723	1722	1071	1177	1423	1641	1027	1107	1304	1454	851	830	872	820	352	136	0
42	0	226	492	828	962	808	891	1250	1289	1017	1050	1410	1416	1088	1097	1464	1466	1113	1097	1442	1448	1073	1045	1354	1309	919	833	988	853	508	235	0
40	0	414	726	727	772	1348	1231	1080	1022	1645	1447	1208	1099	1731	1470	1102	1111	1485	1757	1119	1229	1470	1688	1058	1120	1275	1398	802	753	753	434	0
38	0	449	852	728	814	1190	1269	1003	1051	1445	1477	1120	1135	1511	1506	1170	1175	1532	1538	1157	1136	1482	1479	1085	1041	1313	1244	845	755	886	468	0
36	0	305	611	1183	1120	1011	978	1593	1416	1210	1124	1772	1528	1291	1189	1924	1928	1199	1311	1560	1806	1146	1242	1460	1643	1006	1045	1162	1228	636	321	0
34	0	323	665	1049	1127	928	987	1363	1416	1112	1131	1507	1534	1202	1220	1635	1626	1226	1216	1572	1543	1175	1149	1448	1410	1022	967	1168	1091	693	337	0
32	0	510	941	757	869	1507	1322	1031	1093	1804	1522	1143	1200	1962	1657	1213	1213	1660	1977	1218	1170	1576	1860	1130	1070	1373	1568	910	786	984	535	0
30	0	504	941	758	874	1500	1311	1019	1101	1811	1544	1156	1218	1981	1674	1226	1226	1671	1988	1226	1177	1575	1870	1141	1085	1392	1578	910	793	989	537	0
28	0	323	667	1053	1126	928	986	1371	1430	1128	1157	1549	1588	1236	1259	1689	1685	1247	1239	1603	1574	1197	1173	1495	1449	1058	982	1182	1105	702	341	0
26	0	310	613	1189	1127	1015	986	1619	1444	1240	1158	1832	1593	1351	1249	2011	2005	1242	1353	1607	1863	1184	1285	1508	1701	1040	1074	1186	1254	650	328	0
24	0	455	861	736	825	1214	1311	1031	1084	1496	1530	1167	1194	1605	1628	1239	1233	1602	1604	1199	1191	1575	1550	1129	1085	1370	1291	873	778	913	482	0
22	0	420	738	741	789	1384	1272	1125	1068	1718	1509	1267	1162	1838	1573	1174	1176	1563	1850	1185	1302	1562	1783	1114	1179	1349	1467	840	786	783	446	0
20	0	231	502	849	988	830	924	1324	1376	1068	1104	1497	1500	1149	1169	1574	1560	1170	1167	1554	1548	1145	1115	1434	1385	972	882	1049	902	534	245	0
18	0	135	353	823	879	840	863	1477	1332	1135	1058	1699	1479	1234	1137	1836	1844	1154	1258	1509	1749	1097	1175	1384	1540	905	889	942	877	376	144	0
16	0	0	255	381	624	920	1060	878	948	1321	1345	1054	1073	1429	1435	1110	1110	1475	1460	1098	1082	1383	1353	980	910	1110	968	661	401	274	0	0
14		0	0	219	430	906	928	868	874	1464	1309	1112	1024	1606	1368	1028	1036	1392	1644	1046	1141	1336	1507	900	903	972	952	453	231	0	0	
12			0	159	330	414	640	918	1053	856	921	1268	1285	978	996	1317	1323	1012	1004	1324	1306	950	888	1093	964	670	434	347	167	0		
10			0	0	0	207	412	900	912	833	823	1371	1200	1005	923	1499	1507	936	1033	1243	1418	851	864	948	940	436	217	0	0	0		
08					0	0	328	427	618	870	978	780	815	1101	1104	872	872	1125	1123	837	805	1013	901	642	445	343	0	0				
06						0	160	220	373	812	839	732	727	1175	1046	767	770	1058	1194	737	754	867	841	386	225	166	0					
04						0	0	0	254	347	496	729	852	608	666	949	952	673	617	870	755	513	359	263	0	0	0					
02								0	0	134	228	416	449	306	324	515	517	327	311	460	428	235	138	0	0							
..									0	0	0	0	0	0	0	0	0	0	0	0	0	0	0	0								

HZP calculations with POLCA7 using PHOENIX Cell Data

```
************
* POWER    *       Assembly avg distribution     Unit= -          Scal power = -3
************       -------------------------     -------------    ---------------

                            Avg value = 1000.00
                            Max value = 1664.79    Assy = 18/47
                            Min value =  212.28    Assy = 60/17
```

Y/X	..	01	03	05	07	09	11	13	15	17	19	21	23	25	27	29	31	33	35	37	39	41	43	45	47	49	51	53	55	57	59	..
..									0	0	0	0	0	0	0	0	0	0	0	0	0	0	0	0								
60								0	0	212	329	618	662	431	444	721	724	452	440	678	643	345	221	0	0							
58						0	0	0	390	437	628	949	1096	735	801	1156	1162	814	755	1127	979	657	457	409	0	0	0					
56						0	255	296	457	1016	1021	864	831	1393	1222	808	818	1247	1417	853	900	1084	1066	476	315	274	0					
54					0	0	453	510	739	1060	1125	843	853	1236	1233	852	857	1233	1259	880	870	1199	1107	781	545	492	0	0				
52			0	0	0	304	488	1088	1088	914	838	1446	1247	1000	863	1451	1460	875	1024	1296	1512	880	969	1168	1179	532	329	0	0	0		
50			0	265	462	502	748	1077	1190	855	879	1249	1253	861	851	1219	1226	857	881	1313	1322	922	909	1288	1187	817	528	492	278	0		
48		0	0	305	518	1103	1082	927	849	1464	1249	1009	872	1409	1196	826	837	1211	1438	898	1065	1348	1598	947	1026	1201	1196	555	322	0	0	
46	0	0	404	467	757	1108	1194	857	878	1246	1225	875	856	1212	1221	834	833	1209	1231	883	909	1355	1370	979	963	1325	1189	804	497	428	0	0
44	0	219	451	1055	1093	939	868	1486	1272	991	880	1425	1220	952	843	1402	1398	831	959	1251	1478	922	1077	1408	1642	943	1004	1147	1115	480	230	0
42	0	342	653	1083	1190	869	907	1278	1283	894	889	1235	1210	830	819	1144	1143	809	826	1233	1269	921	948	1417	1418	977	926	1254	1138	690	363	0
40	0	640	978	901	868	1510	1303	1050	906	1472	1275	969	824	1320	1107	753	770	1119	1335	832	987	1314	1545	971	1126	1393	1605	916	949	1036	682	0
38	0	682	1140	872	892	1310	1345	921	896	1280	1283	847	810	1118	1101	770	774	1111	1135	830	855	1285	1329	946	959	1392	1397	941	912	1202	723	0
36	0	441	776	1466	1302	1061	922	1491	1275	989	852	1348	1128	890	782	1329	1330	785	908	1170	1387	871	1018	1314	1538	950	1105	1359	1530	813	471	0
34	0	470	852	1305	1306	929	914	1278	1267	869	840	1130	1108	792	799	1128	1114	790	812	1171	1178	863	891	1277	1305	946	953	1341	1351	878	475	0
32	0	760	1230	876	918	1557	1311	878	877	1467	1194	785	795	1373	1155	762	769	1152	1375	807	812	1239	1505	896	906	1344	1596	937	885	1254	780	0
30	0	760	1232	879	921	1561	1302	880	880	1478	1217	811	819	1397	1193	774	777	1159	1379	808	806	1232	1516	906	915	1363	1595	916	876	1251	780	0
28	0	473	862	1327	1333	932	922	1293	1288	888	869	1186	1174	827	837	1205	1184	806	816	1168	1181	878	922	1329	1348	954	955	1331	1328	871	483	0
26	0	459	794	1506	1338	1082	935	1534	1317	1029	890	1420	1199	951	844	1430	1418	828	944	1204	1433	906	1053	1352	1571	961	1103	1354	1515	805	469	0
24	0	702	1175	902	921	1354	1396	963	944	1354	1355	885	875	1210	1222	837	833	1199	1216	871	909	1373	1381	963	971	1392	1381	920	905	1193	720	0
22	0	665	1014	936	901	1575	1366	1123	971	1577	1353	1031	876	1420	1199	827	830	1193	1434	895	1058	1396	1618	989	1140	1391	1596	911	942	1027	672	0
20	0	358	684	1133	1255	908	973	1414	1421	965	951	1334	1297	875	872	1250	1232	877	897	1349	1367	996	1010	1472	1444	979	927	1236	1118	687	360	0
18	0	230	484	1125	1173	1009	942	1637	1415	1100	959	1550	1320	1010	881	1497	1504	900	1035	1342	1588	994	1129	1446	1665	954	1017	1174	1121	485	235	0
16	0	0	432	507	819	1210	1324	951	981	1421	1407	954	932	1283	1258	878	891	1300	1312	941	975	1428	1420	1001	958	1327	1216	822	509	434	0	0
14		0	0	327	563	1207	1198	1018	941	1638	1404	1107	941	1499	1254	873	884	1288	1540	962	1136	1419	1659	945	1028	1195	1211	567	329	0	0	
12			0	282	502	544	818	1166	1304	931	964	1354	1368	917	908	1295	1312	930	958	1429	1418	998	959	1319	1196	827	544	502	283	0		
10			0	0	0	333	539	1187	1187	996	901	1554	1334	1063	915	1550	1561	930	1098	1411	1633	956	1034	1219	1217	554	337	0	0	0		
08					0	0	497	555	804	1152	1237	890	906	1305	1287	915	921	1296	1334	937	933	1310	1201	831	570	508	0	0				
06						0	284	326	494	1106	1118	924	888	1480	1305	873	879	1326	1507	911	963	1173	1150	508	331	289	0					
04						0	0	0	424	473	674	1000	1158	783	857	1234	1239	865	797	1196	1048	701	488	436	0	0	0					
02								0	0	229	353	655	694	446	472	766	768	477	455	715	678	365	235	0	0							
..									0	0	0	0	0	0	0	0	0	0	0	0	0	0	0	0								

HFP state prior to TT2 test, POLCA7 calculations using PSU Cell Data

```
************
* POWER    *       Assembly avg distribution     Unit= -          Scal power = -3
************       --------------------------    -------------    ---------------

                             Avg value = 1000.00
                             Max value = 1460.35     Assy = 30/25
                             Min value =  293.52     Assy = 56/49
```

Y/X	..	01	03	05	07	09	11	13	15	17	19	21	23	25	27	29	31	33	35	37	39	41	43	45	47	49	51	53	55	57	59	..
..									0	0	0	0	0	0	0	0	0	0	0	0	0	0	0	0								
60								0	0	360	509	573	618	637	653	661	661	654	638	613	577	508	358	0	0							
58						0	0	0	441	725	946	967	1098	1054	1156	1157	1157	1157	1066	1099	957	944	722	438	0	0	0					
56						0	297	474	712	993	966	1147	1067	1297	1154	1110	1103	1152	1297	1081	1145	964	988	700	470	294	0					
54					0	0	512	783	987	895	956	1015	1081	1137	1158	1142	1131	1146	1142	1071	1011	962	889	981	780	510	0	0				
52			0	0	0	457	753	1028	897	771	728	1178	1110	1229	1093	1347	1344	1079	1221	1107	1175	727	769	902	1027	752	455	0	0	0		
50			0	296	514	764	1046	975	971	727	750	1045	1116	1064	1080	1136	1133	1054	1057	1113	1044	751	724	972	975	1045	752	512	295	0		
48		0	0	473	784	1029	975	1154	1017	1165	1028	1227	1098	1273	1099	1066	1066	1086	1268	1098	1229	1033	1171	1016	1160	976	1029	783	473	0	0	
46	0	0	441	711	986	896	970	1010	1058	1074	1089	1094	1080	1046	1038	1019	1017	1030	1053	1086	1090	1114	1083	1071	1018	974	904	986	711	434	0	0
44	0	359	724	991	884	770	727	1165	1076	1183	1054	1285	1068	880	787	1174	1173	781	881	1072	1288	1050	1190	1095	1177	727	772	893	993	725	360	0
42	0	508	944	965	964	727	753	1030	1092	1057	1075	1131	1086	813	799	1027	1026	805	810	1089	1140	1072	1054	1113	1047	755	730	967	968	948	510	0
40	0	571	958	1148	1006	1176	1037	1230	1099	1291	1144	1333	1139	1263	1080	1099	1108	1083	1267	1143	1335	1143	1295	1106	1238	1043	1182	1017	1151	962	580	0
38	0	612	1100	1085	1076	1102	1118	1095	1086	1076	1099	1145	1185	1176	1178	1191	1192	1191	1182	1194	1146	1094	1079	1095	1108	1123	1109	1080	1089	1106	616	0
36	0	630	1068	1304	1143	1228	1075	1281	1060	886	818	1270	1179	1343	1187	1452	1453	1190	1348	1184	1273	819	889	1064	1284	1072	1238	1155	1308	1073	643	0
34	0	655	1161	1160	1166	1094	1086	1107	1044	788	804	1086	1183	1190	1223	1286	1277	1224	1192	1195	1090	813	794	1037	1111	1092	1105	1160	1164	1166	659	0
32	0	662	1161	1118	1143	1361	1147	1091	1031	1187	1036	1116	1199	1457	1288	1284	1284	1288	1458	1199	1118	1046	1188	1031	1094	1153	1363	1153	1113	1166	666	0
30	0	653	1160	1117	1151	1356	1145	1077	1037	1187	1046	1119	1210	1460	1281	1278	1284	1288	1458	1199	1118	1038	1188	1032	1097	1154	1365	1145	1119	1166	667	0
28	0	653	1159	1159	1155	1091	1081	1105	1043	790	808	1093	1199	1195	1229	1281	1288	1216	1191	1195	1089	812	795	1047	1106	1104	1105	1168	1164	1167	659	0
26	0	637	1057	1301	1149	1231	1068	1281	1061	889	822	1277	1189	1353	1197	1460	1457	1191	1347	1183	1272	817	890	1065	1287	1074	1240	1155	1309	1074	643	0
24	0	611	1099	1084	1075	1103	1126	1098	1089	1080	1102	1151	1198	1189	1203	1202	1198	1193	1182	1181	1148	1102	1082	1093	1110	1126	1110	1081	1089	1106	616	0
22	0	571	958	1148	1006	1177	1040	1236	1105	1296	1147	1339	1148	1273	1093	1110	1115	1086	1269	1146	1340	1151	1301	1110	1242	1055	1185	1018	1153	963	575	0
20	0	508	946	965	964	724	753	1047	1114	1056	1075	1144	1093	813	805	1043	1033	803	813	1097	1148	1084	1068	1118	1051	758	733	971	972	952	512	0
18	0	360	731	991	884	771	726	1177	1097	1193	1053	1291	1073	883	786	1180	1181	791	884	1067	1293	1063	1196	1099	1178	729	776	902	1001	738	361	0
16	0	0	434	710	985	896	974	1027	1074	1095	1106	1100	1084	1047	1029	1025	1018	1043	1048	1083	1099	1105	1085	1071	1018	975	901	992	711	445	0	0
14		0	0	472	782	1027	976	1160	1026	1175	1044	1233	1101	1273	1093	1076	1078	1096	1276	1093	1231	1034	1171	1016	1159	978	1032	786	476	0	0	
12			0	294	511	751	1043	967	972	726	755	1046	1116	1065	1091	1143	1143	1093	1067	1118	1046	755	729	973	977	1049	756	514	296	0		
10			0	0	0	455	751	1025	894	769	723	1175	1100	1228	1089	1353	1354	1089	1224	1109	1177	722	770	896	1030	765	458	0	0	0		
08					0	0	511	781	982	881	961	1003	1071	1128	1143	1150	1141	1151	1127	1070	1003	963	882	983	783	514	0	0				
06						0	297	478	700	987	962	1144	1080	1295	1156	1129	1129	1155	1293	1064	1143	962	987	700	472	297	0					
04						0	0	0	438	721	941	954	1094	1053	1158	1163	1163	1157	1051	1092	962	942	721	438	0	0	0					
02								0	0	357	506	569	608	626	653	663	663	652	626	608	570	507	358	0	0							
..									0	0	0	0	0	0	0	0	0	0	0	0	0	0	0	0								

HFP state prior to TT2 test, POLCA7 calculations using PHOENIX Cell Data

```
************
* POWER    *       Assembly avg distribution     Unit= -          Scal power = -3
************       -------------------------     -------------    ---------------

                         Avg value = 1000.00
                         Max value = 1417.46    Assy = 30/25
                         Min value =  393.82    Assy = 12/05
```

Y/X	..	01	03	05	07	09	11	13	15	17	19	21	23	25	27	29	31	33	35	37	39	41	43	45	47	49	51	53	55	57	59	..
..									0	0	0	0	0	0	0	0	0	0	0	0	0	0	0	0								
60								0	0	487	609	686	736	766	782	790	787	778	760	730	689	613	488	0	0							
58						0	0	0	564	767	989	993	1135	1090	1189	1186	1186	1190	1095	1134	989	990	767	565	0	0	0					
56						0	397	566	744	1026	982	1144	1077	1312	1175	1108	1110	1178	1310	1079	1146	990	1027	745	569	400	0					
54					0	0	598	807	1014	913	972	1004	1066	1140	1164	1124	1118	1141	1142	1065	1010	978	919	1015	812	604	0	0				
52			0	0	0	602	793	1052	917	761	695	1169	1091	1180	1053	1312	1311	1041	1178	1091	1170	689	763	931	1062	794	606	0	0	0		
50			0	398	598	797	1066	981	981	693	712	1032	1095	1016	1031	1106	1106	1017	1012	1102	1035	713	690	991	1001	1075	792	599	400	0		
48		0	0	566	807	1051	979	1157	1013	1163	1018	1195	1070	1234	1068	1030	1030	1067	1235	1066	1199	1027	1174	1017	1168	1000	1060	811	569	0	0	
46	0	0	559	738	1009	910	976	1003	1050	1062	1071	1066	1049	1024	1019	981	981	1021	1037	1050	1065	1101	1074	1058	1016	992	925	1015	747	564	0	0
44	0	478	758	1020	905	758	689	1155	1064	1128	1010	1250	1046	831	727	1139	1139	725	833	1048	1251	1008	1137	1074	1168	690	762	919	1028	770	486	0
42	0	604	982	987	971	692	712	1010	1075	1017	1035	1113	1073	752	742	1002	1003	743	751	1075	1114	1034	1011	1096	1032	714	690	976	993	989	613	0
40	0	677	980	1142	1000	1170	1026	1198	1071	1255	1123	1297	1115	1224	1047	1061	1087	1056	1230	1117	1298	1125	1260	1069	1202	1033	1177	1009	1146	989	688	0
38	0	720	1127	1083	1062	1090	1111	1071	1056	1053	1083	1119	1157	1141	1138	1152	1158	1159	1148	1161	1123	1083	1058	1056	1067	1106	1098	1068	1081	1133	729	0
36	0	742	1090	1307	1133	1189	1036	1243	1041	836	755	1227	1139	1271	1137	1404	1406	1138	1276	1148	1232	757	837	1030	1237	1023	1186	1142	1310	1094	758	0
34	0	771	1186	1175	1160	1063	1048	1079	1025	730	746	1051	1145	1140	1183	1259	1242	1178	1141	1166	1054	747	730	1003	1079	1044	1052	1152	1177	1188	765	0
32	0	773	1183	1117	1131	1323	1118	1041	986	1147	1006	1088	1169	1414	1258	1255	1268	1258	1413	1165	1090	1023	1147	985	1044	1120	1321	1130	1110	1183	785	0
30	0	773	1182	1114	1132	1320	1114	1037	987	1148	1023	1097	1169	1417	1261	1245	1262	1258	1413	1169	1089	1008	1149	987	1046	1125	1322	1113	1109	1185	788	0
28	0	771	1186	1174	1161	1047	1041	1072	1020	730	750	1061	1164	1146	1186	1255	1264	1162	1140	1160	1058	748	734	1025	1076	1049	1065	1161	1175	1189	782	0
26	0	755	1087	1309	1144	1182	1018	1237	1028	836	757	1234	1149	1282	1146	1416	1412	1140	1275	1146	1234	758	838	1034	1243	1028	1188	1150	1311	1096	765	0
24	0	717	1126	1082	1059	1084	1106	1069	1057	1055	1084	1118	1161	1153	1169	1175	1166	1166	1145	1161	1121	1085	1059	1060	1071	1105	1098	1052	1083	1134	734	0
22	0	678	978	1140	996	1166	1019	1200	1071	1260	1122	1298	1117	1232	1060	1092	1096	1054	1231	1118	1302	1131	1266	1072	1205	1042	1176	1003	1144	988	685	0
20	0	606	983	984	970	682	711	1027	1091	1013	1041	1114	1075	752	747	1017	1008	747	754	1075	1120	1046	1034	1107	1034	718	694	973	984	989	613	0
18	0	484	773	1023	907	757	684	1162	1077	1140	1012	1255	1051	832	725	1140	1141	728	833	1046	1256	1022	1145	1082	1166	689	763	916	1029	777	486	0
16	0	0	560	742	1010	913	980	1011	1051	1091	1105	1068	1059	1022	1009	975	977	1017	1022	1049	1073	1103	1073	1054	1008	982	919	1017	749	567	0	0
14		0	0	564	808	1052	990	1157	1013	1174	1040	1201	1071	1232	1063	1024	1025	1063	1235	1063	1200	1026	1171	998	1158	994	1055	810	569	0	0	
12			0	394	595	793	1066	975	979	685	714	1031	1095	1010	1034	1111	1115	1041	1028	1106	1034	718	697	983	993	1070	792	598	398	0		
10			0	0	0	603	792	1050	913	756	680	1160	1080	1173	1038	1314	1317	1045	1182	1100	1170	694	763	918	1057	800	605	0	0	0		
08					0	0	596	805	1007	902	968	994	1054	1124	1139	1135	1124	1140	1129	1058	1000	977	908	1013	810	599	0	0				
06						0	399	565	737	1020	982	1138	1078	1305	1172	1111	1113	1177	1307	1076	1142	988	1023	743	565	400	0					
04						0	0	0	561	762	981	976	1123	1086	1187	1183	1183	1186	1086	1127	987	982	759	561	0	0	0					
02								0	0	482	604	677	720	743	772	778	778	771	740	720	677	603	477	0	0							
..									0	0	0	0	0	0	0	0	0	0	0	0	0	0	0	0								

APPENDIX 6 – PEACH BOTTOM 2 RPV NODALIZATION IN POLCA-T

The RPV model was developed and verified in [5] and [21].